The Paton WELDING JOURNAL

March 2000 # 3

English translation of the monthly «Avtomaticheskaya Svarka» journal published in Russian since 1948

«The Paton Welding Journal» monthly is published by the E.O. Paton Electric Welding Institute of the National Academy of Sciences of Ukraine with the support rendered by the International Association «Welding».

Promotion group:
V.N.Lipodaev, V.I.Lokteva
A.T.Zelnichenko (Exec. director)

Editorial and advertising offices are located at PWI, Dept. 51, 11, Bozhenko str., 252650, Kyiv, Ukraine.
Tel.: (38044) 227 67 57
Fax: (38044) 268 04 86
E-mail: paton@i.kiev.ua; paton@iptelecom.net.ua

Subscriptions:
$460, 12 issues

«The Paton Welding Journal» Website:
http://www.nas.gov.ua/pwj

CONTENTS

PATON Evgeny Oscarovich

On March 5, 2000, 130 years have passed since the birthday of Paton Evgeny Oscarovich (1870 – 1953), the outstanding scientist in the field of metal structures and welding, academician of the Academy of Sciences of UkrSSR (1929), Honoured Scientist of UkrSSR (1940), laureate of Stalin prize of USSR (1941), Hero of Socialist Labour (1943), founder and permanent director of the Institute of Electric Welding (1934 – 1953), vice-president of Academy of Sciences of UkrSSR (1945 – 1953). E.O.Paton went down in history of science as the author of classical manuals on bridge construction, the designer of unique projects of bridges, the head of a scientific school on the problems of welding which is recognized all over the world.

Evgeny Oscarovich is well characterized by his own words: «I have never been attracted by the work directed to the solution of subjects abstracted and isolated from practice. I tried to make my works and the works of my staff to be useful for the national economy. The best award for the man is to see the embodiment of ideas and results of works into the life.» Different scientists including those involved in engineering estimate their achievement in different ways. Some of them are satisfied with receiving unique formula and consider their mission finalized. But such an achievement for Paton E.O. is only a step on the way to the main aim.

All life he was tireless at his work. He taught students, wrote manuals, improved methods of design of bridges, created unique projects and participated in their realization. He invited students to these works, fascinating them with his ideas, imparting the habits of a creative approach to the solution of technical problems.

In the 20s E.O. Paton realized that the technology of fabrication of metal structures will be based on an electric welding and decided to study this technological process. He founded the Electric Welding Laboratory which in 1934 was transformed to the Institute of Electric Welding. Evgeny Oscarovich considered the development of a high-efficient method of welding suitable for manufacture of critical structures as one of the important aims of the Institute. By the end of the 30s the Institute managed to develop such method as the submerged arc welding. The war began. By the request of Evgeny Oscarovich the Institute was evacuated to the Urals where the mass production of tanks was organized. In the severest conditions it was necessary in the shortest terms to create the technology of welding of hard-to-weld armoured steels, to set the manufacture of welding automatic machines and flux. At that time Evgeny Oscarovich and his colleagues accomplished a really heroic deed in realizing all this. The famous tanks T-34, welded by the automatic machines, were continuously leaving the plant conveyor. The submerged arc welding was also mastered at other defense plants owing to the efforts of E.O. Paton and his staff.

In postwar years the Institute was working in collaboration with hundreds of plants. New technologies of manufacture of ship hulls, large-diameter pipes, power, petrochemical and other equipment were created. At the same time Evgeny Oscarovich returned to his main idea, i.e. to the construction of all-welded bridges. The program of research works was scheduled and successfully fulfilled. This program envisaged the specifying of requirements to steel for welded structures, creation of rational welded joints and study of their strength, development of technology of welding both under shop and site conditions. At that time a method of welding vertical welds with a forced weld formation was also developed. The works of that period made a good start for a thorough study of materials science problems of welding, problems of strength of welded joints for different conditions of service, contributed to a wide application of mechanized methods of welding in site conditions. The first long all-welded bridge designed and constructed under the direct supervision of Evgeny Oscarovich and named after him was put into service in Kyiv in 1953.

E.O. Paton paid a great attention to the works made from the orders of the industrial enterprises. He considered an agreement with a customer as a certificate of recognition of usefulness of the research works. At a present transition to the market principles of organizing the economy, the progressiveness of the vital positions of the outstanding scientist becomes more evident.

E.O. Paton left us the property, the paton traditions, which are followed now at the Electric Welding Institute headed by Paton Boris Evgenievich. In spite of hard times in the country economy, the Institute, which bears the name of its founder, PATON EVGENY OSCAROVICH, is still one of the most authoritative research centres in the field of welding and allied technologies. This is proved by its wide-spread relations both with Ukrainian enterprises, and with R & D centres and companies of many foreign countries.

Student of Drezden Polytechnic Institute (1892)

Ceremonial opening of the E. Bosh road bridge through the Dnieper river (Kyiv, 1925)

Dean of the engineering faculty and chairperson of bridges of Kyiv Polytechnic Institute (1906)

Arch bridge over the Petrovskaya alley (Kyiv, 1910)

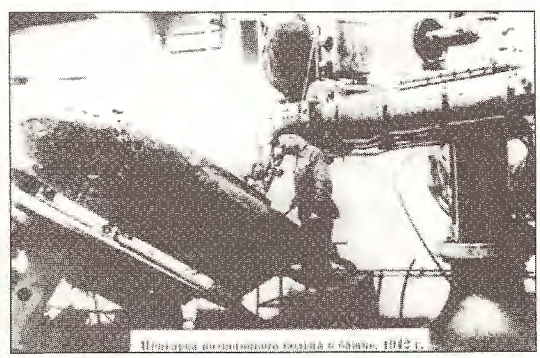

Welding of a supporting ring to the tank gun turrets (Nizhny Tagil, Uralvagonzavod, 1943)

Dismountable bridge for crossing the river (years of the I World War)

After tests of tank T-34 (1943)

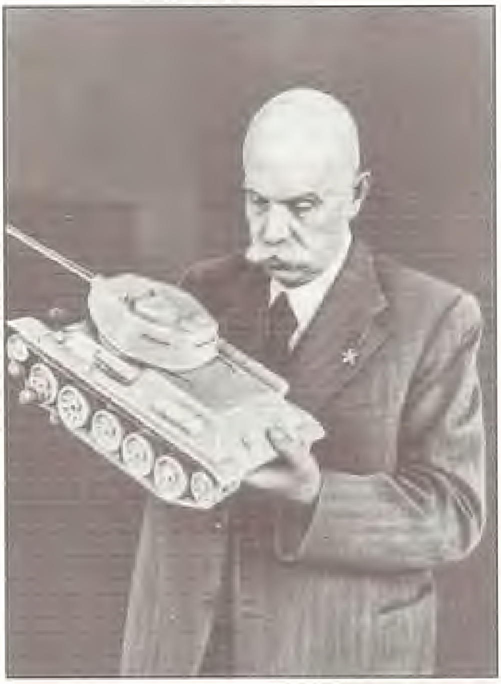

E.O. Paton with a medal presented him by the staff of the tank plant (Nizhny Tagil, 1945)

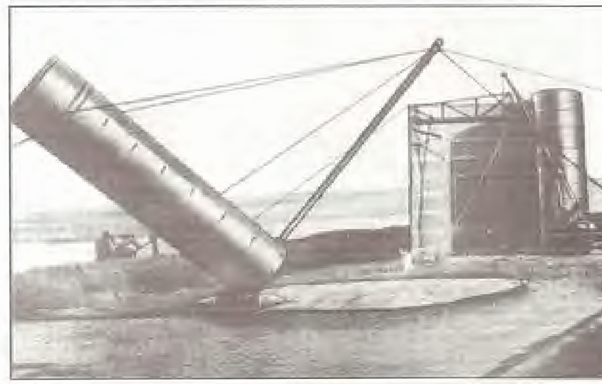

Erection of a large-sized tank (1948)

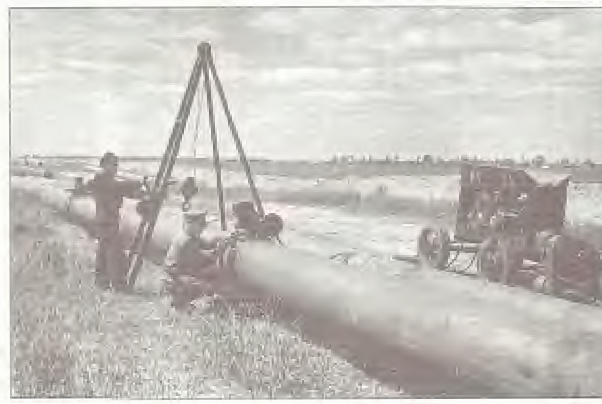

Automatic welding of pipeline in Dashava-Kyiv route (1949)

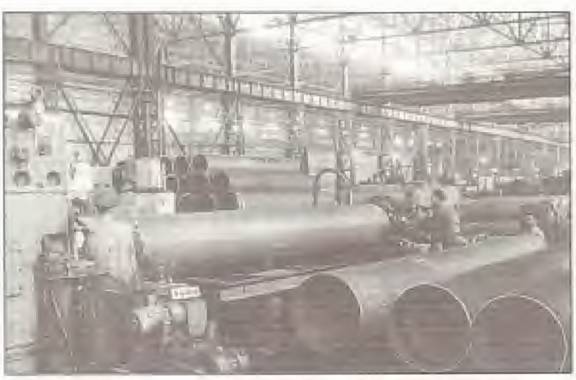

Pipe-welding shop of the Khartsyzsk pipe plant (1950)

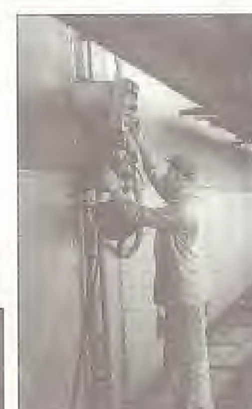

Automatic welding of vertical welds with a forced formation in the bridge span (1952)

I-beam of a span structure of the all-welded bridge (Dnepropetrovsk, 1952)

Hardfacing of a roll (1949)

PECULIARITIES OF WELDING T-JOINTS MADE FROM HIGH-STRENGTH STEEL 12KhGN2MFDRA

L.I. MIKHODUJ[1], V.D. POZNYAKOV[1], B.G. VASILJEV[1], A.K. YUSHCHENKO[1], Yu.I. BARYSHNIKOV[2] and V.A. STARODUBTSEV[2]
[1]The E.O. Paton Electric Welding Institute, NASU, Kyiv, Ukraine
[2]JSC Uralmashzavod, Russia

ABSTRACT

Mechanical properties of high-strength alloyed steel 12KhGN2MFDRA and peculiarities of formation of welded joints in making fillet welds are investigated. It is shown that steel acquires high values of mechanical properties, such as $\sigma_{0.2} \geq 980$ MPa; $\sigma_t \geq 1078$ MPa; $\delta_5 \geq 10$ % and $KCV^{-50} \geq 29$ J/cm^2 after quenching in combination with tempering. It is established that in T-joint welding within the range of 6 – 15 mm thicknesses the rate of cooling ($w_{6/5}$) of HAZ metal of web and flange is varied from 1.8 to 60 °C/s. Within this interval of cooling rates the structure of HAZ metal is mainly formed in martensitic and bainitic regions with hardness HV 303 – 375.

Key words: *high-strength steel, hot-rolled sheets, heat treatment, microstructure, mechanical properties, cold resistance, T-joints, thermal cycle, flange, web, minimum cooling rate.*

The low-alloyed high-strength steels with 600 – 800 MPa yield strength are successfully used in manufacture of critical welded structures in machine-building and construction. Steel of 12KhGN2MFDRA grade differs from many known high-strength thermally-strengthened steels (13KhGMRB, 12GN2MFAYu, 14KhG2SAFD, 14KhGN2MDAFB and others) by not only higher complex of its service properties ($\sigma_{0.2} \geq 980$ MPa, $\sigma_t \geq 1078$ MPa, $\delta_5 \geq 10$ % and $KCV^{-50} \geq$ ≥ 29 J/cm^2), but also by peculiarities of its use. This steel is supplied to the plant-manufacturer in the form of hot-rolled sheets of 4 – 20 mm thickness. Steel 12KhGN2MFDRA acquires the required complex of properties after heat treatment during manufacture of parts and separate elements of structures, such as box-type members in which T-joints and overlap joints are dominated.

In the opinion of the authors of [1] steel of the C–Mn–V–B alloying system possesses a sufficient hardenability, therefore, the introduction of nickel increases negligibly its hardness after quenching and high tempering, however, it can deteriorate the weldability. Some other drawbacks of this system are observed, such as: susceptibility to weakening, insufficient cold resistance at nickel content up to 2.5 % (as compared with its content not exceeding 0.5 – 1.0 %).

Therefore, the present work is aimed at investigation of mechanical properties of steel 12KhGN2MFDRA after different heat treatments and peculiar formation of welded joints in making fillet welds.

For investigation the metal of 6, 10 and 15 mm thicknesses and of the following chemical composition was used, %: 0.10 – 0.13 C; 0.29 – 0.33 Si; 1.08 – 1.12 Mn; 0.96 – 1.09 Cr; 1.96 – 2.05 Ni; 0.49 – 0.53 Mo; 0.10 – 0.12 V; 0.58 – 0.62 Cu; 0.001 – 0.002 B; 0.010 – 0.019 S; 0.012 – 0.019 P.

Microstructure of the as-delivered hot-rolled steel is martensitic-bainitic (Figure 1, *a*) with hardness HV 257 – 309. Mechanical properties and impact strength of the hot-rolled steel are given in Table 1 and in Figure 2, *a*, *b*. The impact strength of metal of 5 and 10 mm thickness is at the sufficiently high level, in spite of a negligible share of a tough constituent (20 %) in fracture of specimens with a sharp notch (0.25 mm radius) even during tests at 20 °C temperature.

Normalization with tempering did not cause the change in structure and properties of steel 12KhGN2MFDRA. Taking into account that after such treatment the required strength characteristics of the metal were not provided the further investigation for its use in welded structures seemed not to be rational.

Quenching with tempering (Table 1) contributes to the formation of a sorbite structure (Figure 1, *b*) in the steel investigated, which is more homogeneous as compared with the structure of the hot-rolled steel. In addition, the hardness (HV 300 – 343) and also values of strength and toughness of steel to the level of requirements specified by the technical specifications are increased.

Such nature of the structure of the parent metal may significantly influence the formation of properties of the HAZ metal and its resistance to a delayed fracture. In this connection it was rational to determine the parameters of cooling the HAZ metal of steel 12KhGN2MFDRA relative to conditions of manufacture of real structures. Single-pass fillet welds were performed in T-joint specimens made from steel 12KhGN2MFDRA of 6 – 15 mm thickness using a mechanized welding in

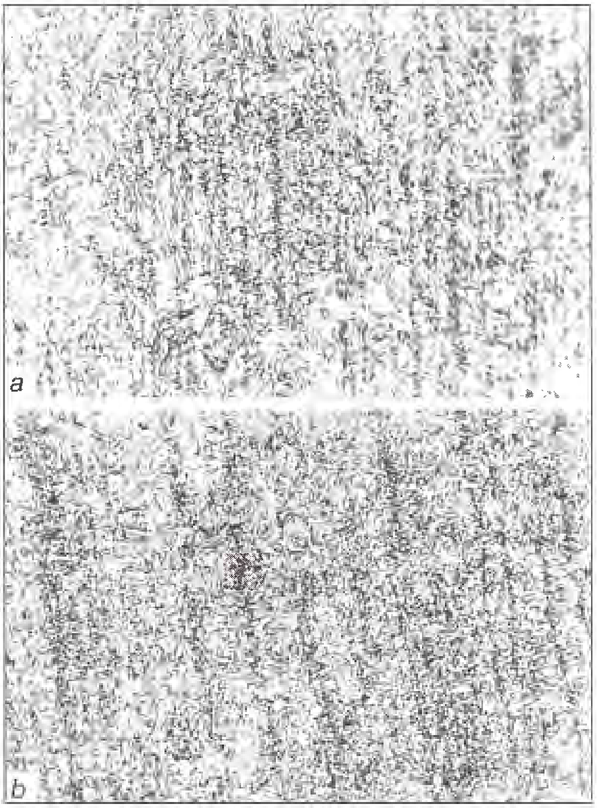

Figure 1. Microstructure of steel 12KhGN2MFDRA in hot-rolled state (*a*) and after quenching with tempering (*b*) (×320) (reduced by 0.67).

Ar + CO_2 mixture and 1.2 mm diameter wire. Leg of welds was equal to 0.7 – 0.8 of the web thickness, but not more than 8 – 9 mm. The conditions of welding of specimens were similar to the shop conditions of making these welds. Cooling rate of welded joints was controlled by changing the preheating within the interval 80 – 150 °C. Temperature in a central part of the T-specimens at the boundary of weld metal with HAZ metal from the side of flange and web was measured by a chromel-alumel thermocouple of 0.5 mm diameter. Typical curves of cooling HAZ metal of T-joints are given in Figure 3.

Almost straight relationship between the temperature and time at an ascending region of the temperature curve is observed for investigated welding conditions. Maximum temperature of metal heating at the point of thermocouple arrangement was 1230 – 1300 °C. When analysing the process of cooling T-joints of steel 12KhGN2MFDRA the following parameters were determined on the descending part of the curves: time of cooling from 800 to 500 °C ($t_{8/5}$, s), cooling rate within the temperatures 600 – 500 °C ($w_{6/5}$, °C/s) and instantaneous cooling rates at temperatures 500 and 300 °C (w_{500} and w_{300}, °C/s, respectively). Ratios of investigated thicknesses of web h_2 and flange h_1, welding conditions, temperatures of preheating T_{pr} and mentioned parameters of cooling curve are given in Table 2.

As the analysis showed, the HAZ metal from the flange side is under the most unfavourable conditions. In this case the intensive heat dissipation to both sides from the site of weld occurs, thus causing the large difference in intensity of cooling metal of flange and web. This situation is more pronounced in welding T-joints with different thicknesses of flange and web (15 and 6 mm, respectively).

The investigation showed that at selected welding conditions the cooling rate $w_{6/5}$ of HAZ metal of T-joints can vary within the wide ranges: from 2.7 to 50.0 °C/s. This wide range of cooling rates is beyond the limits which are usually established in welding of high-strength steels [2]. This can greatly influence both the structure and properties of HAZ metal of the high-strength steel and its resistance to a delayed fracture. Rational use of the thermokinetic diagrams of decay of austenite will give approximate information about the formation of structure and hardness, thus giving an opportunity to predict the changing in properties of alloyed steels under the action of the welding thermal cycle.

Thermokinetic diagram of decay of austenite of steel 12KhGN2MFDRA (Figure 4) was plotted using a quick-response dilatometer. Specimens of different sizes were heated by a passing current up to 1300 – 1350 °C, and then cooled in accordance with welding thermal cycles.

Within cooling rates interval 100.0 – 0.3 °C the austenite (A) transformation occurs in a martensitic (M) region. Metallographic examination showed that at $w_{6/5}$ = 100 °C/s the lath marten-

Table 1

Initial state of steel	*Steel thickness, mm*	$\sigma_{0.2}$, *MPa*	σ_t, *MPa*	δ_5, *%*	φ, *%*
Hot-rolled sheets	5	672	798	21.3	63.0
	10	676	845	20.6	55.0
	15	714	872	16.0	46.0
After heat-treatment					
Normalizing at 900 °C, tempering at 580 °C	5	686	868	20.0	53.2
	10	679	870	20.0	50.7
	15	728	915	20.0	50.7
Quenching at 880 °C, tempering at 580 °C	5	984	1053	19.6	62.0
	10	1054	1130	16.0	45.5
	15	1015	1124	17.3	50.8

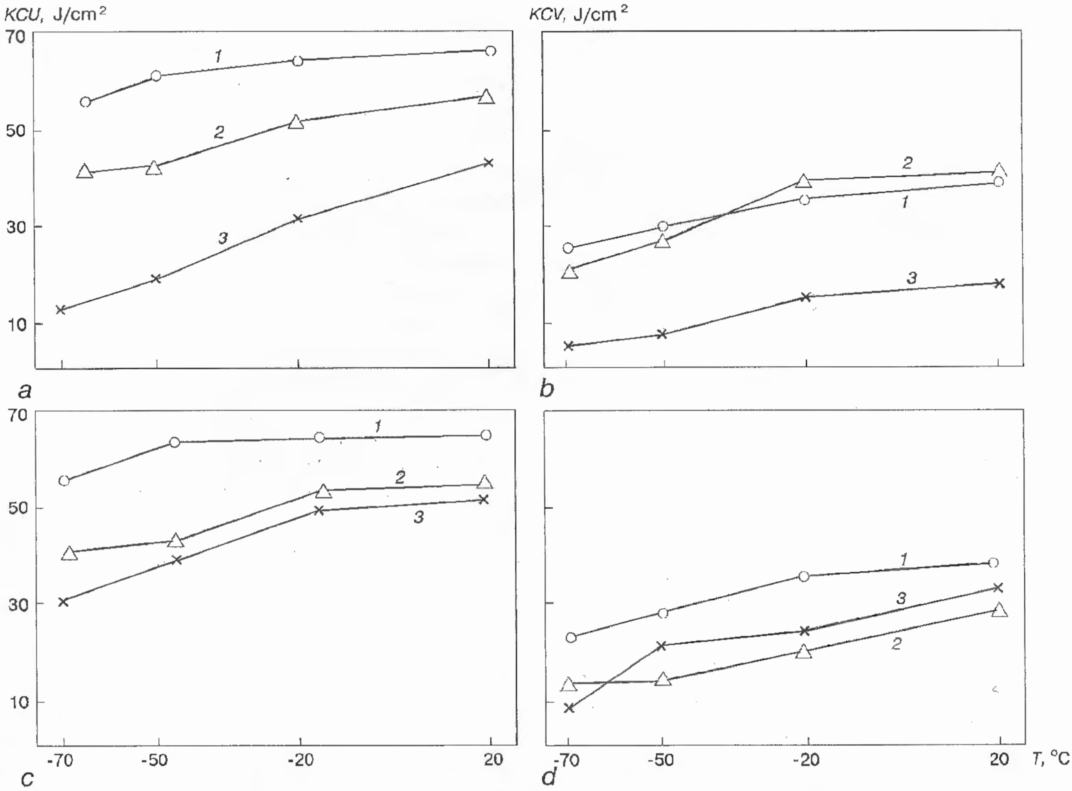

Figure 2. Relationship between the toughness of steel 12KhGN2MFDRA in initial state (*a*, *b*) and after quenching with tempering (*c*, *d*) and test temperature at metal thickness 5 (*1*); 10 (*2*) and 15 (*3*) mm.

sites are oriented to each other under 60° angle, which is typical of a quenching martensite, and also separate regions of a tempering martensite are also observed (Figure 5, *a*). With decrease in cooling rate the width of laths is increased reaching maximum at $w_{6/5}$ = 14.0 – 8.5 °C/s (Figure 5, *b*). In the cooling rates range 100.0 – 8.5 °C/s the temperature of a beginning of the martensite (M_b) transformation is 450 °C, and the hardness of low-carbon martensite is decreased negligibly — from *HV* 375 to 365.

At $w_{6/5}$ = 6.5 °C/s the bainitic (B) transformation is started and at $w_{6/5}$ = 6.0 °C/s its amount in structure is amounted to 6.0 %. With decrease in cooling rate the temperature of beginning the transformation is increased and at $w_{6/5}$ =

Table 2

$h_1 + h_2$, mm	Welding condition			leg, mm	Element	T_{pr}, °C	$t_{6/5}$, s	Cooling rate, °C/s		
	I_w, A	U_a, V	v_w, m/h					$w_{6/5}$	w_{500}	w_{300}
6 + 6	200 – 220	26 – 27	22.2	5.0	Web	20	24.0	7.0	6.25	1.50
						80	34.0	5.1	4.70	1.00
						150	59.0	2.7	2.10	0.80
					Flange	20	11.0	14.3	11.90	5.30
						80	24.0	8.4	6.30	2.50
						150	35.0	5.2	2.50	1.10
10 + 10	200 – 220	26 – 27	10.3	8.9	Web	20	20.0	11.0	9.25	1.90
						80	38.0	5.6	4.50	1.25
						150	56.0	3.3	3.10	0.30
					Flange	20	11.0	16.6	16.00	2.50
						80	18.0	11.0	6.90	1.00
						150	32.0	5.3	3.75	0.60
15 + 6	200 – 220	26 – 27	22.2	5.0	Web	20	8.0	28.0	21.00	7.50
						80	11.0	18.5	15.00	3.75
						150	18.0	12.0	9.20	0.90
					Flange	20	3.5	50.0	46.00	12.50
						80	7.0	32.0	28.30	2.80
						150	8.0	26.0	23.50	1.10

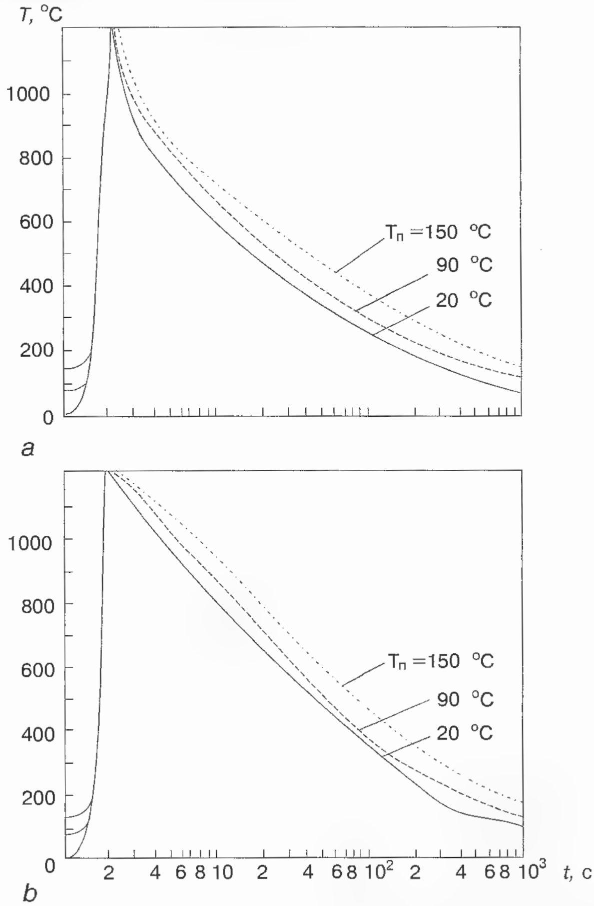

Figure 3. Thermal cycles of heating and cooling of HAZ metal in flange (*a*) and web (*b*) of T-joints of steel 12KhGN2MFDRA of 10 mm thickness in mechanized welding in Ar + Co_2 mixture.

= 0.3 °C/s it is 560 °C. At cooling rates to 1.6 °C/s an acicular structure is preserved that is typical of a lower bainite (Figure 5, *d*).

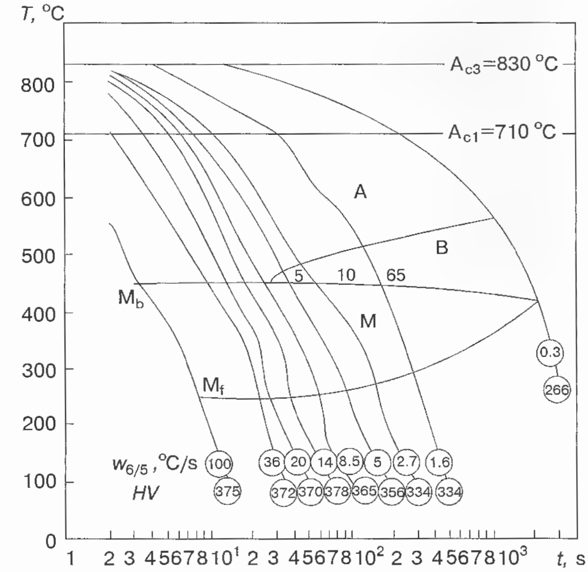

Figure 4. Thermokinetic diagram of decay of austenite of steel 12KhGN2MFDRA.

At $w_{6/5}$ = 0.3 °C/s the region of a martensitic transformation is finished (M_f), only bainitic transformation takes place, the structure has a granular nature (Figure 5, *e*) that is typical of an upper bainite. With decrease of cooling rates from 5.0 to 0.3 °C/s the metal hardness is decreased from *HV* 365 to 266.

In cooling with rate 100.0 – 2.7 °C/s the point M_f is below 300 °C. The further decrease in cooling rate leads to the increase in temperature of an end of the martensitic transformation to 400 °C.

Analysis of thermodynamic diagram indicates that within the range of real conditions of welding steel 12KhGN2MFDRA ($t_{8/5}$ = 7 – 60 s; $w_{6/5}$ = = 1.8 – 25.0 °C/s) the martensitic or martensitic-

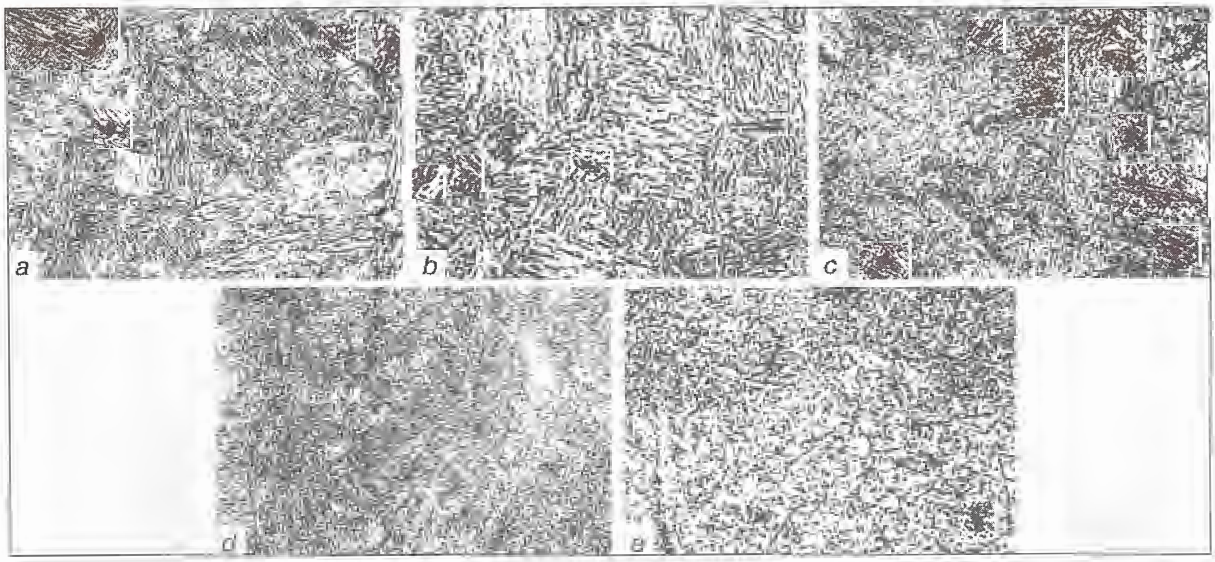

Figure 5. Microstructure of steel 12KhGN2MFDRA in cooling with different rates, °C/s : *a* — 100; *b* — 14; *c* — 5.0; *d* — 1.6; *e* — 0.3 (×320) (reduced by 0.73).

bainitic structure with hardness HV 303 – 370 will be formed in HAZ metal.

This change in structure and hardness of steel 12KhGN2MFDRA under the action of welding cycles may considerably influence the resistance of HAZ metal to a brittle fracture. Taking into account that the width of HAZ in welded joints of high-strength steels does not usually exceed 3 – 4 mm, it is very difficult to perform tests on real specimens. In this connection the HAZ metal resistance to brittle fracture was evaluated using simulation samples which were heated and cooled by a preset cycle in the MSR-75 type installation [3]. In the present investigation the 13×13×150 plates of 12KhGN2MFDRA steel were treated under the following conditions: heating up to temperature 1300 – 1350 °C at 250 – 300 °C/s rate and subsequent cooling at 1.5 – 20.0 °C/s rate ($t_{8/5}$ = 11 – 50 s).

From the specimens-simulators the standard samples of 10×10×55 mm size were manufactured, the Charpy and Mesnager notches were made and then the samples were subjected to impact bend test at temperature –50 °C.

The test results show that with decrease of $w_{6/5}$ from 20.0 to 1.5 °C a monotonous decrease in impact strength of samples with both types of notches is occurred (Figure 6). Samples with V-notch (Charpy type) were most sensitive to the changing in cooling conditions. At $w_{6/5} \le 3.0$ °C/s the impact strength of HAZ metal of the specimens-simulators is decreased below the values obtained in testing specimens of parent metal and regulated by the requirements specified to the welded structures from the service conditions. Probably, this cooling rate can be considered as minimum admissible for 12KhGHN2MFDRA steel to provide the necessary cold resistance of the HAZ metal.

The results of the investigation prove that in welding T-joints of 6 – 10 mm thickness (with equal thicknesses of web and flange) it is rational to limit the temperature of their preheating within 80 – 150 °C to keep the above-mentioned conditions of joint cooling. This technological procedure allows the rate of cooling HAZ metal of flange to be 2.0 – 3.0 times delayed within the 800 – 500 °C interval of temperatures and 4.0 – 4.5 times delayed at 300 °C. This provides not only optimum structures in HAZ metal but also creates the favourable conditions for desorption of diffusive hydrogen from the welded joints, thus contributing to improvement of their resistance to a delayed fracture.

For T-joints with other ratios of thicknesses of web and flange such limitations are not correct, as the selection of optimum conditions of welding (maximum values of cooling, temperature of preheating and other parameters) depends mainly on the necessity of prevention of the delayed fracture of the welded joints.

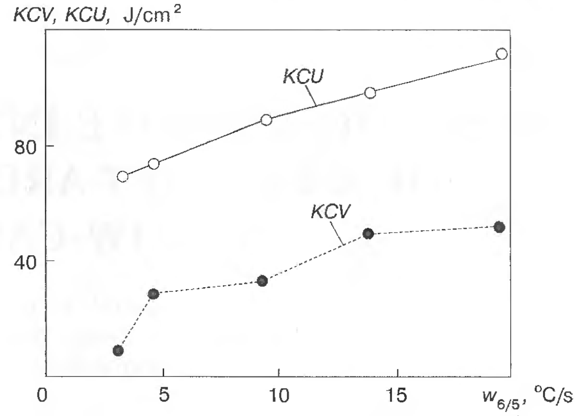

Figure 6. Effect of cooling rates on impact strength of HAZ metal of steel 12KhGN2MFDRA at temperature –50 °C.

CONCLUSIONS

1. Low-carbon alloyed high-strength steel of 12KhGN2MFDRA grade after quenching and tempering meets the requirements specified to it as to the characteristics of strength, ductility and impact strength. However, the investigation carried out testify about instability of properties of steel and a negligible share of a tough constituent in fractures of specimens after the impact bend tests.

2. In welding high-strength steel 12KhGN2MFDRA the rate of cooling of HAZ metal of T-joints ($w_{6/5}$, °C/s) in 6 – 15 mm thicknesses is changed within the rather wide range (from 1.8 to 60.0 °C/s) that can significantly influence the delayed and brittle fracture.

3. Thermokinetic diagram of transformation of austenite of steel 12KhGN2MFDRA during simulation of welding thermal cycles shows that within the cooling rates $w_{6/5}$ = 1.6 – 100.0 °C/s the HAZ metal structure is formed mainly in martensitic, and also in bainitic regions (hardness HV 303 – 375).

4. To provide the required cold resistance of welded joints of steel 12KhGN2MFDRA, the combination of welding conditions and temperatures of preheating should be selected in such a way that the minimum rate of cooling of HAZ metal was not lower than 3.0 °C/s.

REFERENCES

1. Gladshtein, L.I., Bobylyova, L.A., Litvinenko, D.A. *et al.* (1973) Improvement of cold resistance of high-strength structural steel. *Stal*, **6**, 541 – 546.
2. Lobanov, L.M., Mikhoduj, L.I., Gordonny, V.G. (1998) State-of-the-art and prospects of using high-strength steels with an improved weldability in welded structures. *Avtomaticheskaya Svarka*, **12**, 29 – 34.
3. Sarzhevsky, V.A., Sazonov, V.Ya. (1981) Installation of simulation of welding thermal cycles on the base of MSR-75 machines. *Ibid.*, **5**, 69 – 70.

EFFECT OF ADHESIVE INTERLAYER ON FORMATION OF A CONTACT AREA IN SPOT WELDING OF LOW-CARBON STEELS

L.M. LOBANOV[1], **Yu.S. VASILJEV**[1] and **A.N. KUKSIN**[2]
[1]The E.O. Paton Electric Welding Institute, NASU, Kyiv,Ukraine
[2]Institute of Macromolecular Chemistry of NASU, Kyiv, Ukraine

ABSTRACT

Theoretical and experimental investigations of a contact area formation in producing adhesion-welded joints using a resistance spot welding (RSW) of mating surfaces of the parts having a pre-deposited layer of an adhesive with different reological characteristics are presented. A mechanism of influence of a boundary layer of the adhesive on the formation of contact at increasing and decreasing of compression force at the welding machine electrodes has been established. Recommendations are given for the creation of adhesive-bonded compositions having required reological characteristics to produce the adhesion-resistance spot welded joints along the adhesive layer.

Key words: *adhesion, adhesive-bonded compositions, weldbonded joints, resistance welding, boundary friction, developments.*

One of the methods of producing adhesion-welded joints is the resistance spot welding (RSW) on the preliminary deposited layer of an adhesive on the mating surfaces. This method does not impose any limitations to a width of overlapping and some other design-technological parameters of the product, but specifies sufficiently high requirements to the physical and chemical properties of the adhesive.

Polymeric adhesive-bonded compositions both in a solid and liquid state are dielectrics. To perform RSW it is necessary to extrude an adhesive completely from a contact by the time of welding current supply. This requirement should also be fulfilled due to the fact that destruction of the unextruded adhesive disturbs not only a geometric shape of the welded spot and structure of a nugget, but also leads to an intensive evolution of gaseous products, which during escape from an overlap, destroy the continuity of an adhesive layer of the adhesion-welded joint.

This work presents theoretical and experimental investigations of formation of a contact area using adhesives with various reological characteristics. Two successively proceeding stages of the process are considered: 1) extrusion of an adhesive between the parts by the moment of contacting the largest in height roughnesses of their surfaces; 2) formation of a contact area by the moment of interruption of contact between these surfaces under the conditions of a plastic deformation.

The process of extrusion of liquids between the contacting solid surfaces has been studied rather comprehensively at relatively large thicknesses of a layer of viscous media. The quantitative relationships of duration of contacting the surfaces which were confirmed in practice by many researchers and used for a large number of technological recommendations in different branches of engineering have been suggested. Nevertheless, when investigating RSW along the adhesive layer the authors [1] encountered certain difficulties in evaluation of adaptability of different adhesive-bonded compositions. According to the calculations the RSW can be made on the adhesive-bonded compositions of a viscosity of not more than 0.1 Pa·s. At the same time there is a lot of information concerning welding even on paste-like adhesive-bonded compositions of a viscosity of more than 100 Pa·s.

Thus, it was necessary to perform an additional analysis of the process of contacting the surfaces taking into account the following assumptions: 1) as the adhesive cannot move along the weld the adhesive flow occurs from the center of applied compression forces by electrodes to the edges of an overlap (Figure 1); 2) electrode of the welding machine is moved with a constant speed (w) until the moment of contact with parts; 3) surfaces of parts to be welded possess a certain roughness, however, before the contact of roughnesses they can be considered as «mirror high-elastic» planes, because the adhesive makes levelling of the microgeometric profile of a surface and the friction depends on the adhesive viscosity.

The plane flow of the viscous adhesive (for Newton liquids) can be expressed [2] by equations:

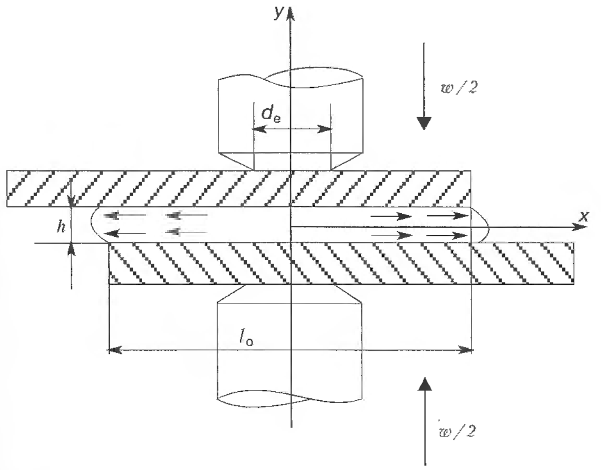

Figure 1. Scheme of adhesive extrusion between the plane parts.

$$\frac{\partial\sigma}{\partial x} + \eta\Delta v_x = 0; \quad \frac{\partial\sigma}{\partial y} + \eta\Delta v_y = 0; \quad \Delta\Delta\psi = 0, \qquad (1)$$

where η is the adhesive viscosity; $\sigma = \frac{\sigma_x + \sigma_y}{2}$ is the mean normal stress; v_x, v_y are the components of liquid flow rate; $\Delta = \frac{\partial^2}{\partial x^2} + \frac{\partial^2}{\partial y^2}$ are the Laplas's operator; ψ is the function of flow determined by ratios

$$\frac{\partial\psi}{\partial y} = v_x; \quad \frac{\partial\psi}{\partial x} = -v_y.$$

As a result of solution of system (1) it was established that for the accepted physical model and boundary conditions there is a critical thickness of an adhesive layer in the process of an adhesive extrusion, at reaching of which the force of compression by electrodes and the resistance of the adhesive layer to the contact of plates are equalized (region I of Figure 2):

$$h_{cr} = \frac{l}{2}\sqrt[3]{\frac{3\eta w d_e l_o^3}{F}},$$

where h_{cr} is the critical thickness of an adhesive layer; w is the rate of contact of electrodes; d_e is the electrode diameter; l_o is the overlap length and F is the force of compression by electrodes.

The further extrusion of the adhesive (region II of Figure 2) occurs at a constancy of the force of compression at the electrodes and decrease in rates of contact of the surfaces. The duration of this stage until the moment of contact of maximum in height roughnesses of surfaces can be calculated from the following formula:

$$t = \frac{3\eta\, d_e\, l_0^3 (h_{cr}^2 - h_b^2)}{16 F h_{cr}^2\, h_b^2},$$

where h_b is the thickness of a boundary adhesive layer.

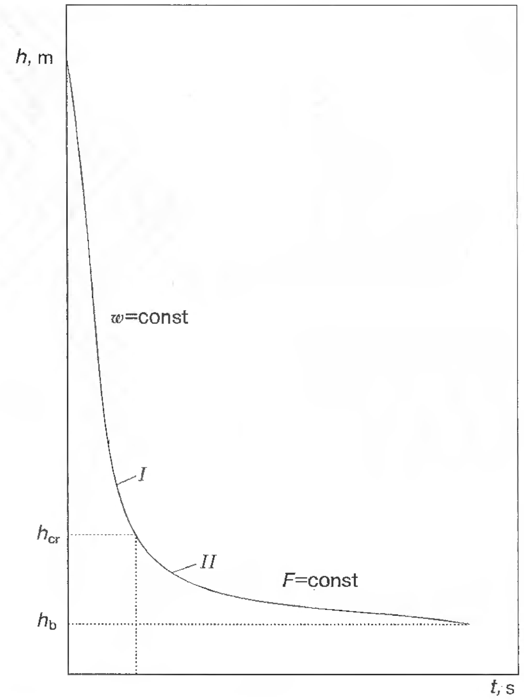

Figure 2. Contact of plates during the adhesive extrusion.

Investigation of reological properties of experimental adhesive-bonded compositions (Figure 3) showed that their viscosity does not almost depend on a shear stress, i.e. the selected polymeric systems are governed by the Newton law of flow and the theoretical relationships obtained can be used for calculation of welding conditions and development of special adhesive-bonded compositions, not preventing the RSW.

For example, at overlap adhesion-welded joint ($l_o = 12\times10^{-3}$ m; $d_e = 4\times10^{-3}$ m; $h_b = 10^{-5}$ m) and a rate of increasing the compression force at the electrodes of 5 kN/s, it is possible to perform RSW along the adhesive of viscosity 80 Pa·s.

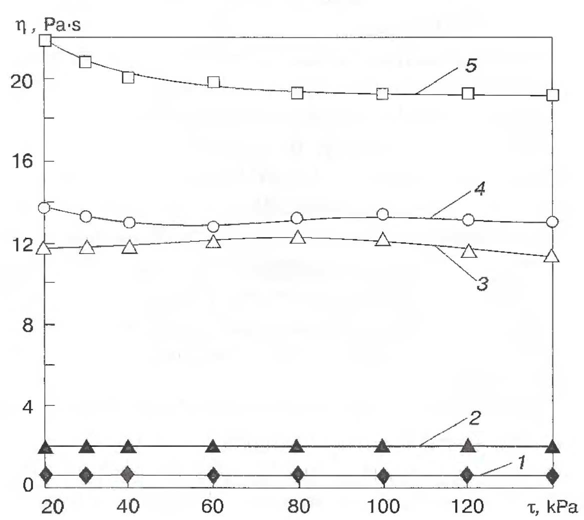

Figure 3. Relationship between the effective viscosity of selected adhesive-bonded compositions and the shear stress (τ): *1* — UG-7; *2* — DEG-1; *3* — ED-20; *4* — «Styk»; *5* — L-19.

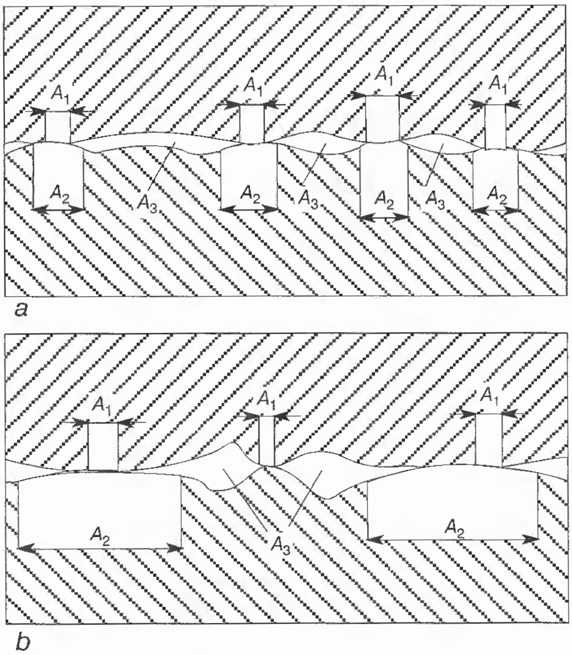

Figure 4. Region of metal-to-metal contact at the presence of an adhesive layer: *a* — initial moment of compression; *b* — moment of stabilizing the contact resistance; A_1 — RAC; A_2 — CAC; A_3 — zone of all-sided compression of adhesive.

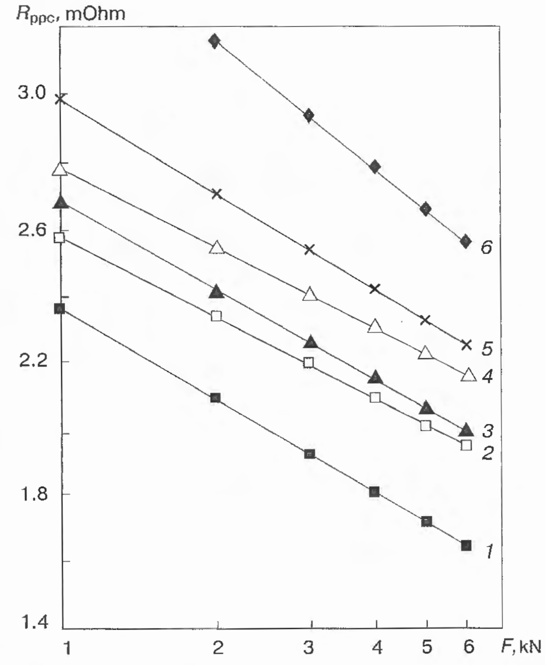

Figure 5. Variation of contact resistance depending on the compression force from electrodes for different adhesive-bonded compositions: *1* — without adhesive; *2* — UG-7; *3* — «Styk»; *4* — ED-20; *5* — L-19; *6* — KLT-30.

The formation of a contact area is peculiar by that the both the metallic contacts and a film of the adhesive are subjected to the loading of compression from electrodes. It should be noted that main laws of taking the load by metallic contacts and a boundary layer are differed not only by a physical nature of forces, but also by a character of dependence of these forces on pressure. A real area of contact (RAC) of metal is increased with a load growth due to the appearance of new spots. Moreover, the mean size of the spot remains almost constant. Such increase in RAC leads to the redistribution of the adhesive in a geometric profile of a contact area and to the formation of zones of a compressed adhesive film in the region of a contoured area of the contact (CAC) (Figure 4).

As is shown in [3], it is necessary to create a specific pressure 80 – 100 MPa for extrusion of polymolecular layers of the adhesive beyond the contact area and compression of a monomolecular layer of CAC with an orientation of the adhesive molecules along the contact surface. Thus, the compression forces from electrodes can be insufficient for the adhesive to flow away completely from the contact area.

Experimental investigation of effect of different adhesive-bonded compositions on the formation of a contact was carried out by the method of measuring the contact resistances. The compression of 0.8 mm thick samples of St.08 steel (rimmed) was made by 4 mm diameter plane-surface electrodes in the welding machine K-242 with an open secondary circuit. The current in a measuring circuit was preset with the help of a DC power source within 3 – 10 A. Voltage drop at the regions of electrode-part, part-part, part-electrode was varied by a digital voltmeter. During measurements the voltmeter was connected in turn to the welding zone regions with the help of a commutator. The commutator switching, voltmeter starting for measurement, record of data of voltage drop and calculation of a contact resistance were realized by a computer.

The results of measurements (Figure 5) show that for the range of selected loading conditions a linear relationship is observed taking logs of the following expression [4]:

$$R_{\text{ppc}} = \frac{r_{\text{cc}}}{F^{\alpha}}, \tag{2}$$

where R_{ppc} is the contact resistance of the part-part; r_{cc} is the «specific» cold contact resistance of the contact and α is the dimensionless coefficient which characterizes the ratio between the pure metallic and nominal surfaces of the contact.

It should be noted that the equation (2) is not regarded similarly. Thus, it is indicated in [5] that there is no regularity in the formula, while in [6] the doubt is shown in its applicability to a wide range of pressures used in RSW, and in [7] the equation is considered to be not applicable, since it does not reflect physical processes taking place in a contact. Nevertheless, the presence of selected adhesive-bonded compositions does not change the mentioned regularity, though leads to the increase in the contact resistance within the whole measured range of compression forces, i.e. the adhesive is not extruded completely from a contact area even at the compression force of 6 kN.

In RSW practice, the parts to be welded are preliminary pressed by electrodes with a forging force, exceeding twice the compression force in welding. The efficiency of this technological procedure is shown in Figure 6, where a certain hysteresis of a contact resistance was observed. This phenomenon was mentioned in [6], however, the presence of the adhesive changes the hysteresis shape. It is known that the recommended conditions of RSW of low-carbon steels create the elasto-plastic conditions of formation of a contact area. Moreover, microroughnesses are deformed plastically and the surfaces are contacted due to deformation of waves in the elastic region. Therefore, during unloading by a definite moment, the RAC and CAC are changed negligibly, i.e. the contact resistance remains almost constant.

The presence of the adhesive changes the mechanism of this process. The elastic constituent of deformation of the surface waves is only a part of energy consumed for the compression of parts by electrodes. The adhesive contained in a closed intercontact space, is also deformed elastically and contributes to the separation of surfaces during unloading. Simultaneously, the adhesive flows from the zone of all-sided compression to the zone of CAC and separates the contact surfaces, thus reducing the electric conductivity.

It follows from the analysis of results obtained that it is not practically rational to use a preliminary pressing for definite adhesives, because when reducing the compression force to a value of the welding force the resistance of a cold contact is increased as if the pressing was not made.

The investigation of kinetics of formation of a contact area was carried out by changing the contact resistance of the welding zone in the process of increasing the compression force at the electrodes of the welding machines ARO-537 and K-242. The results of measurement (Figure 7) make it possible to evaluate the duration of adhesive extrusion by the time of contact of roughnesses (appearance of a signal in the oscillograph) and to observe the nature of formation of a contact area and also the effect of the adhesive on the total resistance of the welding zone R_{eec} (electrode-electrode) by changing the conductivity of contact.

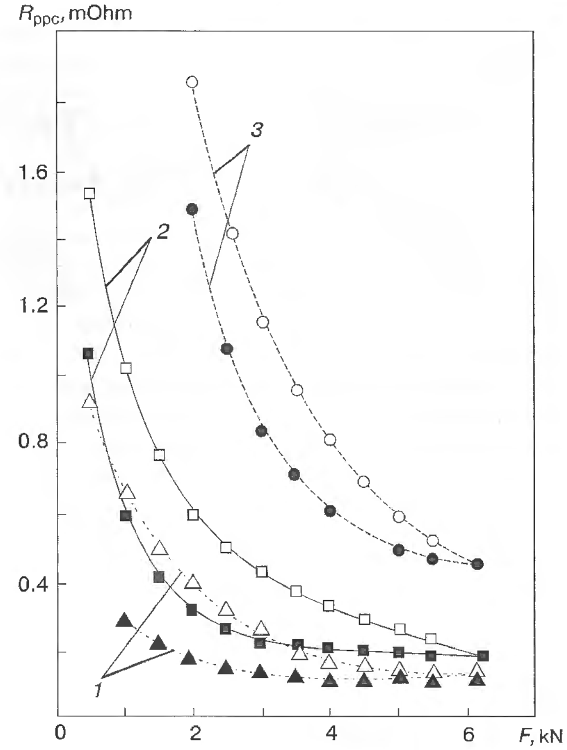

Figure 6. Variation of contact resistance at increasing (○, □, △) and post reduction (●, ■, ▲) of compression force by electrodes for different adhesive-bonded compositions: *1* — without adhesive; *2* — «Styk»; *3* — KLT-30.

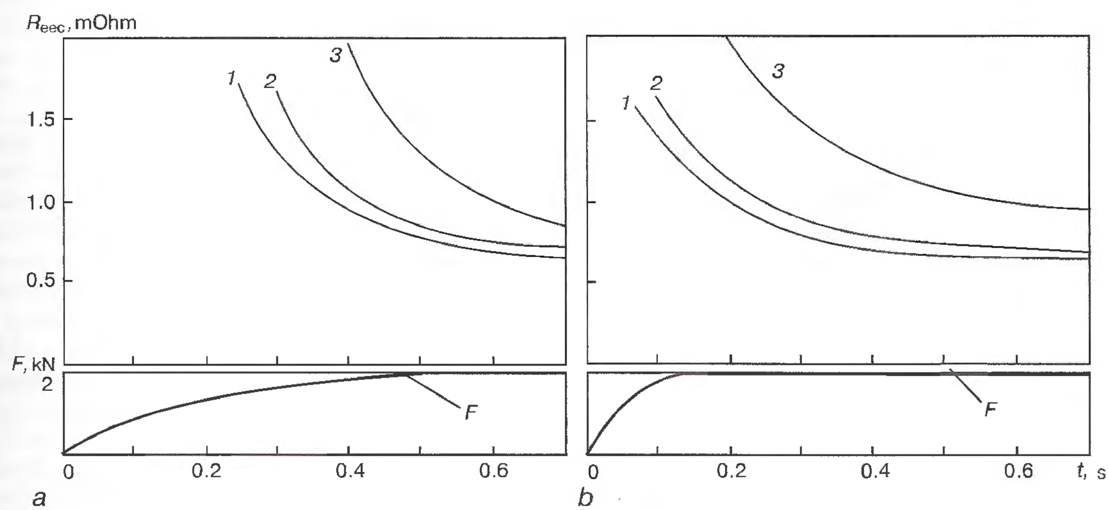

Figure 7. Dynamics of variation of contact resistance in welding using ARO-537 (*a*) and K-242 (*b*) depending on the compression force at different viscosity of the adhesive: *1* — without adhesive; *2* — 10 Pa·s adhesive viscosity; *3* — 60 Pa·s.

In the process of formation of the contact area without an interlayer of adhesive the values R_{eec} for each level of loading are comparable with those stated under the static conditions, i. e. reological processes of deformation and yielding of microroughnesses are proceeding very quickly. The presence of the adhesive of viscosity up to 10 Pa·s does not almost influence the kinetics of formation of the contact area, however R_{eec} is higher than that at the absence of the adhesive. When the adhesive of 40 – 80 Pa·s viscosity is used the process of stabilization of R_{eex} is completed for 0.4 – 0.6 s (Figure 7), i.e. for welding machines with a high rate of compression force increment it is necessary to increase the time before the welding current supply. The use of the adhesives of viscosity of more than 80 Pa·s requires the preliminary pressing using a forging force during 0.5 – 1.0 s.

REFERENCES

1. Shavyrin, V.N., Ryazantsev, V.I. (1981) *Adhesion-welded structures*. Moscow: Mashinostroyeniye.
2. (1973) *Calculation of processes of plastic yielding of metals*. Edited by A.D. Tomlev. Moscow: Nauka.
3. Adamson, A. (1979) *Physical chemistry of surfaces*. Moscow: Mir.
4. Holm, R. (1961) *Electrical contacts*. Moscow: Izdat. Inostr. Literatury.
5. Merl, V. (1962) *Electrical contact*. Moscow: Gosenergoizdat.
6. Orlov, B.D., Dmitriev, B.V., Chakalov, A.A. *et al.* (1975) *Technology and equipment of resistance welding*. Moscow: Mashinostoyeniye.
7. Kochergin, K.A. (1987) *Resistance welding*. Leningrad: Mashinostroyeniye.

OPTIMIZATION OF THE HEAT SOURCE LOCATION IN GLOW-DISCHARGE BONDING

G.P. BOLOTOV
Chernigiv Technological Institute, Chernigiv, Ukraine

ABSTRACT

The method proposed for analytical estimation of the optimal location, with respect to a joint, of the zone affected by the normally distributed heat source, i. e. medium-pressure glow discharge, is based on analysis of distribution of heat flows in parts joined. The method allows the time consumed for pre-production experimental-technological works to be reduced and waste of expensive materials to be avoided.

Key words: *bonding, glow discharge, dissimilar materials, parts of different sizes, heat source location, heating.*

Diffusion bonding is an efficient method for joining parts of simple or complicated shapes made from similar or dissimilar materials. However, joining parts which substantially differ in thermal-physical and geometrical characteristics involves problems associated with a difficulty of producing a uniform temperature field in the parts joined, when they are subjected to surface heating. In turn, this gives no way of producing desirable mechanical properties of the bonds.

This drawback could be eliminated to some extent by heating the parts due to heat generated in a contact plate (located in a gap between the parts to be joined [1]) using heating screens, which are placed between the heat source and the parts to equalize the heat flow coming to them [2], or by heating one of the parts and removing heat by the radiation mechanism from the other part heated from the heat source, the distance between the parts being $(3-5)\times10^{-3}$ m [3].

However, these methods require the use of special fixtures and rather sophisticated clamping devices, which is not always reasonable, especially under conditions of single-unit or repair production, and leads to a much larger consumption of electric power than in direct heating of the parts. Therefore, it seems more advantageous to form the required temperature field in the parts by creating conditions for desirable redistribution of heat flows between them through thermal conductivity of materials of the parts, providing that there is no thermal resistance within the zone of their contact.

The search for methods for equalizing the temperature fields in the parts with substantially differing geometrical and thermal-physical characteristics, primarily near their contact zone, by using a direct glow-discharge heating, was done on a model of the cathode unit of a high-power gas-discharge device. The device comprised (Figure 1) a rather massive molybdenum target 0.03 m in diameter and a water-cooling jacket made from 12Kh18N10T steel with a wall thickness of 0.0028 m. The character of distribution of the current density j in the cathode spot is schematically shown in the Figure.

The glow discharge is a normally distributed heat source which provides the maximum energy release at the centre of the cathode spot located on side surfaces of the parts joined. Therefore, to increase the heating efficiency, the wire anode of the discharge, having the form of a closed loop, is placed in front of the joining zone. However, with this diagram of heating, as shown by the results of measurement of the temperature fields in the parts joined, at a bonding temperature of 1423 – 1473 K for a given pair of metals (Figure 1, point *1*) [4] an overheating of 160 – 180 K occurs in a thin-walled part in a region located at a distance of $(8-10)\times10^{-3}$ m from the joining zone. Heating was

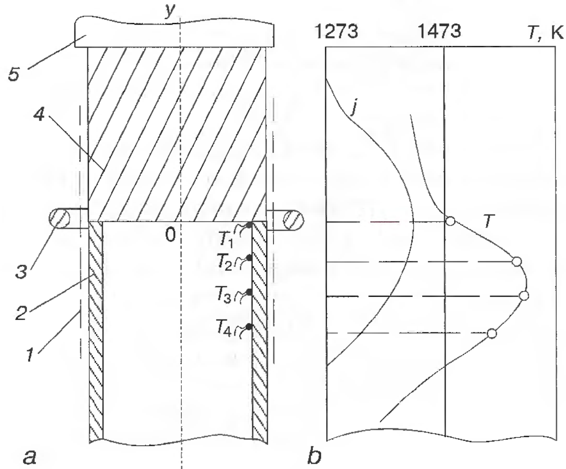

Figure 1. Diagram of measurement (*a*) and character of temperature distribution (*b*) in a workpiece: *1* — cathode spot of the discharge; *2, 4* — parts being joined; *3* — anode; *5* — clamping device; T_1-T_4 — temperature control points. Heating parameters: discharge current 5 A, gas pressure 5.32 kPa.

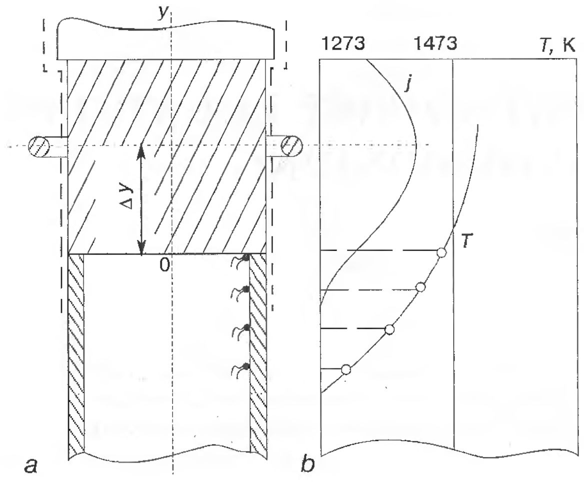

Figure 2. Diagram of measurement (*a*) and character of temperature distribution (*b*) with the heat source shifted along the axis to a distance of Δ_y = 0.023 m from the joint.

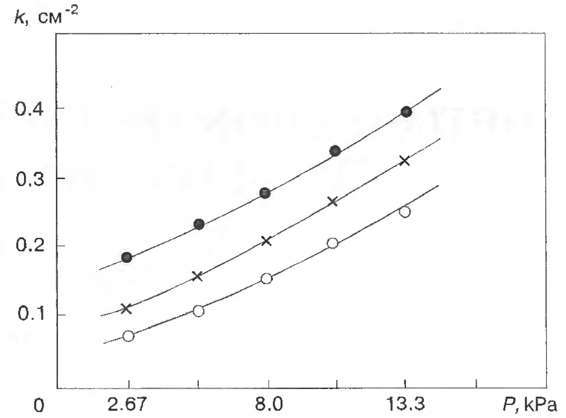

Figure 3. Dependence of the coefficient of concentration of the glow discharge in the cathode spot upon the pressure of argon at discharge current *I*, A: ● – 3; × – 4; ○ – 8.

done in argon under a pressure of 5.32 kPa. Thermal measurements were made using chromel-alumel thermocouples with a spacing of 0.006 m (Figure 1). As the gas pressure in the chamber is decreased to 10.64 kPa, the width of the overheating zone, which stands out sharply against the parts joined, decreases with a simultaneous increase in temperature of 40 – 50 K. In this case the region of the maximum temperatures approaches the bond to a distance of up to $(5-7)\times10^{-3}$ m. A compression force of 4.9 – 9.8 MPa applied to the parts leads to a barrel-shaped distortion of the thin-walled part. Regions of surface melting in the steel part were observed in a number of experiments.

This behaviour in heating the parts differing not only in sizes, but also in thermal-physical characteristics (thermal diffusivity a of molybdenum and steel is 4×10^{-5} and 7×10^{-6} m^2/s, respectively) is well explicable. Overheating can be eliminated by decreasing the discharge power. Nevertheless, the bond will not be formed because of an insufficient thermal activation of the molybdenum part, this being caused by a decrease in temperature of its mating surface.

It seems to be a good practice to heat the molybdenum part to a bonding temperature with a subsequent heat transfer (through thermal conductivity of this part, which is sufficiently high) into the bonding zone and then into the steel part. For this, it is necessary to change location of the heat source with respect to the bonding zone ($y = 0$) by displacing the anode (the glow-discharge axis) upward to a distance of Δ_y (Figure 2). As established by the results of several experiments, under the said heating conditions (see Figure 1) the optimal displacement should be 0.023 m and the sufficiently uniform temperature field is formed near the bonding zone (Figure 2). At the same discharge current but under a gas pressure of 10.64 kPa, the displacement can be decreased to 0.016 m. This seems to be associated with an increase in the discharge concentration coefficient k from 0.13 to 0.28 cm^{-2} (Figure 3).

This problem, as well as many other similar problems which can be handled by the methods of diffusion bonding, could be solved much faster and much more efficient, if it were possible to preliminarily define the required zone affected by the heat source using analytical methods. In order to develop the analytical dependence for the heat source under consideration, it is advisable to make use of the possibility, which was proved in previous investigations [5], of reducing the glow-discharge heating process for the majority of the combinations of parts to a diagram of heating the rod-shaped samples with a fixed plane heat source. In a stationary state, the temperature in the rods, which are affected by this heat source located within their contact zone, will be determined by the following relationship [6]:

$$T = \frac{q}{c\rho F\sqrt{ba}} \exp\left(-\sqrt{by^2/a}\right) = \frac{q}{2F\sqrt{\lambda c\rho b}} \exp\left(-\sqrt{by^2/a}\right), \qquad (1)$$

where q is the heat source power; $c\rho$ is the heat capacity of the materials of the parts per unit volume; λ is the thermal conductivity; F is the cross section area of the parts and b is the thermal diffusivity.

It follows herefrom that the thermal state of the parts being heated is determined by their ability of accumulating heat and providing its transfer to more remote metal layers. The first is characterized by thermal-physical peculiarities of the materials of the parts, such as the $\sqrt{\lambda c\rho}$ parameter, and the second is characterized by their geometrical features in a direction of heat propagation.

With the heat source located symmetrical about the mating surfaces, the temperatures of cross sections of the parts, which are equidistant from the heating zone, will be diffcrent and their relationship, with allowance for formula (1), can be written as follows:

$$\frac{F_1\sqrt{\lambda_1\rho_1 b_1}\,\exp\left(-\sqrt{b_2 y^2/a_2}\right)}{F_2\sqrt{\lambda_2\rho_2 b_2}\,\exp\left(-\sqrt{b_1 y^2/a_1}\right)} = A. \quad (2)$$

As we are interested in the thermal state of the parts in the vicinity of their contact zone, values of exponents in expression (2) approach unity, i.e. they can be cancelled.

Distribution of specific heat flows, q_2, in the cathode spot of the glow discharge obeys the normal law

$$q_2 = q_0 \exp(-ky^2), \quad (3)$$

where q_0 is the heat flow at the discharge axis.

It follows from expression (3) that, in the case of surface heating of the parts using the normally distributed heat source, the thermal effect on the part, i.e. a thin-walled part in this case, can be decreased by shifting the heat source along the axis towards a less massive part to a distance of Δ_y. With this, the heat flows coming to the surfaces of the parts will fit their ability of absorbing the heat. According to Figure 2 and expressions (2) and (3), this can be written as follows:

$$\frac{F_1\sqrt{\lambda_1 c_1\rho_1 b_1}}{F_2\sqrt{\lambda_2 c_2\rho_2 b_2}} = \frac{q_0}{q_0 \exp\left[-k(\Delta_y)^2\right]}, \quad (4)$$

which then can be reduced to the following form:

$$A = \exp\left[k(\Delta_y)^2\right].$$

As a result, the displacement from the heat source axis will be as follows:

$$\Delta_y = \sqrt{|\ln A|/k}. \quad (5)$$

Logarithm in formula (5) is taken to the modulus, as the result of taking the logarithm may also be negative, depending upon the characteristics of the parts joined, which allows the direction of displacement of the heat source along the axis to be determined with respect to the bond.

Displacements Δ_y, calculated from expression (5), for the part under consideration and for the same coefficients of concentration of the discharge as those used in the experiments, are 0.029 and 0.02 m, respectively, i.e. they differ from those obtained experimentally by 19 – 20 %. The experimental validation of the suggested method done on homogeneous cylindrical samples of steel 20 (with the ratio of their cross section areas equal to 1/2) and on dissimilar titanium-steel samples in the form of hollow cylinders (with a diameter of 0.04 m and a homogeneous wall thickness of 0.0025 m) shows that the calculation error in the determination of the optimal location of the heat source is 17 – 21 %. Given that heating affects mostly the part which is characterized by a higher ability of accumulating the heat and in which the temperature gradients cannot be significant, the result obtained can be considered satisfactory and the method can be recommended for practical application.

In particular, this method was employed for the development of the technology for glow-discharge diffusion bonding of magnetostrictive transducers. The latter consist of a stack of plates of iron-cobalt alloy EP-207 (the characteristics of which are deteriorated under conditions of a long-time holding at a temperature which is much higher than Curie point) and a massive waveguide made from steel 45.

In addition, this method can also be utilized to determine the optimal location of the heat source for other welding processes, where heating is done using the normally distributed heat sources. For example, as it was experimentally found, in arc welding of copper-aluminium plate contacts 0.008 – 0.012 m thick [7], the arc should be shifted towards the copper plate to $(4-8)\times10^{-3}$ m to achieve the required melting of both materials joined. According to this method, to set up relationship (2) it is necessary to make use of the calculation diagram based on a linear heat source acting in an infinite plate and the corresponding calculation dependencies given, e.g. in [8]. The calculations made in accordance with (5) at the arc concentration coefficients equal to $k = 3-2$ cm^{-2} yield $\Delta_y = (3.6-6.2)\times10^{-3}$ m, which is in a satisfactory agreement with the experimental results.

The suggested method used for the analytical determination of the optimal zone of action of a normally distributed heat source, such as the glow discharge, with respect to the joint allows the time of the experimental-technological operations that precede the commercial production to be shortened and losses of expensive materials to be decreased. It appears most efficient for diffusion bonding of materials and parts whose geometrical dimensions may be distorted and physical-mechanical properties deteriorated at increased temperatures.

REFERENCES

1. Kochergin, A.K., Shestakov, A.I. (1971) *Pressure bonding of metals with a low degree of distortion*. Leningrad: LDNTP.
2. Kochergin, A.K. (1967) The use of heating screens for diffusion bonding of metals. In: *Bonding in radio electronics and instrument making*. Leningrad: LDNTP.
3. Kvasha, A.N., Medvedev, D.N., Nichushkin, V.V. (1968) Investigation and development of the technology for vacuum diffusion bonding of bimetal inserts in pipings of alloys greatly differing in melting points. In: *Proc. of the V Inter-University Sci. and Techn. Conf. on Vacuum Diffusion Bonding of Metals, Alloys and Non-Metallic Materials*. Moscow: PNILDSV.
4. (1981) *Diffusion bonding of materials*. Handbook. Edited by N.F. Kazakov. Moscow: Mashinostroyeniye.
5. Chernysh, V.P., Bolotov, G.P., Kotelnikov, D.I. *et al.* (1984) Calculation of a heating temperature in glow-discharge diffusion bonding. *Avtomaticheskaya Svarka*, **9**, 54 – 56.
6. Rykalin, N.N. (1951) *Calculation of heat processes in welding*. Moscow: Mashgiz.
7. Rabkin, D.M., Ryabov, V.R., Gurevich, S.M. (1975) *Joining of dissimilar metals*. Kyiv: Tekhnika.
8. (1970) *Theory of welding processes*. Edited by V.V. Frolov. Moscow: Vysshaya Shkola.

PLASMA HARDENING OF SURFACES OF WHEELSET RIDGES

S.V. PETROV[1], **A.G. SAAKOV**[1], **T.G. TARANOVA**[2], **G.M. GRIGORENKO**[2] and **V.A. KOSTIN**[2]
[1]Research and Production Company TOPAS, Kyiv, Ukraine
[2]The E.O. Paton Electric Welding Institute, NASU, Kyiv, Ukraine

ABSTRACT

Surface treatment of steel parts and units with a high-temperature plasma is an efficient, cost-effective and practicable process. Plasma hardening of sliding surfaces of wheels and tyres of railway trains, combined with slow cooling within a temperature range of 800 – 400 °C, leads to an improvement of the quenching structures and increase in the hardened zone sizes.

Key words: *plasma treatment, hardening, quenching structure, microhardness, performance.*

The experience gained in service evidences that reliability of wheels of railway trains has dramatically decreased in the last 15 – 20 years. First of all, it is attributable to increased wear of ridges of wheelsets of locomotives and cars, caused by changes in design of running gears and tracks, as well as by the use of heat treatment and other factors [1, 2].

Service life of the new and repaired parts can be extended by hardening their surface layer. Plasma hardening, which is a relatively recent method, as compared with other surface hardening methods, has passed a serious practical validation in industry. This method is based on the use of a high-temperature plasma to affect the workpiece surface. As a result, hardness of the treated layer increases from 300 to 700 *HV*. Out of all methods of heat treatment involving highly concentrated heat sources, the plasma method is most cost-effective and efficient. It is characterized by reduced costs, affordability of the process equipment and larger sizes of the hardened zone. Plasma treatment provides hardening to a depth of 6 mm. In this case the effective layer has a depth of 1.0 – 3.0 mm. Surface hardness of this layer is 650 – 700 *HV*, which is 30 – 50 points higher than in conventional hardening.

Plasma hardening causes an increase in wear resistance and fatigue strength which is proved by many investigations and examination of the plasma treated surfaces of wheels under actual service conditions [3, 4]. Plasma hardening provides the clean surface, having no traces of oxidation or decarburization.

Data are available on thermal processes occurring in plasma hardening of surfaces of wheelsets [5] and the resulting metal quality [6]. Laboratory investigations into wear resistance and in-service tests indicate that wear of the wheels can be decreased from 2 – 3 to 4 – 6 times [3, 4] through selecting the optimal parameters of hardening. The hardened zone in surface heating using the circular plasma jet has the shape of a segment. The simplest case, which involves no special measures, is the production of the hardened zone with a high-hardness martensitic structure. The transition zone between the hardened layer and base metal in this case is small in size and features a considerable spread of properties [7].

The purpose of this work was to produce the plasma hardened zone with optimal parameters to improve performance of the wheel-rail set.

Samples for investigations were cut out from the hardened wheel surface. Structural state of the hardened surface was investigated using the JEOL scanning electron microscope JSM-840 equipped with a system of the «Link Analytic» and «Ortek» microanalysers. Investigations were conducted in the mode of secondary electrons at an acceleration voltage of U = 20 kV and an electron beam current of $10^{-7} - 10^{-10}$ A. Microhardness was measured with the LECO hardness meter M-400 under a load of 100 g with a spacing of 0.1 mm. Averaging was done over 20 measurements. To reveal microstructure, the samples were subjected to electrolytic etching in the following chemical solution: 20 g oxalic acid per 100 ml distilled water with an addition of a few droplets of sulphuric acid. The etching conditions were as follows: U = 20 V, t = = 15 s. Steel investigated had the following chemical composition, %: C — 0.56; Cr — 0.34; Mn — 0.77; Si — 0.60; V — 0.10; Fe — balance. Microstructure and microhardness were studied on transverse sections of the samples through thickness of the treated layer to the base metal.

The use of the jet of the combustion products plasma spreading along the surface provides the

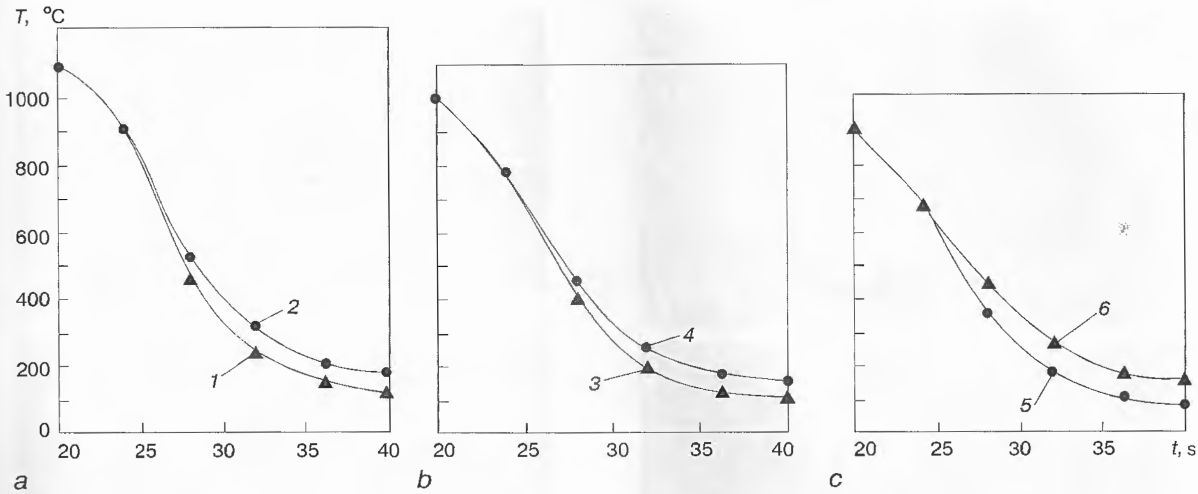

Figure 1. Thermograms of heat treatment of wheels at a stage of cooling depending upon the heating temperature, °C: *a* — 1100; *b* — 1000; *c* — 900; *1* – *6* — sample numbers corresponding to those given in the Table.

surface hardened zone of substantial sizes (25 – 35 mm wide and 2.5 – 3.5 mm deep in a single pass) [7]. Structure of the hardened layer can be controlled by varying the plasmatron working parameters [8].

In this study the authors used actual operating conditions of the plasmatron, which are indicated in the Table below. The Table also gives three modes of heating and cooling for plasma jet hardening. Extra heat treatment of the hardened layer with a thermal cycle as shown in Figure 1 was employed to increase wear resistance of the hardened layer and avoid the negative effect of the stressed state of the transition layer (to decrease the probability of cracking or spalling). The temperature of surface heating was increased from 900 to 1100 °C, i.e. approximately in proportion to an increase in heat input of 30 %. The rate of cooling in the case of heating up to 1100 °C was decreased by 11 %, while in the case of heating up to 900 °C it was decreased by 30 % (Figure 1, *a, b*).

Metallography was done on the samples in accordance with the parameters indicated in the Table [9]. The samples were grouped in pairs and compared. The difference between them was only in the cooling rate. At an accelerated heat treatment

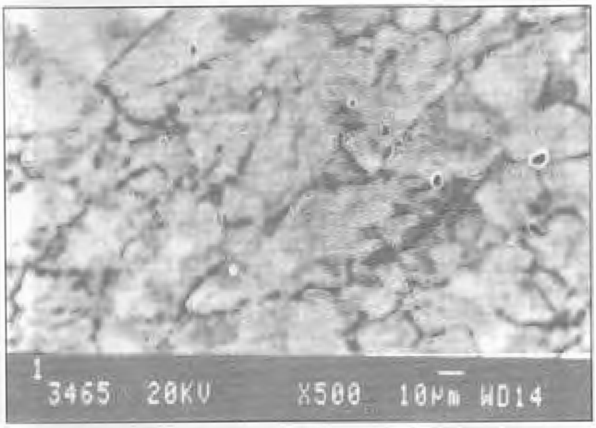

Figure 2. Microstructure of St.60 wheelsets in the as-received condition.

the hardened layer undergoes a number of phase and structural transformations, leading to the formation of the following characteristic zones:

I — the zone of complete recrystallization (heating temperature is above A_{c3});

II — the zone of intercrystalline range (temperatures ranging from A_{c1} to A_{c3});

III — the zone of partial recrystallization;

Parameters of plasma hardening of samples

Mode for a group of samples	*Sample No.*	*Arc current, A*	*Voltage, V*	*Factor of air excess in plasma mixture*	*Extra heating*	*Hardness of surface layer, $HV_{(50)}$*	T_{max}, °C	*Depth of the treated layer, mm*	*Layer width, mm*
I	1	240	210	1.0	–	822	1100	3.00	28
	2	240	210	1.0	+	800	1100	3.25	33
II	3	200	230	0.8	–	750	1000	2.60	30
	4	200	230	0.8	+	705	1000	3.00	32
III	5	200	210	1.0	–	613	900	2.25	27
	6	200	210	1.0	+	550	900	2.25	29

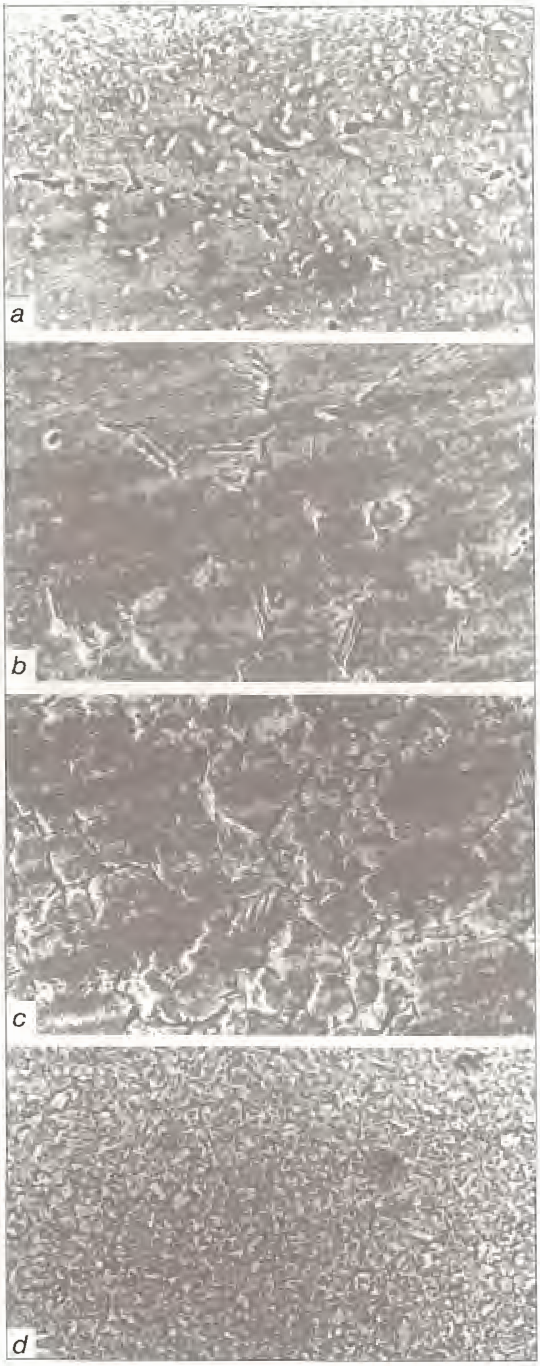

Figure 3. Microstructure of the hardened layer of the samples treated by plasma according to mode I: *a* — zone I, 0.75 mm dia.; *b* — zone II, 0.5 mm dia.; *c* — zone III, 0.5 mm dia.; *d* — zone IV, 1.25 mm dia. (×1000) (reduced by 0.60).

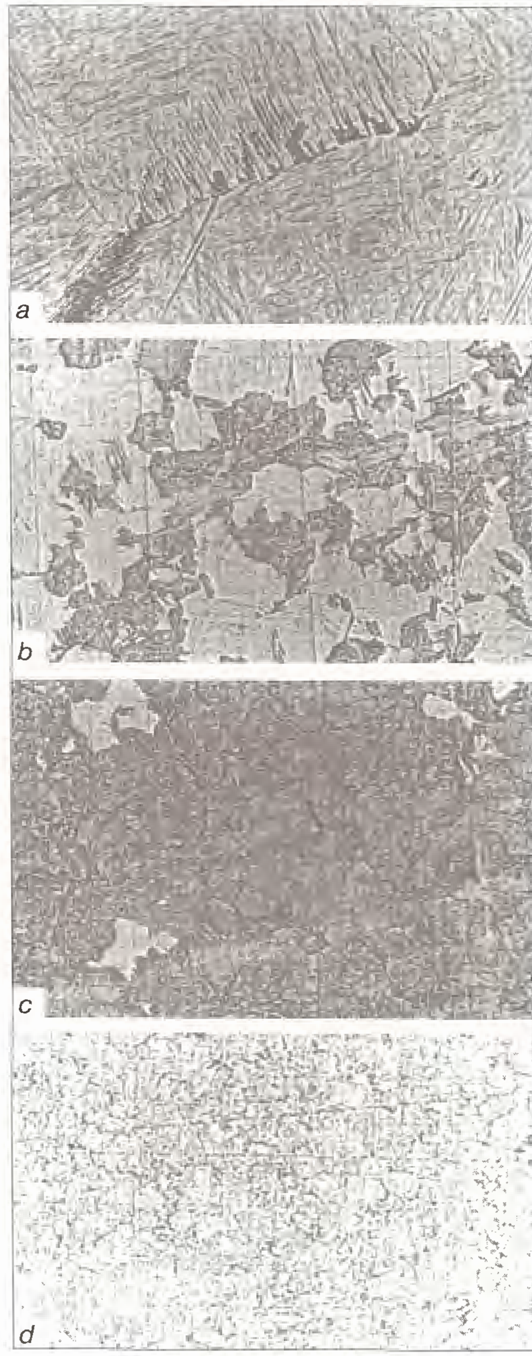

Figure 4. Same as in Figure 3, except for treatment according to mode I using a heating gas (×1000) (reduced by 0.60).

IV — the fine-grained zone (temperatures from A_{c1} and below);

V — the base metal zone.

Structure of the base metal in this steel is a ferritic-pearlitic mixture with an initial grain 30 – 40 μm in size. Its hardness is 270 – 280 *HV* under an indentor load of 50 g (Figure 2). Interlayers of hypoeutectoid ferrite have thickness of 2 – 3 μm and a smooth defect-free (slightly etched) surface. The pearlite colonies are equiaxed, have an average diameter of 5 – 15 μm and a lamina spacing of about 0.15 μm.

Mode I includes samples *1* and *2*, 0.75 mm in size. They were hardened by an accelerated heat treatment at a temperature of above A_{c3}. The width of the hardened layer in sample *1* is 28 mm and in sample *2* — 33 mm. In zone I, the martensitic structure of different types can be formed on the sample surface (Figures 3, *a*; 4, *a*). In sample *1*, the finely dispersed structure consisting of tempered low-

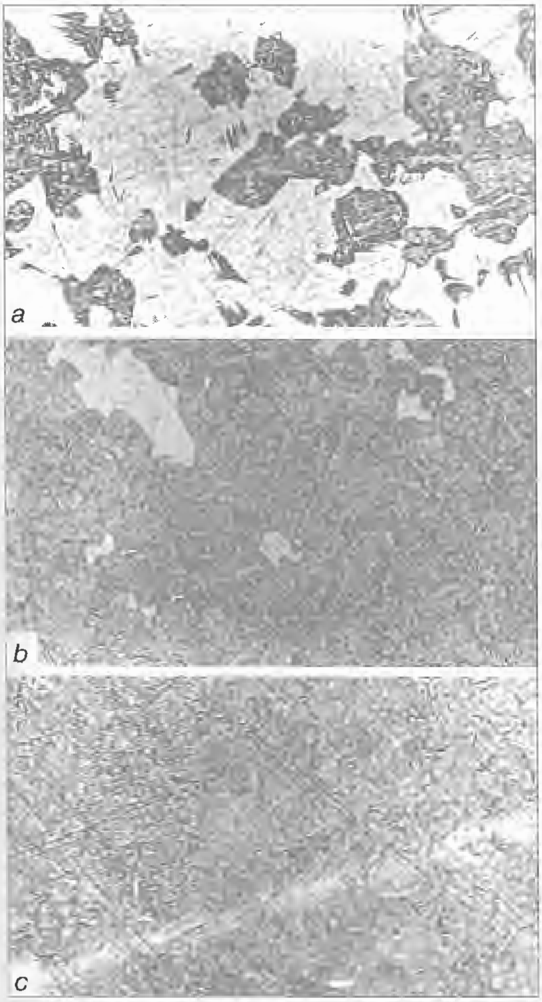

Figure 5. Microstructure of the hardened layer of the samples treated by plasma according to mode III: *a* — zone II, 0.25 mm dia.; *b* — zone III, 0.25 mm dia.; *c* — zone IV, 1.75 mm dia. (×1000) (reduced by 0.60).

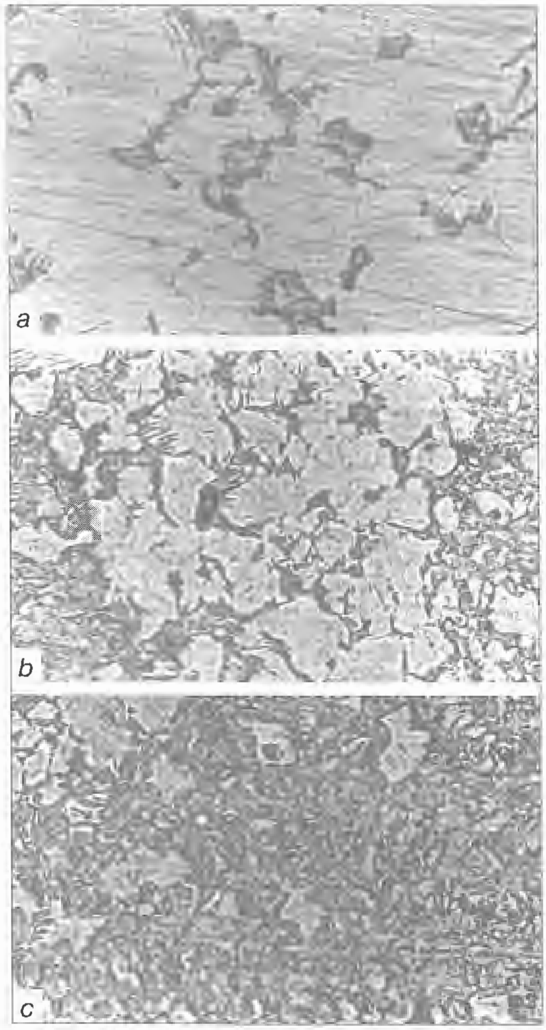

Figure 6. Same as in Figure 3, except for treatment according to mode III using a heating gas (×1000) (reduced by 0.60).

carbon martensite and uniformly distributed redundant carbides (Figure 3, *a*) is formed on the surface 20 μm in size. Microhardness of this structure is 760 – 780 N/mm^2. Boundaries of the fine austenite grains are smeared and martensite stacks are seen, extending from the grain boundaries. Microstructure of sample *2* consists of the equiaxed coarse martensite grains with a high carbon content [10]. The martensite laminae are formed in grains, having needles 2 – 3 μm thick and 7 – 10 μm long, and hardness of 720 – 740 N/mm^2 (Figure 4, *a*). This difference in structure of the given area in samples *1* and *2* is attributable to different cooling rates. In sample *2*, the cooling rate was decreased due to technology factors (see the Table) and its austenite grain was coarser. This sample contains remainders of cementite located along the grain boundaries.

Zone II for this group of the samples is 0.5 mm in size. Sample *1* exhibits clearly defined boundaries of grains 10 – 40 μm in size. The martensite needles extend in the bulk of these grains between the boundaries (Figure 3, *b*), microhardness is much lower and amounts only to 460 N/mm^2.

In sample *2* this zone is characterized by a combination of martensitic and pearlitic transformations — the upper part of this zone is occupied mostly by martensite (light regions), which makes approximately 60 vol.% (Figure 4, *b*), while the dark regions consist of bainite. In transition to zone III, the content of the martensite component decreases through the sample thickness until it forms individual islands, which is caused by redistribution of carbon in austenite. This results in the formation of bainite (Figures 3, *c*; 4, *c*). The size of this region is 0.5 mm, microhardness decreases through the thickness and is 430 – 350 N/mm^2.

Zone IV, which is 1.25 mm in size, has a structure of sorbite. Microstructures shown in Figures 3, *d* and 4, *d* comprise precipitates of finely dispersed carbides in a ferrite matrix. This type of the microstructure is responsible for a microhardness of 300 – 320 N/mm^2. This zone extends into the base metal. Metallography allowed tracing the difference between structural components of this group

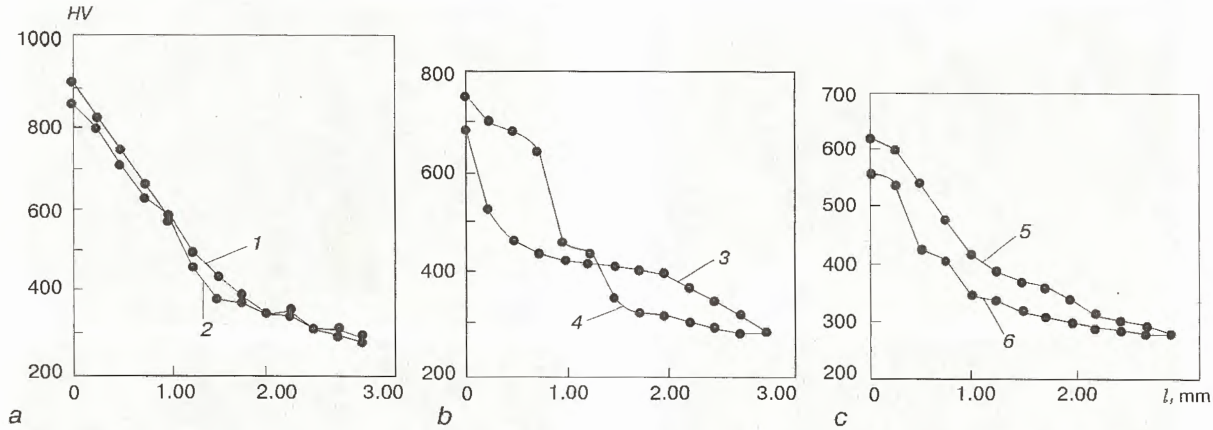

Figure 7. Gradient of microhardness through thickness of the surface layers depending upon the temperature, °C: *a* — 1100; *b* — 1000; *c* — 900; *1* – *6* — sample numbers corresponding to those given in the Table.

of the samples which were subjected to heating and cooling with somewhat different temperature and rate characteristics.

In the second group of the samples (*3, 4*) the heating temperature was 100 °C lower, and microstructure hardly differed from that in the previous group of the samples, except that zone I of martensitic hardening is much narrower and is about 0.1 mm in size.

Microstructure of the layer subjected to plasma hardening according to mode III comprises no zone of complete recrystallization of type I. Zones II and III in samples *5* and *6* are 0.25 mm in size, i.e. they are somewhat different from those in the previous samples. In this case, given that the temperature-time region is wider (Figures 5, *a*; 6, *a*), the microstructure consists of martensite grains of different sizes, as well as of rosette-shaped troostite (bainite). The ratio of these components in zone II is 80 to 20 % in sample *5*, and 60 to 40 % in sample *6* (Figures 5, *a*; 6, *a*). Then a decrease in the martensitic regions is seen in sample *5* and the ratio of the martensite to bainite components becomes 50 to 50 % (Figure 5, *b*). In sample *6* the martensitic regions (Figure 6, *b*) are seen to split into individual islands. In this group of the samples zone IV is larger than in the previous samples and amounts to 1.75 mm. In sample *5*, the microstructure is nonhomogeneous yet and still comprises some insignificant regions with the martensite component (Figure 5, *c*). However, the microstructure in sample *6* is already fully homogeneous and of the sorbite type (Figure 6, *c*). In these samples treated by plasma according to mode III, zones II and III are almost half as large, as compared with the previous samples treated according to the first two modes, while zone IV is 0.5 mm larger and its microstructure is an equiaxed finely dispersed sorbite mixture. Hardness of this group of the samples is substantially lower.

Therefore, the resulting structure is sufficiently homogeneous, has an optimal combination of properties and is characterized by high functional capabilities.

Analysis of peculiarities of structurization of the surface layer of a wheel subjected to plasma hardening indicates to a positive effect of extra heating. Figure 7 shows the microhardness profile which corresponds to the thermal cycle used (see Figure 1), varying in dynamics through the entire thickness, i.e. from surface to base metal. In all the cases the surface hardness decreases and the rate of this decrease through the thickness slows down.

CONCLUSIONS

1. Surface heating using plasma of the air and fuel hydrocarbon gas combustion products is efficient, cost-effective and affordable in technology and equipment. It can be recommended for the use as a method of heat treatment of railway wheels.

2. Plasma hardening of local regions of surfaces of all-rolled wheels and tyres used for repair under the railway car shop conditions provides the surface layer with a hardness ranging from 350 to 780 *HV* to a depth of down to a few millimeters.

3. Microstructure of the layer hardened by plasma treatment is a combination of different structural components. By controlling these components, it is possible to achieve the optimal combination of strength properties.

4. Delayed cooling of the hardened region on the surface within a temperature range of 800 to 400 °C leads to a decrease in the hardness gradient, increase in size of the hardened zone and formation of the homogeneous finely dispersed structure.

REFERENCES

1. Lashko, A.D., Savchuk, O.M. (1997) Strategy of «Ukrzaliznytsya» in solving the problem of avoidance of excessive magnetic wear of the «rail-wheel» set. *Zalizn. Transport Ukrainy*, **2/3**, 2 – 4.
2. Uzlov, I.G., Podolsky, S.E., Perkov, O.N. (1997) Materials science aspects of the problem of the wheel service life. *Ibid.*, 26 – 27.

3. (1998) *«Znamenka» locomotive shed*. Kirovograd: Narodna Osvita.
4. Lashko, A.D., Petrov, S.V., Saakov, A.G. (1997) Surface plasma hardening of wheelsets. *Zalizn. Transport Ukrainy*, **2/3**, 22 – 25.
5. Kolesnik, V.V., Orlik, V.N., Petrov, S.V. *et al.* (1998) Investigation of thermal phenomena in surface plasma hardening of wheelsets. *Ibid.*, **1**, 77 – 82.
6. Petrov, S.V., Saakov, A.G., Grigorenko, G.M. *et al.* (1998) Microstructural peculiarities of surface layers of steel treated by plasma. *Problemy Spets. Electrometallurgii*, **2**, 31 – 34.
7. Petrov, S.V., Saakov, A.G. (1997) Plasma surface hardening of wheelsets. In: *Proc. of XI Int. Conf. on Surface Modification Technologies,* Paris, Sept. 8 – 10. Bharboroujy: MTPT.
8. Kolesnik, V.V., Orlik, V.N., Petrov, S.V. *et al.* (1998) Prediction of properties of plasm hardened surface layers of steel. In: *Advanced equipment and technology in machine building, instrument making and welding.* Kyiv: KPI.
9. (1988) *Theory of welding processes*. Edited by V.V. Frolov. Moscow: Vysshaya Shkola.
10. Shorshorov, M.Kh. (1965) *Metals science of welding of steel and titanium alloys*. Moscow: Nauka.

«UKRNIIPROEKTSTALKONSTRUKTSIA» INSTITUTE – ITS PAST, PRESENT AND FUTURE

V.N. SHIMANOVSKII
Corresp. Member of the NAS of Ukraine, academician of the Academy of Construction of Ukraine, Kyiv, Ukraine

In 1944 the USSR People's Commissariat on Construction issued an order to approve setting up a network of self-financing organisations on design, fabrication and mounting of metal structures, including the Special Design Bureau No. 3 in Kyiv, having its own balance, as part of the Proekstalkonstruktsia trust. This way, more than 50 years ago the foundations were laid down of an organisation specializing in design of building metal structures, which has now become the leading in Ukraine research and design Ukrniiproektstalkonstrutsia Institute capable of solving at a high technical level the issues of development and improvement of metal structures in an integrated manner, together with their fabrication and mounting.

In the initial period the main task of the Design Bureau was development of designs for restoration of the bridges, industrial facilities and other constructions in Ukraine, destroyed during the years of the World War II. Designs have been developed for restoration of blown-up bridges across the rivers Dnestr in Zaleshchiki, Yuzhnyi Bug in Pervomaisk and Vinnitsa, of a railway bridge in Kyiv, of mine head-frames in Donbass, of shops of metallurgical, cake and by-product processing and mechanical engineering plants in the cities of Donetsk, Krivoi Rog, Makeevka, Enakievo, Lisichansk, Kharkov, Nikolaev, etc. The core of leading experts at that time was made up by building engineers – war veterans.

Formation of the Bureau as a specialised design organisation was promoted by a government assignment to design the Navodnitskii bridge across the Dnieper river in Kyiv (now E.O. Paton bridge), which was performed in close creative co-operation with the Electric Welding Institute and directly with academician E.O. Paton. He initiated development of a variant of all-welded frameworks of a bridge with application of solid-wall primary trusses. It was decided to study and jointly find a solution for a new design of a bridge, welded joints of the primary trusses, joining of transverse elements, ties, bridge roadway with provision of a high reliability and fatigue life. With this purpose calculations and theoretical studies were performed, and the variants of welded joint and component design were verified experimentally. The field welded joints of solid-wall primary trusses and the machine for their automatic welding were developed for the first time, and killed, easily weldable steel for all-welded bridge frameworks was proposed.

The approach, in which development of welded components and joints providing reliable operation at below zero temperatures, dynamic and cyclic loads on critical structures, is based on the results of the theoretical and experimental investigations of advanced designs of welded structures, became a tradition in the practical work performed by Proektstalkonstruktsia.

Among other bridge constructions, note the suspension bridge across the Dnieper river to the Trukhanov island in Kyiv (180 m span); the first rope bridge across the bay in Kyiv (144 m span); all-welded bridge across the river Smotrich in Kamenets-Podolsk (150 m span), built for the first time using high-strength steel and with orthotropic plate of the roadway; suspension bridge across the Teterev river in the city of Zhitomir (with 160 m main span and 62 and 75 m bank spans) and an original pedestrian suspension bridge 102 m long across the Uzh river in the town of Korosten, with one pylon. Later on, bridges on a curve in plane with a lighter-weight orthotropic plate (bridge across the forebay, flyover above the locks) and ingenious console design of anchorage in the dam body were constructed on the Dneproges dam, thus widening the passage two times

Organisational and structural changes were made in the 50 – 60s. In 1953 the Bureau was reorganised into a design office and in 1960 into Ukrproektstalkonstruktsia State Design Institute. The engineering and technical potential of the Institute also increased considerably. A team of graduates of the civil engineering colleges of the country joined the Institute staff. Among them were the future chief project engineers and department heads. The Institute staff increased up to 400 people, branches were opened in Kharkov, Donetsk, Mariupol, Lugansk, and later in Poltava and Odessa. The Institute developed projects of any level of complexity, the range of its activity was continuously expanding. A major success of engineering work of Ukrproektstalkonstruktsia was construction of very tall all-welded TV towers in the USSR cities. New designs of high-rise constructions adaptable to fabrication and mounting were developed in co-operation with PWI. The regular flange joints leading to excess consumption of steel and great labour consumption, were replaced by welded joints of elements. The first all-welded TV tower of 317 m height of our design and under author's supervision together with PWI was constructed in Leningrad, followed by original designs of TV towers in Erevan and Tbilisi. Construction of the most advanced design of the TV tower in Kyiv, built by the incremental method with automatic welding of tubular chords from a high-strength steel, was marked by a State Award of Ukraine. The staff members of the Institute were among the prize winners.

A prominent place in the Institute's activity is taken up by design of industrial facilities and constructions. The large ship-assembly shop of Leninskaya Kuznitsa Works and mechanical shops of Bolshevik Works in Kyiv, shops of metallurgical works in Donetsk, Makeevka, Dneprodzerzhinsk, Mariupol and other industrial centers of Ukraine were built from the designs developed by the Institute. The scope of design of high-rise communication facilities, power transmission line supports, special sheet structures (water towers, air heaters, gasholders, tanks) became wider.

The scientific-technical potential incremented for many years, the gained experience and high level of qualifications of its specialists enabled the Institute to extend its activity to other USSR republics and foreign countries and to become established as a leading design organisation in the field of metal structures. The Institute was active in design and construction of such large-sized and complicated metallurgical works as Novo-Lipetsk, Orsk-Khalilovsk, Rustav, Sarkanais Metalurgs, as well as in Korea, China, Pakistan, Hungary, India, Bulgaria, Algiers, Nigeria, and other countries. Special mention should be made of design of critical steel structures of buildings with large spans such as the Large high-voltage hall in Zaporozhje (60 m span, 60 m height), some of the largest assembly shops in Feodosia (96 m span, 50 m height, with up to 200 t rated load capacity hoists) and in the shipyard in Nikolaev (two spans of 48 m, 45 m height), hangar buildings with 48 to 136 m spans in Borispol, Donetsk, Nikolaev, Sheremetjevo, Vnukovo, Kuibyshev, Yakutsk, Magadan. A large hangar building with 108 m span was designed and built in Cuba.

As designer general of the plants for fabrication of metal structures, the Institute was continuously working on improvement of the production technology. Our designs were used for reconstruction and construction of I.V. Babushkin Metal Structure Plant (MSP) in Dnepropetrovsk; Mariupol, Zaporozhje, Nikolaev MSP, Zhitomir Plant of Enclosure Structures and Zhitomir MSP, Kamenets-Podolsk Light Metal Structure Plant, as well as in Russia in Shadrinsk, Bataisk, Vyksun, Novokuznetsk MSP. The only in Ukraine aluminium metal structures plant in Brovary was built by the Institute's design.

The design and construction of the Large high-voltage hall in Zaporozhje, shops of cold and hot rolling of carbon steels in Novo-Lipetsk Metallurgical Works, as well as reconstruction of the plant of radial drilling machines in Odessa were rewarded by USSR Soviet of Ministers Prizes, whose winners were some of our staff members.

Alongside the production facilities, the Institute also participated in designing the metal structures of large civil buildings such as «Ukraine» Palace with the large-span roofing in the form of a system of crossgirders, «Kyiv» hotel, House of Commerce, V.I.Vernadskii National Library of Ukraine, Opera Houses in Kharkov and Kyiv, «Ukrainian house» (former Lenin Museum). The work on design and construction of the Motherland sculpture of the Great Patriotic War Museum in Kyiv was very complicated. For development of the latter two designs the Institute's specialists received high government awards of Ukraine and the USSR.

A new stage in the Institute's development was its re-organising in 1983 into a design and research institute. The USSR State Committee on Science and Technology made the Institute the principal organisation on the highly urgent issue of renewal of buildings and facilities. A group of talented scientists in the field of structural mechanics and investigation of metal structures design joined the Institute. Investigations related to scientific problems of designing structure, buildings and constructions, enabled the Institute's staff members to receive academic titles. The staff increased up to 900 people.

In the middle of the 80s the problem of reconstruction of the existing buildings and constructions became one of the main areas of the scientific activity of the Institute, in connection with equipment renewal and changes in the technology. The urgency of the problem was determined by a considerable lagging behind in improvement and development of new technologies, need for restructuring the industry, as well as failures and accidents of the load-carrying metal structures which became more frequent as a result of wear of the capital assets. In order to solve this problem and perform the work, the Institute formed teams for in site technical inspections of the existing structures, theoretical analysis and development of reinforcement of the load-carrying structures. With changes in the technological process, increase of the rated load capacity of cranes and other equipment, the problem of reinforcement of the building frame, reinforcement or replacement of the crane rail track structures was addressed. It was often necessary to solve the problem of increasing the height with raising of the existing roofing structures in keeping with the new technological requirements and overall dimensions of the equipment. Here, the problem of reconstruction was solved without interruption of production, which called for an integrated design allowing for the technology and sequence of construction-erection work. The norms and standards were improved with active participation of the Institute's experts. Sections 20* of SNiP II-23–81, «Additional requirements to design of structures of buildings and facilities in reconstruction» and a manual to complement SNiP on design of steel structure reinforcement were developed.

Development and study of new types of designs of buildings and constructions became a different, but not less important scientific field of the Institute's activity. An integrated R&D unit with research facilities was formed which focused on development of advanced designs of buildings from light-weight metal structures characterised by high adaptability to fabrication and mounting, material saving, better aesthetic features. In particular, new types of unified roofing for buildings were developed based on panel-strut frame systems with few elements and a wide use of sheet membranes, whose characteristics were much superior to those of the existing ones, thus opening up new possibilities for effective development of the industry of Ukraine in the field of light-weight metal structures.

In order to try out the critical components, as well as test the full-scale samples of structures in development of complex constructions, bridges, specialised facilities, large industrial and civil buildings, as well as new designs, the Institute built well-equipped experimental facilities with 7000 m^2 production area. Among the most important fields of the Institute's activity are expert evaluation of the metal structure designs and of the existing metal structures of the entire range of buildings and constructions, methods of reinforcement of building structures, renewal and re-equipment of enterprises, functions of the leading center of certification of building products in the field of metal structures. As author of «Ukrytie» («Sarcophagus») project, the Institute took part in the programs of localising the consequences of the accident in the Chernobyl NPP and turning «Ukrytie-1» into an ecologically-safe object.

The Institute is solving with success the problem of design and research automation. At one time it was a pioneer in «mechanising» calculations in structural design. The then developed principles of programming the engineering calculations in key-operated automatic machines were used at the Institute for some time starting from 1959 and for programming of the first computers. To-day the Institute uses the most advanced computers allowing more effective automation of the design computational and graphic operations and other areas of the Institute's activity. The software packages developed by the Institute's experts, namely OSKAR, PARSEK, SUDM, SETI, PROMET are widely used.

More than 300 author's certificates and patents for inventions in the field of advanced engineering solutions are an indication of the high technical level of the Institute's developments, and creative activity of its specialists. The scientists and engineers of the Institute published more than 400 papers and reports, 30 monographs, with more than 45 monographs written with participation of the Institute's staff or using the material of its design and research work. For the significant contribution into introduction of the scientific achievements into production and training of scientists, the Institute's director V.N. Shimanovskii, Corresp. Member of the NAS of Ukraine, received the Honorary diploma of the Presidium of the Supreme Soviet of Ukraine. In 1994 he was awarded the State Prize of Ukraine for «Theory of design of spatial structures for static and dynamic loading» series of publications. More than 40 staff members received high government awards during the years of existence of the Institute.

Thus, during the 55 years of its activity the Kyiv Proektstalkonstruktsia has developed into a large highly efficient research and development institute, leading in Ukraine and known abroad. The former USSR Gosstroi organisation included only two research institutes of the first USSR grade in terms of salary level, namely Melnikov TsNiiproektstalkonstruktsia in Moscow and Ukrniiproektstalkonstruktsia in Kyiv. To-day only one research and design institute of steel structures — Ukrniiproektstalkonstruktsia is functioning in the building industry of Ukraine, which is capable of conducting a common technical policy in the field of metal fabrication.

The restructuring begun in the Soviet Union, followed by its disintegration, Ukraine gaining its independence, drifting towards market economy and the wish to join the European Union — all this poses new tasks and problems for the Institute. The main fields of its activity are influenced by participation in elaboration of recommendations for the government bodies as regards overcoming the economic crisis by the industry and the country as a whole. The Institute was one of the initiators of the Cabinet of Ministers of Ukraine passing the resolutions of 05.05.1997 No. 409 on «Provision of reliability and safe service of buildings, constructions and utilities» and of 08.09.1997 No. 985 on «Elimination of the critical situation in the motor-road bridge on the Dneproges dam», of setting up the Interdepartamental Scientific-Technical Council on reliability and safe service of buildings, constructions and utilities. Together with the Zaporozhje city administration and Kharkov Hidroproekt the Institute is working under a program to eliminate the critical situation in the motor-road bridge of Dneproges. Work is being conducted to elaborate the construction codes and them harmonize with the world and European codes.

Considerable changes have taken place in the form of the Institute's property. In keeping with «On corporatisation of enterprises» Act No. 210 of 15.06.1993 of the President of Ukraine the Institute was transformed into an open stock-company, whose founder was the Ukrmontazhspetsstroi State Corporation.

Despite the difficulties due to restructuring, the Institute managed to retain the highly-qualified experts and continues playing its leading role in the field of building metal structures. Its financial position is stable. In the rating of research organisations the Institute, by the decision of the Government Commission on certification of the industrial research organisations, was classified in category A of those which should be supported by the state, was included into the list of research organisations which are of a strategic importance for the economy and safety of the country (Act of 21.03.1997 No. 991 of the Cabinet of Ministers of Ukraine) and of enterprises having a monopoly in the national market (Decision of the Antimonopoly Committee of Ukraine of 18.02.1997 No. 38-r). The Institute put in a lot of effort to stay together as a collective and retain its property, as in the intensive process of privatisation and together with it, the Institute could have been lost more than once already for all its «strategic importance for the economy and safety of the country». The Institute was accorded the 1997 International Honour — «Diploma of Achievement» for success in retaining the intellectual potential and personnel under the conditions of transition economy. In 1997 the Institute received the «Commercial Prestige» prize of the World Market International Journal, and in 1998 the Great Golden Prize for fruitful activity in the field of construction and world recognition of its achievements. The author of these lines believes that the diploma received by him in recognition of his scientific achievement and efficient management and the Honorary Diploma «Man of the Year 1997» of the International Committee on Scientific Achievement of the American Biographical Institute granted him as a man of science who has contributed to the world community and his field, also rightfully belong to the Ukrniiproektstalkonstruktsia.

The Institute has compiled a data base of the designed facilities which form a considerable industrial and defence potential of Ukraine, CIS countries, some other countries of Europe, America and Asia. It contains more than 15 thousand constructions, including the designs of road flyovers, hangars for repair of flying vehicles, general layouts of plants for fabrication of steel and aluminium structures, etc. The importance of this base is growing with time, as a considerable part of metal structures have aged physically and morally and require certain measures for maintaining them in the working condition (on the whole, by the data of the Institute, more than 130 mln. t of building metal structures are in service in FSU territory, of which one fourth are in Ukraine).

The Institute is open to co-operation in all the fields of its activity. With the beginning of the growth of production in the key sectors of the national economy, the role of the Institute as a leading research and design institution should be enhanced in connection with such tasks of national importance as reconstruction in ferrous metallurgy and coal mining industry using advanced ecologically safe technologies, construction of Trans-European transport lanes, prospecting and local production of oil and gas, in particular, in the shelf, participation in international projects on processing and transportation of products, ecologically safe power engineering, and space research.

SETTING UP COMMERCIAL PRODUCTION OF THE Sv-08Kh20N9G7T WELDING WIRE AT DNEPROSPETSSTAL

K.A. YUSHCHENKO[1], L.V. CHEKOTILO[1], Yu.N. KAKHOVSKY[1], V.G. GORDONNY[1], V.M. KIRIAKOV[1], A.V. KLAPATYUK[1], V.A. LEIBENZON[2], V.N. KRENDELYOV[2], V.G. KNOKHIN[2], S.B. KALASHNIK[2] and V.Ya. BRIGIDIN[3]

[1]The E.O. Paton Electric Welding Institute, NASU, Kyiv, Ukraine
[2]Open Stock-Holding Company Dneprospetsstal, Zaporizhzhya, Ukraine
[3]State Company V.A. Malyshev Works, Kharkiv, Ukraine

ABSTRACT

Results of setting up the production of the Sv-08Kh20N9G7T grade wire with a diameter of 2–5 mm by Dneprospetsstal are presented. The wire is shown to provide high welding-technological properties of the joints, meeting requirements of the transport engineering standards. The wire is delivered according to TU 14-143-506–98 and GOST 2246–70.

Key words: *welding, steel making, casting, forging, rolling, high-strength quenching steels, high-alloy welding wire, spattering, tear cracks, mechanical properties.*

High-strength alloyed steels find an increasingly wide application in engineering [1]. There is a special group among these materials which includes high-strength structural quenching steels. These steels have a carbon content of 0.30 – 0.45 % and are alloyed with chromium, nickel, molybdenum, copper, manganese, vanadium, silicon, boron and other elements. In particular, this group includes steels of such grades as 30KhN2MFA, 45Kh3N3M, 38KhN3MFA, 30KhGSNA, 30Kh2N2M, 30KhN4MD, etc. [2 – 4].

In addition to typical defects, such as pores and solidification hot cracks, fusion welding of steels belonging to this group can result in the formation of cold quenching cracks in the weld metal and tear cracks in the heat-affected zone of the base metal [4, 5].

The risk of their formation increases in welding restrained (non-compliant) pieces of steels of increased thicknesses. In the cases where the requirement of providing welded joints with strength equal to that of the base metal is not essential, these steels are welded using wires of the austenitic grade. The wire most commonly used for these purposes is that of the Sv-08Kh20N9G7T grade. This wire was developed by the E.O. Paton Electric Welding Institute in the 1950s.

Until recently the Sv-08Kh20N9G7T grade wire has been produced in Russia. Then, as Ukraine had to start up its own production and because of other circumstances Dneprospetsstal* carried out comprehensive investigations aimed at improvement of welding-technological properties of this wire. New high-strength quenching steels have been developed and found its way into commercial application in the last decades. Welding such steels imposes increased requirements for the quality of the welding wire.

The investigations conducted by PWI with participation of Dneprospetsstal and some industrial customers resulted in refining chemical and phase composition of the Sv-08Kh20N9G7T wire, development of the technology for steel making and refining, as well as testing the commercial batches of the wire at the customers'. Delivery of the wire is done in compliance with TU 14-143-506–98 and GOST 2246–70.

Based on new requirements, Dneprospetsstal melted Sv-08Kh20N9G7T steel in 30 t electric-arc furnaces and cast it into 1 t round ingots. The ingots were forged by the advanced method using the RKM-1000 type radial-forging machines first into squares 180×180 mm in size, and then using the second RKM-340 type machine — into squares 95× × 95 mm in size. Wire rods 8 mm in diameter were made using the small-section mill of the 200 type. Drawing the wire was done with the single-stand mills with of the 1/700 and 1/550 types.

* In 1996 – 1998 Dneprospetsstal also started up the production of welding wires of the Sv-04Kh19N9 and Sv-04Kh19N11M3 grades with a diameter ranging from 2 to 5 mm [6, 7].

Table 1. Results of comparative tests of the Sv-08Kh20N9G7T welding wire to hot crack resistance of the weld metal

Welding method	*Welding consumable, manufacturer*	*Welding procedure*	*Evaluation criterion*	
			Maximum rate of bending a sample until a hot crack is formed in weld metal, mm/min	*Maximum welding current until a hot crack is formed in weld metal, A*
Mechanized CO_2	Sv-08Kh20N9G7T wire, 2 mm dia., heat No.145991, Dneprospetsstal	Welding the 1st bead into a groove	–	380
		Welding by bending a sample	9.5	–
Automatic submerged-arc using AN-22 flux	Same	Welding the 1st bead into a groove	–	420
		Welding by bending a sample	11.0	–
Mechanized CO_2	Sv-08Kh20N9G7T wire, 2 mm dia., heat No.2187, Izhevsk Metallurgical Works	Welding the 1st bead into a groove	–	220
		Welding by bending a sample	5.0	–
Automatic submerged-arc using AN-22 flux	Same	Welding the 1st bead into a groove	–	240
		Welding by bending a sample	5.5	–

This welding wire with a diameter ranging from 2 to 5 mm meets requirements of GOST 2246–70 and TU 14-143-506–98 in all its basic parameters (chemical composition, geometrical sizes, quality of the surface, strength properties, etc.).

The finished Sv-08Kh20N9G7T wire 2 mm in diameter (heat No. 145991), manufactured by Dneprospetsstal, has the following chemical composition, %: C – 0.07; Mn – 6.5; Si – 0.51; Cr – 19.47; Ni – 9.4; Ti – 0.76; S – 0.002; P – 0.021; Cu – 0.09; Mo – 0.12; W, Sn, V, Zn and Nb – traces; Al – 0.28; Sb, Pb, Bi and As – no.

The gas content of metal of the finished Sv-08Kh20N9G7T wire 2 mm in diameter (heat No. 145991) is as follows, %: O – 0.0045, H – 0.0008 (8.8 cm^3 / 100 g) and N – 0.023 (prior to the gas content analysis the surface of the wire was thoroughly cleaned and polished).

Tensile strength of the improved Sv-08Kh20N9G7T welding wire with a diameter from 2 to 5 mm, manufactured by Dneprospetsstal, is within a range of 1000 – 1200 MPa and corresponds to requirements of GOST 2246–70. This allows it to be used for welding and for manufacture of welding electrodes.

This welding wire is characterized by good welding-technological properties. No hot cracks were detected in multilayer claddings made by argon or carbon dioxide welding, and in submerged-arc welding using the AN-22 flux on austenitic steel of the 08Kh18N10T grade 30 mm thick and on high-strength quenching steel of the 30Kh2N2M grade 80 mm thick.

Metal of the investigated batches of the Sv-08Kh20N9G7T wire and metal deposited with this wire in argon are characterized by an increased purity. The content of non-metallic inclusions in the wire and deposited metal is not higher than point 1 of the ShZ scale, GOST 1778–70. The inclusions are small in size. They can be identified only at a magnification of not less than 1000 power.

Table 2. Evaluation of cold tear crack resistance of the welded joints in high-strength quenching steel 25 mm thick, made using the Sv-08Kh20N9G7T wire*

Welding method	*Welding consumable*	*Manufacturer*	*Maximum bend of welded samples, mm*	
			To formation of tear crack in the HAZ	*To full fracture caused by tear crack formed in the HAZ*
Mechanized CO_2	Wire 2 mm dia., heat No. 145991	Dneprospetsstal	6.5	10.5
Automatic submerged-arc using AN-22 flux	Same	Same	6.8	11.8
Mechanized CO_2	Wire 2 mm dia., heat No. 2187	Izhevsk Metallugical Works	5.2	8.5
Automatic submerged-arc using AN-22 flux	Same	Same	6.0	9.0

*The rate of bending the samples is constant.

Table 3. Mechanical properties of metal deposited with the Sv-08Kh20N9G7T wire 2 mm diameter manufactured by Dneprospetsstal (heat No. 145991)

Shielding atmosphere of the arc	*Mechanical properties at room temperature*				
	σ_y, *MPa*	σ_t, *MPa*	δ, *%*	ψ, *%*	*KCU, MJ / m²*
Argon	324.5	617.1	47.3	66.3	–
	332.2	620.2	46.1	61.2	–
CO_2	391.0	611.6	41.3	71.4	1.37
	404.9	621.4	47.3	71.4	1.36

Table 4. Mechanical properties of weld metal produced by CO_2 welding of high-strength quenching steel using the Sv-08Kh20N9G7T wire (heat No.145991)

Welding conditions	*Mechanical properties at room temperature*				*KCU, MJ / m² at T, °C*	
	σ_y, *MPa*	σ_t, *MPa*	δ, *%*	ψ, *%*	*+20*	*–40*
Multipass, groove 30 mm deep, plate 80 mm thick	324 – 337 / 332	627 – 644 / 638	44.5 – 46.8 / 45.2	54.3 – 56.2 / 55.2	1.66 – 1.82 / 1.74	1.54 – 1.62 / 1.58

Table 5. Mechanical properties of welded joints in high-strength steel 25 mm thick made using the Sv-08Kh20N9G7T wire manufactured by Dneprospetsstal (heat No.145991)

Welding method	*Mechanical properties at room temperature*				*KCU, MJ/m² at T, °C*	
	σ_y, *MPa*	σ_t, *MPa*	δ, *%*	ψ, *%*	*+20*	*–40*
Mechanized CO_2	305.0 – 340.0 / 325.0	610.0 – 635.0 / 620.5	52.5 – 57.5 / 54.5	56.5 – 60.5 / 58.5	1.65 – 1.76 / 1.69	1.44 – 1.65 / 1.52
Automatic submerged-arc using AN-22 flux	330.0 – 355.0 / 342.5	632.0 – 641.5 / 638.2	50.5 – 58.5 / 56.5	55.5 – 61.5 / 59.0	1.56 – 1.88 / 1.76	1.52 – 1.60 / 1.57

In metal purity, this wire is superior to samples of similar wires investigated earlier. The sulphur and phosphorus content of the wire is lower, and it contains almost no low-melting point impurities, such as tin, lead, bismuth, arsenic, antimony and zinc.

Commercial batches of the Sv-08Kh20N9G7T wire were tested by the methods accepted in transport engineering. The initial evaluation of hot crack resistance of the welds was conducted by the method based on static bending of the butt samples during welding. In this case the evaluation criterion was the maximum rate of bending of the butt samples, at which no hot cracks were yet detected in a single-pass weld (Table 1). Also, no cases of formation of such defects were registered in welding restrained samples under technological conditions accepted in transport engineering. Resistance of the weld metal to hot cracking was tested by depositing beads into grooves 30 mm deep made in the 80 mm thick plates of high-strength quenching steel.

The amperage was increased in welding each next sample. The rest of the parameters remained unchanged. The maximum welding current at which no hot cracks were yet detected in the beads was used as the evaluation criterion (Table 1).

Resistance of welded joints to the formation of cold tear cracks in the fusion zone between the austenitic weld metal and quenching steel was evaluated by the method that involved bending of the samples which had been cooled to room temperature after welding under technological conditions. The maximum bend of a sample at which no tear cracks were yet formed in metal of the heat-affected zone was used as the evaluation criterion (Table 2).

Tests of the Sv-08Kh20N9G7T wire conducted by the methods described gave positive results. This allowed it to be used in mass production.

In welding a batch of standard pieces of high-strength quenching steel using the 2 mm diameter Sv-08Kh20N9G7T wire, no cases of discarding because of hot cracks in the weld metal or cold tear cracks in the HAZ metal were reported.

This wire exhibits high practicability in welding. The metal is characterized by good spreading in submerged-arc welding of steel using the AN-22 flux, as well as in CO_2 welding into a deep groove. Spattering in CO_2 welding is insignificant, i.e. maximum 4.5 % (the value of 10 % is considered acceptable), detachability of oxide films from the bead surface is good.

The deposited metal (Table 3), weld metal (Table 4) and welded joints (Table 5) of high-strength quenching steel, 25 and 80 mm thick, made using the improved Sv-08Kh20N9G7T wire, meet all requirements for mechanical properties in compliance with standards in force in transport engineering. The static tension and impact bending tests were conducted in compliance with GOST 6996–66, types of specimens — II and VI. The deposited and weld metal is characterized by high ductility and impact toughness at room temperature and at -40 °C, which is especially important for elimination of cold tear cracks in the HAZ metal of welded joints.

The Sv-08Kh20N9G7T wire produced by Dneprospetsstal is recommended for welding high-strength quenching steels and manufacture of welding electrodes.

REFERENCES

1. (1980) *Development of metallurgy in the Ukrainian SSR*. Kyiv: Naukova Dumka.
2. (1989) *Reference book for grades of steels and alloys*. Edited by V.G. Sorokin. Moscow: Mashinostroyeniye.
3. Makara, A.M., Mosendz, N.A. (1971) *Welding of high-strength steels*. Kyiv: Tekhnika.
4. (1974) *Technology for electric fusion welding of metals and alloys*. Edited by B.E. Paton. Moscow: Mashinostroyeniye.
5. Gordonny, V.G., Gaivoronsky, A.A., Sarzhevsky, V.A. *et al.* (1992) Effect of the type of weld metal on structure, properties and cold crack resistance of high-strength steel joints. *Avtomaticheskaya Svarka*, **11 – 12**, 13 – 16.
6. Yushchenko, K.A., Chekotilo, L.V., Kakhovsky, Yu.N. (1996) Manufacture of welding wire of the Sv-04Kh19N9 grade at Dneprospetsstal. *Ibid.*, **3**, 59.
7. Yushchenko, K.A., Chekotilo, L.V., Kakhovsky, Yu.N. *et al.* (1999) Mastering the production of the Sv-04Kh19N11M3 grade welding wire at Dneprospetsstal. *Ibid.*, **3**, 48 – 50.

EFFECT OF ELECTRODE SHAPE AND HEAT INPUT ON STRUCTURE AND PROPERTIES OF DEPOSITED METAL

V.I. SHCHETININA[1], K.K. STEPNOV[1], N.G. ZAVARIKA[1], S.V. SHCHETININ[1], E.N. SHEBANITS[2], V.S. GOLI-OGLU[2], V.G. BENDRIK[2] and B.E. DUBINSKY[2]

[1]Preazovsky State Technical University, Mariupol, Ukraine

[2]Iljich Metallugical Works, Mariupol, Ukraine

ABSTRACT

The structure and properties of medium-carbon alloyed deposited metal can be regulated in a rather broad range by changing the electrode shape and the heat input value. In general, increase in the metal surfacing rate promotes refinement of the deposited metal structure, reduction of the tempered zone, increase in the values of impact toughness, ultimate strength and reducing of welding stresses.

Key words: *arc surfacing, electrode shape, strip, wire, heat input, structure, mechanical properties, deformation.*

The electrode shape is a basic parameter which defines the method of surfacing. The arc movement along the electrode end and with respect to the pool in accordance with the principle of a minimum of Steenback [1] determines a heat input to the weld pool and also (at a constant surfacing condition) rates of heating and cooling of liquid metal and HAZ metal on which the conditions of pool solidification, diffusion processes, structural and phase transformations [2, 3] and, consequently, the quality of the deposited metal are dependent. The effect of electrode shape on structure and quality of the deposited metal was not studied comprehensively [4, 5].

In addition, with decrease in heat input the probability of cold crack formation is increased due to increase in the cooling rate [2, 6 – 8]. However, the large drop of heat input and corresponding increase in cooling rate can lead to the reducing of probability of the cold crack formation [2].

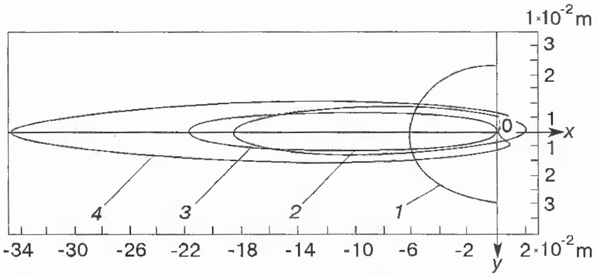

Figure 1. Relationship between the isotherms of melting and electrode shape: *1* — strip located normal to the surfacing direction; *2* — 4 mm dia. wire; *3* — 0.5×45.0 mm strip located along the surfacing direction; *4* — combined electrode consisting of 4 mm dia. wire and 0.5×45.0 mm strip.

To study the effect of electrode shape and heat input on structure and properties of the deposited metal a five-layer surfacing on 30×300×400 mm plates of steel St.3 was made with 4 mm diameter wire Sv-08A, 0.5×45.0 mm strip of steel St.08 (killed), located in longitudinal and perpendicular direction relative to welding axis, and also with a combined electrode which consists of wire Sv-08A of 4 mm diameter and U-shaped 0.5×45.0 mm section strip of steel St.08 (killed). The surfacing was performed at direct current of reverse polarity and optimum conditions for each methods using the flux ZhSN-5. Rectifier VMG-5000 was used as a power source. When surfacing with this flux the chemical composition of the deposited metal corresponded to the type of 25Kh5FMS. The properties of the deposited metal were evaluated by microstructure, impact strength, level of strains and welding stresses.

In accordance with a principle of the Steenback minimum [1] the arc tends to burn at minimum voltage. Therefore, it is moved along the electrode end and the surface of the weld pool. Diameter of a cathode spot is 1×10^{-4} cm, current density at the cathode, according to data of [9] is 1×10^{7} A/cm^2, that was established by photographing the cathode spot with a short exposure and confirmed by a shape and sizes of the weld pool crater when the strip was located along the surfacing direction and also when the surfacing was performed with a combined electrode. As a result of a high current density, and also arc displacement along the electrode end and surface of the weld pool the heat input and temperature field are changed.

In surfacing with a wire electrode the active spot is moved along the fused electrode end, and when a strip electrode is used it is moved along the

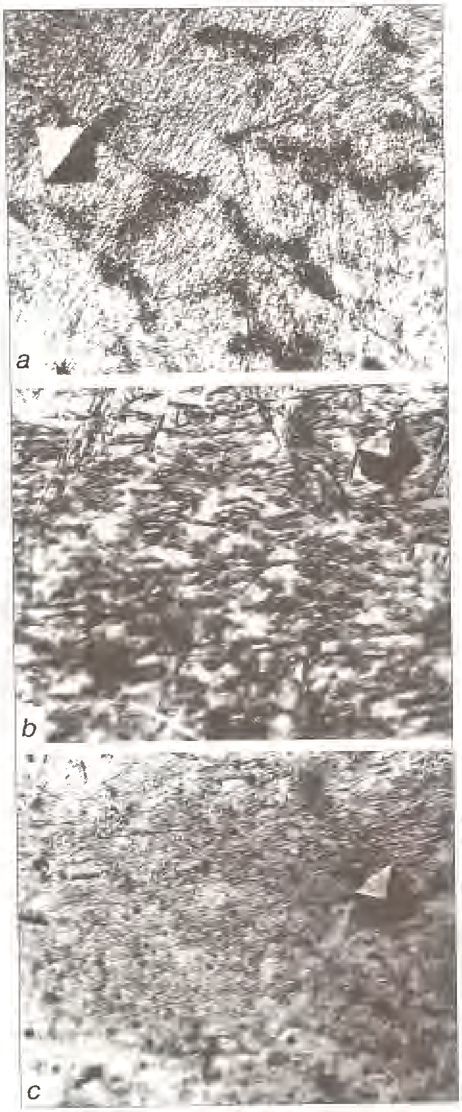

Figure 2. Microstructure of metal deposited with a strip located along the surfacing direction. Here and in Figures 3 – 5 the heat input is 3.6 (*a*); 2.7 (*b*); 1.8 (*c*) MJ/m (×300) (reduced by 0.80).

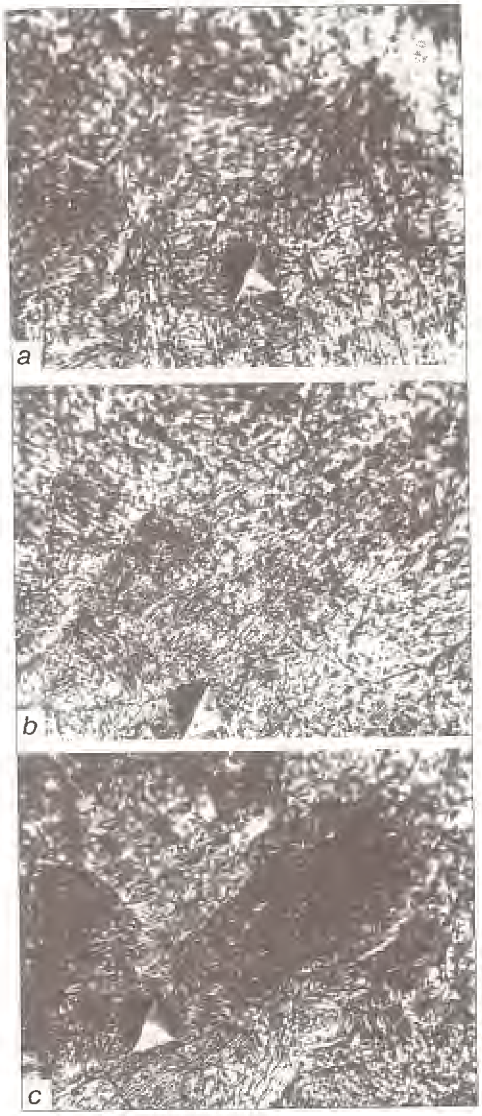

Figure 3. Microstructure of metal deposited with a strip located normal to the surfacing direction (×300) (reduced by 0.80).

electrode end from one edge to another at 45 mm distance. Therefore, in welding and surfacing with a strip electrode the effectiveness of heat input is reduced, which is proved by a decrease in penetration depth.

In accordance with [10] the electrode shape greatly influence the isotherms of melting (Figure 1). In surfacing with a wire electrode at high speeds the isotherms are narrowed and shifted to the region which was already passed by the arc. When the strip is located normal to the surfacing direction the isotherms are expanded, but remain shifted relative to the heat source into the side opposite the surfacing direction, the length of the weld pool is decreased. Arc during displacement from one edge to another is burning mostly in the middle of the weld pool. The duration of arc in the region of side edges of the pool is decreased, therefore, a significant amount of the generated heat is reduced.

When the strip is located along the direction of surfacing, the arc is moved at the electrode end along the weld pool axis. In this case the isotherms of melting are elongated and shifted forward, as compared with those of the wire electrodes.

In surfacing with a combined electrode, when the arc is displaced along the U-shaped strip the duration of arc in the region of side edges of the pool and the amount of heat generated ahead of the arc, burning at the wire, and also the heat input into the regions of side edges of the pool are increased. The isotherms of melting are shifted forward and expanded in the direction normal to surfacing. The temperature gradient in axis O_x is decreased, the length of the weld pool is increased.

When the strip is located along the surfacing direction the microstructure of the deposited metal is coarse-grained and non-homogeneous (Figure 2),

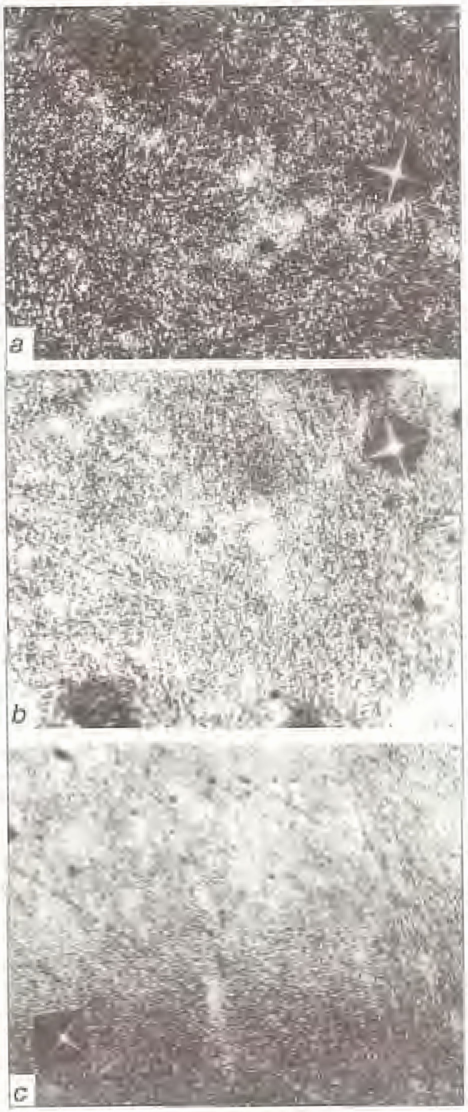

Figure 4. Microstructure of metal deposited with a wire (×300) (reduced by 0.80).

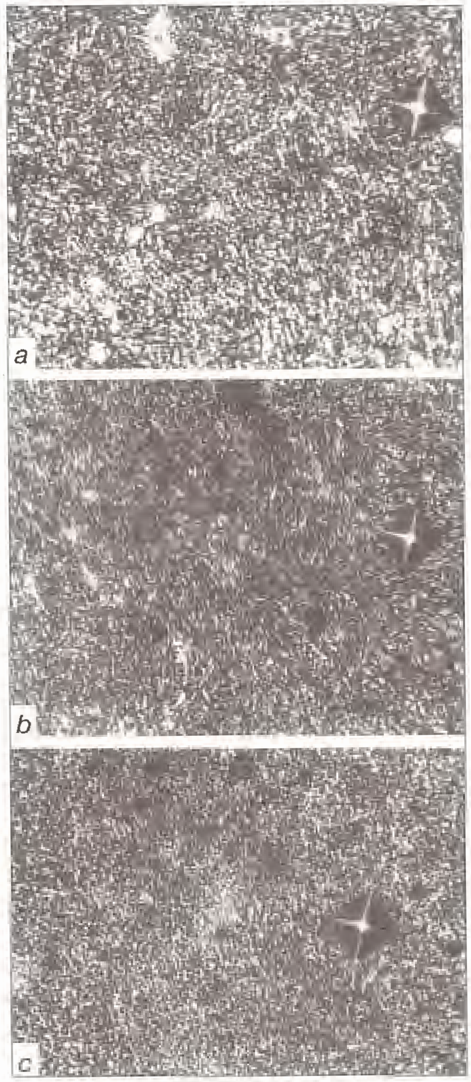

Figure 5. Microstructure of metal deposited with a combined electrode (×300) (reduced by 0.80).

while at a normal location of the strip it is slightly refined, remaining coarse-grained (Figure 3). Surfacing with a wire electrode leads to the microstructure refining (Figure 4). In case of using the combined electrode the microstructure of the deposited metal is most fine-dispersed and homogeneous (Figure 5). At a constant heat input this is a result of a possible changing of chemical composition of the deposited metal and effect of the surfacing speed, because the surfacing with a strip, located along and normal to the welding direction, was performed with speeds of 12, 18 and 24 m/h, with a wire — 20, 30 and 40 m/h, with a combined electrode — 50, 75 and 100 m/h.

The zone of tempering in surfacing with electrodes of different shapes was measured (Figure 6). The minimum zone of tempering typical of surfacing with a strip, located normal to the surfacing direction, is a result of a little-time existence of arc in the region of side edges of the pool and minimum heat input in this region. In surfacing with a strip, located along the surfacing direction, the zone of tempering is increased due to increase in heat input to the regions of side edges of the weld pool. In case of using the combined electrode the zone of tempering is approximately the same as in surfacing with a strip electrode, located normal to the surfacing direction. With a surfacing speed increase, as a result of reducing the heat input, the zone of tempering is decreased, thus contributing to the increase in resistance to separation, because this zone can be a source of a fracture initiation caused by the cold crack formation.

With increase in speed of surfacing with a combined electrode the impact strength is first increased and then it is decreased (Figure 7). The first case is a result of structure refining and decrease in microdistortions of a crystalline lattice, microstresses and density of dislocations which are related to the crack initiation [11]. The second case is caused by some growth of microdistortions of a

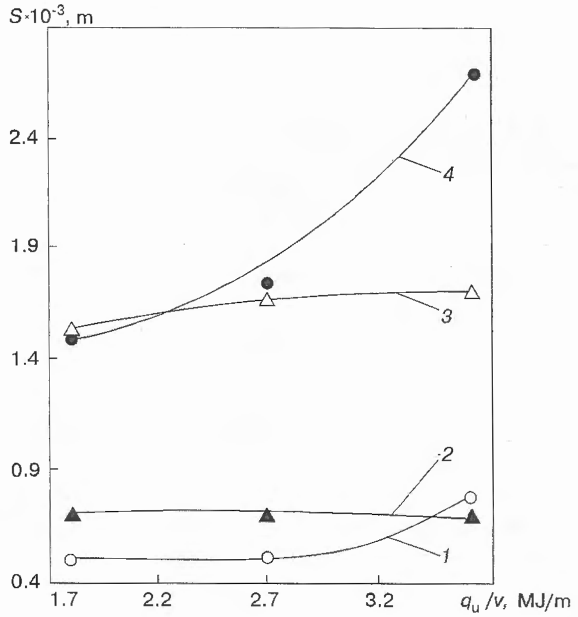

Figure 6. Effect of electrode shape and heat input on the zone of tempering: *1*, *3* — strip located normal and along the surfacing direction, respectively; *2* — combined electrode; *4* — wire electrode; *S* — size of the tempering zone.

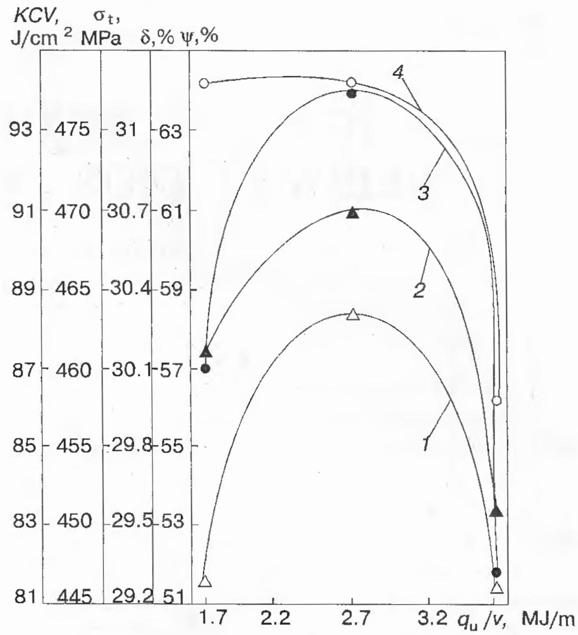

Figure 7. Effect of heat input on mechanical properties of deposited metal: *1* — impact strength; *2* — elongation; *3* — reduction in area; *4* — ultimate rupture strength.

crystalline lattice, microstresses and density of dislocations.

Similar to impact strength, with an increase in surfacing speed the elongation and reduction in area are also changed. In addition the maximum values of impact strength. elongation and reduction in area are coincided. Their high level indicates an increased crack resistance of the metal deposited with a combined electrode.

The ultimate rupture strength is increased with an increase in surfacing speed and decrease in heat input. Its maximum value coincides with that at maximum values of the impact strength, elongation and reduction in area that confirms the validity of the experimental data.

Similar data were obtained during investigation of effect of the electrode shape and heat input on static fracture (Figure 8) which was performed on of 9.0×7.5×20.0 mm samples with V-shaped notch.

As was established, in surfacing with a combined electrode a static loading *P* at similar heat input is 1.2 times higher than that in surfacing with a wire electrode. The maximum static loading is provided at heat input 2.7 MJ/m. Its reduction in surfacing at heat input 1.8 MJ/m can be explained by increase in non-metallic inclusions as a result of increasing the rate of solidification of molten metal of the weld pool and their «trapping» by the deposited metal.

To study the effect of heat input on the deformation of the parent metal the welding of 8×120×900 mm plates and surfacing of 30×120×400 mm plates were performed with a combined electrode at different heat input. As a result, it was established that with increase in the speed and with decrease in heat input the deformation of the parent metal is decreased (Figure 9). This is due to the decrease in heat input and, thus, reduces the welding stresses.

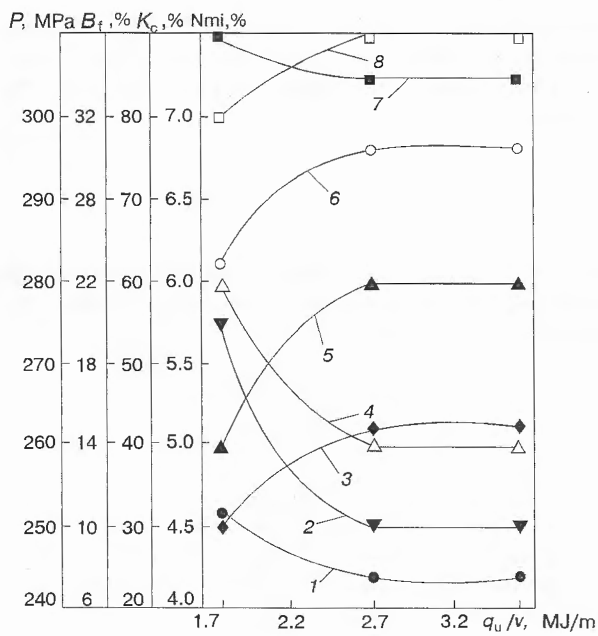

Figure 8. Effect of electrode shape and heat input on the quality of deposited metal: *1*, *3*, *5*, *7* — wire electrode; *2*, *4*, *6*, *8* — combined electrode; *1*, 6 — static load, causing fracture; *2* — tough constituent in fracture B_f; *3* — quasi-cleavage K_c; *4*, *5* — amount of non-metallic inclusions.

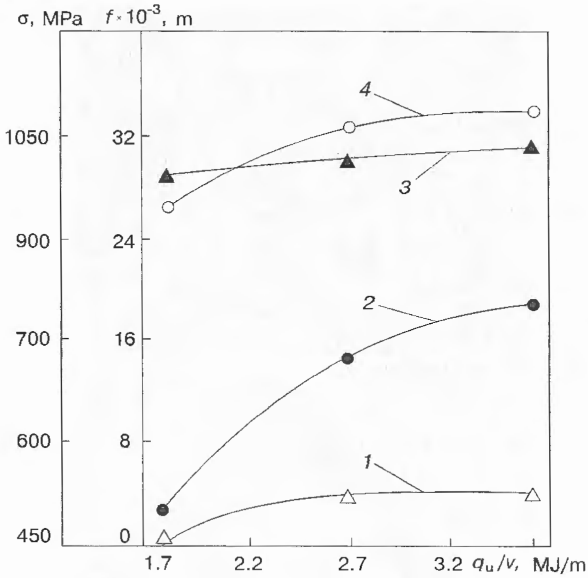

Figure 9. Relationship between welding stresses and heat input: *1, 3* — deformation of plate; *2, 4* — welding stresses; *1, 2* — 30×120×400 mm plates; *3, 4* — 8×120×900 mm plates.

The relationship between the welding stresses and heat input is determined by the expression given in [12]:

$$\sigma \geq \mu E \frac{q_u}{vF},$$

where μ is the Poisson's ratio, which is equal to $0.335 \frac{\alpha}{c\gamma}$ for carbon steel; E is the modulus of elasticity, equal to 19.68×10^{-4} MPa; q_u/v is the heat input and F is the cross-section of the plate.

Deformation of plates depends on welding stresses

$$f = 0.613 l \sqrt{\frac{\sigma - \sigma_{cr}}{E}},$$

where l is the plate length; σ_{cr} is the critical welding stress determined from the following formula:

$$\sigma_{cr} = \frac{\pi^2 E}{12}\left(\frac{s}{l}\right)^2,$$

where s is the plate thickness.

At $\sigma > \sigma_{cr}$ the plate deformation is occurred.

It follows from the above-given expressions that the welding stresses are proportional to the plate deformation

$$\sigma = \frac{f^2}{0.613^2} \frac{E}{l^2} \frac{\pi^2 E}{12}\left(\frac{s}{l}\right)^2.$$

With decrease in heat input at increasing the speeds of welding and surfacing the welding stresses are decreased that significantly improves the crack resistance and serviceability of mill rolls. This was established in surfacing the banded support rolls of mill 3000 at low heat input using the speed of 75 m/h.

CONCLUSIONS

1. Structure and properties of the deposited metal can be regulated by changing the electrode shape and heat input.

2. With increase of the surfacing speed the microstructure is refined, size of tempering zone is decreased, thus leading to the increase in impact strength of the deposited metal and ultimate strength, whose maximum values are characteristic of surfacing with a combined electrode at 2.7 MJ/m heat input.

3. Simultaneous increase in ultimate strength and reduction in welding stresses improves the crack resistance and serviceability of mill rolls during surfacing with a higher speed.

REFERENCES

1. Engel, A., Steenback, M. (1936) *Physics and technique of electrical discharge in gases*. Moscow: ONTI NKTN.
2. Prokhorov, N.N. (1976) *Physical processes in metal during welding*. Moscow: Metallurgia.
3. Shorshorov, M.Kh., Belov, V.V. (1972) *Phase transformations and changing the steel properties during welding*. Moscow: Nauka.
4. Shinko, I.N., Shkolyarenko, G.D., Pozdneev, G.A. *et al.* (1988) Surfacing of parts with electrode strips in ferrous metallurgy. *Chyornaya Metallurgia*, **18**, 8 – 22.
5. Nikolaenko, M.R., Kostenko, S.P., Kashchuk, M.G. *et al.* (1980) Peculiarities of effect of conditions of welding with strip and wire electrodes on sizes and properties of welded joint. *Svarochoye Proizvodstvo*, **11**, 20 – 21.
6. Musiyachenko, V.F., Mikhoduj, L.I., Pozdnyakov, V.D. (1990) Resistance of high-strength T-joints to cold cracking in shielded-gas single-pass welding. *Ibid.*, **2**, 13 – 15.
7. Grezev, A.N., Safonov, A.N. (1986) Cracking and microstructure of Cr–B–Ni alloys deposited by laser. *Ibid.*, **3**, 6 – 8.
8. Lebedev, Yu.M., Letuchii, V.N., Tsyukh, S.M. (1986) Structural transformations in welding steel 30KhGSA and its weldability. *Ibid.*, **12**, 19 – 20.
9. Kasaev, I.G. (1968) *Cathode processes of electric arc*. Moscow: Nauka.
10. Rykalin, N.N. (1947) *Thermal fundamentals of welding*. Moscow–Leningrad: Izdat. AN USSR.
11. Finkel, V.M. (1970) *Physics of fracture*. Moscow: Metallurgia.
12. Vinokurov, V.A., Grigoriants, A.G. (1984) *Theory of welding strains and stresses*. Moscow: Mashinostroyeniye.

INFLUENCE OF DIFFERENT METHODS OF HEAT REMOVAL ON THE ACTIVE ZONE IN WELDING

A.I. GEDROVICH and **A.B. ZHIDKOV**
East-Ukrainian State University, Lugansk, Ukraine

ABSTRACT

The results are given of experimental verification of the effectiveness of various methods of cooling for lowering the welding deformations. It is found that the most effective is showering, cooling by water jets and application of crystalline heat absorbers. Welding with artificial heat removal can be recommended as a promising resources-saving technology.

Key words: *welding, deformation, heat removal, yield lines, active zone, intensity, methods.*

One of the main possibilities for reducing deformations in welded joints is lowering of the plastic deformation of shrinkage, or the width of the zone of its propagation in heating by controlling the thermal impact in welding. It was noted earlier [1], that heat removal during welding is a resources saving measure, not requiring sophisticated and expensive equipment for post-weld treatment. Known is a great number of methods of heat removal during welding [2 – 5]. This paper is exactly devoted to comparison of their effectiveness.

It is convenient to assess the active zone in welding by the yield lines [3]. Experimental verification of various cooling methods as to their effectiveness was performed on samples of VSt.3ps steel of 400×300×2 mm size. Prior to welding the samples were annealed for relieving the internal stresses. The yield lines were revealed by the known procedure [4].

Welding of sheet structures is usually performed in a jig in production, therefore in welding the samples were rigidly fastened in the fixture.

Deposition was performed in the sheet center by coated-electrode manual arc welding (MAW) using VD-306 rectifier, as well as by CO_2 welding in ADG-502 automatic machine with VDU-504 power source with cooling by different schematics. Butt welding of samples was performed by MAW in the same modes for comparison, the sheets having being first assembled by tack welding (tack length is 25 mm, tack spacing being 150 mm).

The welding and deposition modes, the effective and reduced power values are given in Table 1.

In order to reveal the role of heat removal, cooling was performed from one side of the weld and locally in a limited area.

Nine variants of heat removal were studied, namely by a shower; water jet; cooling with crystalline heat-absorbing rods; in a water tank (at

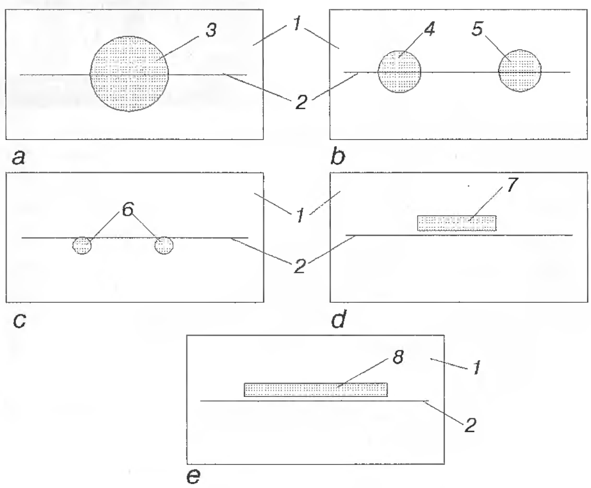

Figure 1. Schematics of heat sink mounting: *a* — water shower; *b* — blowing with air and cooling by a water jet; *c* — application of crystalline heat-absorbing rods; *d* — cooling in a water tank, by heat-absorbing paste, with water-cooled copper backing; *e* — cooling with running water and moist porous materials; *1* — sample; *2* — weld; *3* — showered region; *4* — region blown by air; *5* — region cooled by a water jet; *6* — crystalline heat-absorbing rods; *7* — water tank, heat-absorbing paste, backing; *8* — trough with running water or moist porous material

Table 1. Modes of welding and bead deposition

Welding process	d_{el}/d_{wire}, *mm*	I_w, *A*	U_a, *V*	v_w, *m/h*	v_{wire}, *m/h*	Q_g, *l/min*	q_{ef}, *W*	q_{abs}, *J/m*
MAW	3.0	70 – 75	26 – 30	25 – 27	–	–	1522	2107
Automatic CO_2	1.6	110 – 120	38 – 40	50 – 55	210	5	3140	2153

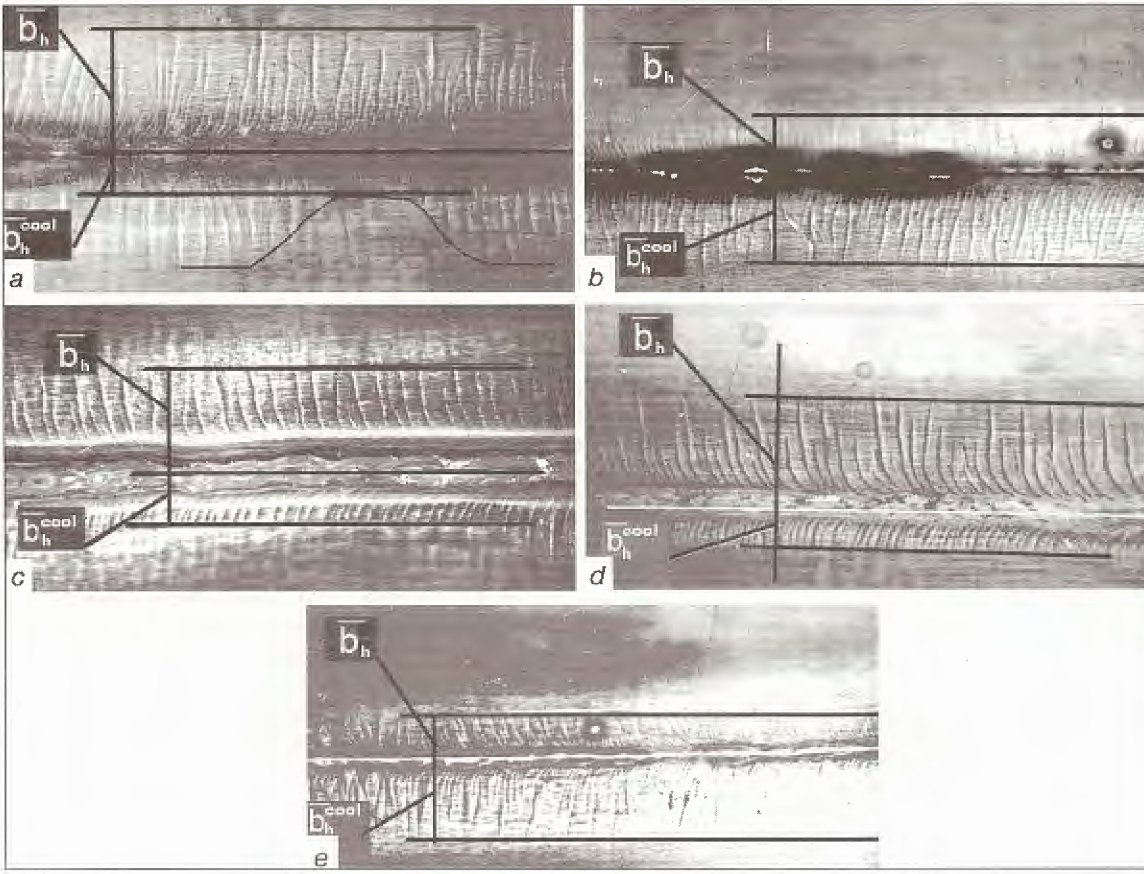

Figure 2. Yield lines and dimensions of the active zone in cooling: *a* — crystalline heat-absorbing rods; *b* – *d* — water in a tank, respectively at T = 0 (ice), 20, 85 °C; *e* — running water.

water temperature 0 °C — ice; 20 °C — normal conditions; 85 °C — hot water); with porous materials impregnated with water; by running water; cooling by heat-absorbing paste; cooling with water-cooled copper substrate (uncoated, coated with liquid glass and tinned with POS-61 solder); blowing with air.

In the case of applying a shower, water was fed under a pressure of 0.2 MPa through a nozzle, in the form of fine drops (drop diameter of 0.2 to 0.5 mm), and hit the reverse side of the sheet from the distance of 25 mm; diameter of the surface being cooled was 120 mm. The water jet was aimed upwards; nozzle diameter was 6 mm, distance to sample surface was 5 mm, spreading spot size was 60 mm. Water consumption was 4 l/min, pressure being 0.1 MPa. The location of the surface being cooled is shown in Figure 1, *a*.

The crystalline heat-absorbing rods were mounted under the samples (Figure 1, *c*) and were spring-loaded with flexible steel plates. When the sample was cooled using a water tank, it was a bottomless bath of 120×25×15 mm size, placed on the sample and sealed with epoxy. Immediately before welding water was poured into the bath or 30 cm^3 of ice were placed into it. For convenience of welding performance, the bath was placed at 10 mm distance from the weld axis (Figure 1, *d*).

When porous materials impregnated with water, were used, glass wool impregnated with water was placed into the trough, and it was then pressed to the sample from below at 5 mm distance from the weld axis.

The heat-absorbing paste (75 % liquid glass, 25 % asbestos) was applied onto the face surface of the sample at 10 mm distance from the weld axis; the thickness of the layer depending on the paste viscosity was 2 to 3 mm.

In cooling with flowing water the trough was placed from below and pressed against the sample at 5 mm distance from the weld axis; sealing was performed using a rubber gasket. In order to remove the air bubbles, a threaded hole was made in the sample, which after the complete filling of the trough with water, was plugged by a screw. Water was fed at a pressure of 0.1 MPa, its consumption being 4 l/min.

The water-cooled copper backing was mounted from the lower side, and was pressed to the sample by spring plates at 5 mm distance from the weld axis. A 10 mm diameter channel was made in the backing body, through which water flowed at a pressure of 0.1 MPa with 4 l/min consumption. The backing surface was left dry in the first experiment, in the second it was coated by a thin layer of liquid glass immediately prior to welding,

Table 2. Results of experimental verification of the effectiveness of various processes of welding with cooling*

Welding process	Half-width of active zone		Intensity of plastic deformation, lines/mm		
	$\bar{b}_h$, mm	Zone narrowing, %	At distance $\bar{b}_h$	At distance $\bar{b}_h/2$	At distance $\bar{b}_h/4$
MAW, bead-on-plate, without cooling	36/–	–	2.00/–	2.4/–	3.0/–
Automatic CO_2, bead-on-plate, without cooling	28/–	–	2.00/–	4.0/–	6.0/–
MAW, butt welding, without cooling	36/–	–	2.00/–	3.0/–	3.0/–
Bead-on-plate with shower, MAW	22/6.0	73.00	4.00/0	5.0/0	5.5/5.0
Bead-on-plate deposition with water jet cooling, MAW	22/7.0	68.00	2.50/0	3.5/0	4.0/5.0
crystalline rod, automatic CO_2	24/9.0	62.50	2.00/0	4.5/1	6.0/6.3
water tank (20 °C), MAW	23/9.0	61.00	2.50/0	3.5/0	4.5/5.0
water tank (85 °C), MAW	35/15.0	57.00	1.50/0	2.7/0	4.0/5.0
water tank (°C — ice), MAW	28/12.0	57.00	1.20/0	2.9/0	5.9/5.6
porous materials impregnated with water, automatic CO_2	26/13.0	50.00	2.00/0	5.0/5.0	6.0/6.0
running water, automatic CO_2	24/16.0	33.30	1.50/0	4.0/4.0	6.5/7.0
water-cooled copper backing coated with a layer of POS-61 solder, MAW	32/22.0	31.25	1.33/0	3.0/3.0	4.0/4.0
water-cooled copper backing coated with heat-conducting paste, automatic CO_2	28/20.0	29.00	2.50/0	3.5/3.5	5.0/4.5
heat-conducting paste, automatic CO_2	28/22.0	21.40	2.00/0	3.0/4.0	6.0/6.5
water-cooled copper backing, MAW	28/26.5	5.40	2.50/0	3.5/3.5	5.0/5.0
blowing with air, MAW	22/21.0	4.50	2.50/0	3.5/3.5	4.0/4.0

*The numerator gives the values for uncooled side of deposited bead and the denominator — for the cooled side.

and in the third experiment it was tinned with POS- 61 solder (1 mm thick tinning layer).

Blowing with air from the reverse side of the sample (Figure 1) was performed at a pressure of 0.3 MPa; the distance between the nozzle and the sample being 5 mm, nozzle diameter being 6 mm.

The produced patterns of yield lines for the cooled and uncooled areas (Figure 2) allowed determination of the average half-width of the active zone in heating $\bar{b}_h$ and the intensity of plastic deformation in heating which is characterised by the number of yield lines per a unit of weld length. Measurements were taken in several areas (in the center and along the edges of the cooled zone) and the average value was determined. The measurement results are given in Table 2.

During experiment performance the following features of welding with cooling were found:

cooling using free water is not adaptable to fabrication, as metal deformation in welding does not allow a reliable sealing of the tank with the water; when cooling of the welded butt with water from below is used, it is difficult to remove the air bubbles from under the surface being cooled;

use of crystalline heat-absorbing rods is adaptable to fabrication in automatic welding, but complicated in manual and mechanised welding, heat-absorbing paste made by the authors had a low viscosity and this did not allow it to be applied in a thick enough layer. The main disadvantage of crystalline heat-absorbing rods and heat-absorbing paste consists in that they are consumable materials, and their mass production has not been organised;

application of the copper backing is the best adaptable to fabrication, as it fits well into the welding fixtures, but its effectiveness is low, application of heat-absorbing paste (liquid glass in the experiment) allowed the effectiveness of the copper backing to be increased, but with a great thickness of the liquid glass layer, its partial boiling was observed, and heat removal in such places was reduced. Application of POS-61 solder also increased the backing effectiveness, but it is desirable to apply a solder with a lower boiling temperature. In order to increase the effectiveness of the backing, it is rational to use substances with a low (below 100 °C) boiling temperature, high (above 1000 °C) boiling temperature, and good heat conduction;

application of porous materials (glass wool) impregnated with water, ensures a high effectiveness of heat removal and is easily adaptable to fabrication;

cooling by blowing with air has a low effectiveness and cannot be used as a method of lowering the welding strains and stresses.

Analysing the results presented in Table 2, the following should be noted:

in welding in the boosted modes (automatic welding) the width of the zone of plastic deformations is smaller than in welding at a low speed (MAW), this being confirmed by published data [2];

in welding of sheets abutted using tack welds in a rigid fixture, the yield line pattern does not differ from the pattern in bead-on-plate welding (same width of the active zone and intensity of plastic deformation);

water temperature when a water tank is used, does not have an essential influence on heat removal, as heat removal occurs mainly at the expense of the latent heat of steam formation (boiling);

application of running water is less effective, as in this case no boiling occurs, and the heat removal coefficient with free convection into water is by two orders of magnitude lower than in boiling [6];

application of heat sink allows an essential narrowing of the zone of plastic deformations; the intensity of plastic deformation in welding with heat removal does not change.

CONCLUSIONS

1. Welding with cooling can be recommended as an effective and resources saving method of lowering the welding stresses and strains.

2. Narrowing of the active zone in welding with cooling depends on the method of heat removal. The most effective method is a shower, cooling by a water jet, cooling by crystalline heat-absorbing rods. In this case narrowing of the width of the active zone is up to 70 to 73 %.

3. Application of water-cooled copper backing coated by a heat-absorbing paste (tinned with a low-melting solder) or of porous materials impregnated with water can be recommended for industry as the most versatile, adaptable to fabrication and highly effective methods.

REFERENCES

1. Gedrovich, A.I., Zhidkov, A.B. (2000) Application of heat-removing devices for lowering the welding strains and stresses. *Avtomaticheskaya Svarka*, **1**, 45 – 49.
2. Kasatkin, B.S., Prokhorenko, V.M., Chertov, I.M. (1987) *Stresses and strains in welding*. Kiev: Vyshcha Shkola.
3. Lobanov, L.M. (1983) *Technological means of lowering the strains and stresses*. Kiev: Znanie.
4. Gedrovich, A.I. (1998) *Plastic deformation in welding*. Lugansk: East-Ukrainian University.
5. Lobanov, L.M. *et al*. *Composition of a heat-absorbing welding paste*. USSR author's certificate **1046052**, Int. Cl. B 23 K 35/36. Publ. 07.10.83.
6. Baskov, A.P., Berg, B.V., Witt, O.K. *et al*. (1991) *Heat engineering*. Edited by A.P. Baskakov. Moscow: Energoizdat.

RESTORATION OF THE DIMENSIONS AND PROPERTIES OF CAST IRON CYLINDRICAL PARTS BY RESISTANCE BUILD-UP WELDING WITH WIRE

A.M. MIKHED and **V.P. CHERNYSH**
National Technical University of Ukraine «KPI», Kyiv, Ukraine

ABSTRACT

It is shown that application of resistance build-up welding of steel with wire for restoration of cast iron surfaces can be technically and economically justified. For this purpose it is necessary to provide a continuous built-up layer with a guaranteed quality of its joining with the a base metal.

Key words: *resistance build-up welding, restoration, cast iron parts, solid-phase joint, building-up modes, mechanical tests, metallographic investigations.*

In car-making, agricultural machinery construction a great number of cast iron cylindrical parts (camshafts, crank and cardan shafts, brake discs, bushings, pistons, etc.) are used, whose surface is subject to wear in operation. These parts need a periodical replacement or conducting repair operations. In many cases restoration of the worn parts (of their working dimensions and surface properties) is more preferable compared to their replacement by new parts, as it saves high-quality metal, power and labour resources. It is known that restoration of the worn parts performance requires 5 to 8 times less technological operations compared to manufacture of new parts [1].

Arc surfacing is widely used in repair production in restoration of steel parts. However, restoration of cast iron parts by arc processes is difficult because of their embrittlement and distortion in intensive heating, and the expense of subsequent treatment of the restored surface, namely deep (up to 2 mm) grinding, press straightening, are comparable with the cost of manufacture (or purchase) of new parts [1, 2].

Rational methods of cast iron parts restoration should meet the following requirements: localised evolution of heat energy providing a small HAZ and absence of the parts distortion, high strength of adhesion of the filler material with the part surface, small allowances for subsequent grinding, reliable and stable quality of the restored surface with minimal porosity, absence of cracks or non-metallic inclusions. Moreover, the treated surface layer should have the hardness not lower than the surface hardness of the parts made in the factory.

The majority of these requirements are met by the process of resistance build-up welding with wire (RBW) which has considerable advantages: low sensitivity to preliminary preparation of the parts for building-up; accessibility, low cost and broad range of wires as a filler material; ability to make the required equipment for building-up with wire by upgrading the existing equipment for resistance spot or seam welding; convenience of automation of the build-up welding process using cycle regulators traditional for resistance welding.

The weakest point in the technology of RBW with wire (Figure 1) is provision of satisfactory quality of joining the side surfaces of wires *1* to each other. Moreover, cavities can form in the root part of this joint in the place of contact of wires *1* with part *2*, these cavities acting as stress raisers and source of corrosion damage.

Depending on the building-up modes and materials used, the process of welded joint formation can proceed with melting of the contact zone and formation of the cast nugget or without melting [2]. In this connection the welded joint also can be produced both in the liquid and in the solid phase. Formation of the cast nugget provides a reliable joint of similar materials with fragmentation, dissolution and mixing of the surface oxides and contamination in the formed pool, but is associated with a larger HAZ in the base metal, which in the case of the cast iron parts leads to their

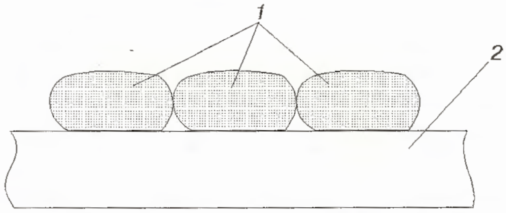

Figure 1. Formation of the joint with the traditional method of RBW with wire.

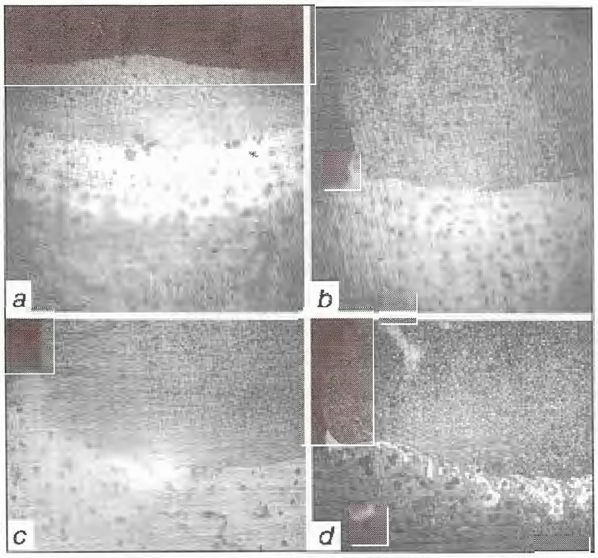

Figure 2. Macrostructures of a built-up layer with different modes of RBW: *a* — «soft», *b* — «stringent» with predominant deformation of the wire; *c* — «stringent» with predominant deformation of the part; *d* — direction of flow of the part metal at the initial moment of the joint formation (×60) (reduced by 0.53).

embrittlement as a result of chilling. Therefore, more rational is the schematic of building-up with welded joint production in the solid phase.

The mechanism of production of the solid phase joint is determined by joint elastic-plastic deformation of the materials being joined in contact, which is accompanied by the effect of shear in the contact plane. The latter not only is a mandatory condition for formation of juvenile pure surfaces and establishment of the physical contact, but in the last stage of the welded joint formation also serves as a source of a significant amount of additional heat energy required for activation of the surfaces being welded [3], and due to its localisation, practically does not have any significant thermal impact on the macro volumes of the metals being joined.

The conditions of plastic deformation differ essentially depending on the modes of building-up with wire. With a relatively long time of the welding pulse («soft modes») (Table 1) the wire has enough time to heat and is flattened over the surface of the massive part, which stays colder as a result of intensive heat removal and less ductile, accordingly (Figure 2, *a*). Grain refinement is visible in

Table 1. Main parameters of «soft modes» of RBW

Parameter	*Value*
Effective value of welding current, A	4000 – 5000
Time of welding current pulse, s	0.2 – 0.3
Forging time, s	0.2
Electrode force, N	1000

the place of the wire contact with the electrode (Figure 2, *a*), this being a consequence of intensive heat removal from the wire into the electrode. Deformation in the contact zone does not always provide a complete removal of contamination and oxides from the surfaces being joined.

With shortening of the welding time and simultaneous increase of the acting pulse of welding current (Table 2) the plastic deformation can proceed by two schematics, namely with predominant plastic deformation of wires in the contact region (Figure 2, *b*) and with deformation of the surface layer of the item metal (Figure 2, *c*). The second case is more characteristic for building-up of a cast iron part with steel wire, this being attributable to lower melting temperature of cast iron.

Investigation of plastic flow in building-up of a cast iron surface by individual contact areas of steel wire showed that in the «stringent modes» the wire practically does not undergo any deformation, and the base material flows from under it to the side, ousting the surface oxides from the contact zone (Figure 2, *d*). Favourable temperature-deformation conditions in the joining zone ensure a reliable welded joint between the steel wire and the cast iron part in the solid state.

In building-up of a cylindrical part with wire along a spiral, in the place of contact of the second and subsequent turns with the earlier deposited ones, the cast iron metal ousted by the earlier deposited wire, becomes an obstacle to formation of a welded joint between the side surfaces of the wires. The surface oxides which together with cast iron have flown out of the zone of contact of the wire and the part, stay between the side surfaces of the wire, thus markedly lowering the quality of the built-up layer. One of the ways to eliminate this drawback, is creation in the joint zone (Figure 3) of such temperature-deformation conditions, in which the metal of cast iron *2* would be ousted between wires *1* to the surface [4]. In order

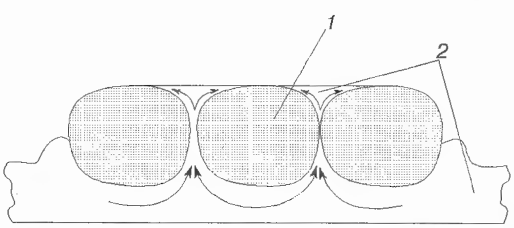

Figure 3. Schematic of plastic deformation in RBW by «KPI» method.

Table 2. Main parameters of «stringent modes» of RBW

Parameter	*Value*
Effective value of welding current, A	9000 – 10000
Time of welding current pulse, s	0.02 – 0.06
Forging time, s	0.2
Electrode force, N	1000

Figure 4. Built-up crankpins of cast iron crankshafts cut out for subsequent testing.

to solve this problem, the Chair of Electric Welding Units of NTU «KPI» proposed the process of RBW with wire and developed the equipment for its implementation [5]. The essence of this process consists in a simultaneous feeding under the electrode of a pack of several wires (Figure 3) located at a certain distance from each other, and their welding on by one pulse of welding current. In this case, the temperature-deformation conditions of the part-filler system are preserved, and simultaneous welding on of several wires arranged in a row ensures ousting of the ductile metal of the part between the wires to their surface. This process can be considered a development of the known process of wire deposition into a pressed out groove by the method of B.M. Askinazi [2]. However, the «KPI» process consists in combining in time and in terms of power consumption, the operations of the groove pressing out and wire welding on.

The effectiveness of this process was assessed by the results of welding on wires of steels 65G (of 2 mm diameter) and 70 (of 1 mm diameter) to the surface of crankpins of cast iron crankshafts. In order to perform the subsequent testing, the built-up part of the shaft was cut out (Figure 4), some of the thus prepared samples were faced and ground in a round-grinding machine for surface hardness measurement, others were cut along the

Table 3. Results of mechanical tests of built-up layer

Parameter	*Value*
Surface hardness of built-up layer after grinding, HRC	55 – 65
Surface finish after RBW, mm	0.1 – 0.5
Shear strength of adhesion of the built-up layer to the base metal, MPa	300 – 350
Base metal, HAZ depth, mm	0.1 – 0.3
Filler metal, HAZ depth, mm	0.1 – 1.0

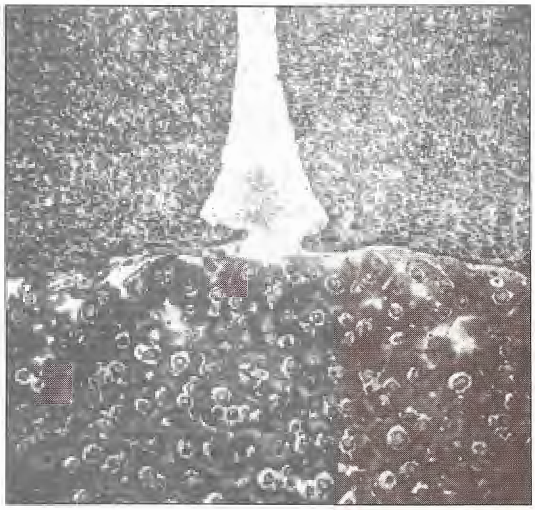

Figure 5. Structure of a joint of high strength cast iron with spring steel wire (×60) (reduced by 0.80).

shaft axis for performance of metallographic investigations. The results of mechanical tests of the samples are given in Table 3.

The strength of the produced steel-cast iron joint was determined by cutting off the welded-on steel layer from the cast iron shaft surface with measurement of its force and subsequent determination of the joint area. The testing results showed that the welded joint has equivalent strength, the shear goes through the base metal with «tearing out» of the cast iron particles, whereas the strength (300 – 350 MPa) corresponds to the strength of cast irons of this type [6].

The results of metallographic investigations showed (Figure 5) that joining of the wire and the part takes place in the solid phase uniformly over the entire area of the wire contact with the part, also between the side surfaces of the wire and the interlayer of cast iron pressed out between them. Cast iron with globular graphite partially undergoes structural changes in the place of contact with the wire at the depth of up to 0.3 mm, related to work hardening and chilling. The short time of the welding process (of the order of 0.02 s), does not allow the chilling to be completed, and globular graphite of unchanged shape is also found in the upper part of the interlayer between the wires.

CONCLUSIONS

1. Application of RBW with steel wires for restoration of the dimensions and properties of cylindrical cast iron surfaces is justified in economic and technical terms. However, the traditional methods of RBW do not ensure the homogeneity and stability of the built-up layer because of unreliable formation of the joints between side surfaces of the wires and concentration of discontinuities and contamination in these areas.

2. In order to produce a solid built-up layer with a guaranteed quality of its joining with the base metal, it is necessary to ensure during the RBW process, the flowing of the base metal between the wires with the aim of ousting the oxides and contamination from the joint zone to the wire surface.

3. RBW by «KPI» method which combines the operations of making a groove on the surface being restored, placing wire into the groove and its welding on around the groove perimeter in the solid phase (in «stringent modes»), provides a uniform built-up layer with the specified properties with surface finish not lower than 0.1 – 0.5 mm.

REFERENCES

1. Molodykh, N.V., Zenkin, A.S. (1989) *Restoration of parts of machines*. Ref. Book. Moscow: Mashinostroyenie.
2. Klimenko, Yu.V. (1978) *Resistance surfacing*. Edited by E.S. Karakozov. Moscow: Metallurgia.
3. Kochergin, K.A. (1987) *Resistance welding*. Leningrad: Mashinostroyenie.
4. Mikhed, A.M., Chernysh, V.P. (1998) Optimisation of the method of resistance restoration of part surfaces. In: *Welding and allied technologies – into the XXI century*. Kiev: PWI.
5. Mikhed, A.M. (1999) UEKN 01 unit for resistance building up with wire. *Welder*, **2**, 7.
6. (1991) *Cast iron*. Ref. Book. Edited by A.D. Sherman, A.A. Zhukov. Moscow: Metallurgia.

SOME FEATURES OF FORMATION OF SILVER COATINGS AT DIFFERENT GRAVITY*

B.E. PATON[1], V.F. LAPCHINSKII[1], E.S. MIKHAILOVSKAYA[1], A.A. GORDONNAYA[1], V.N. SLADKOVA[1], V.F. SHULYM[1] and L.O. NEZNAMOVA[2]

[1]The E.O. Paton Electric Welding Institute, NASU, Kyiv, Ukraine

[2]RSC Energia, Moscow, Russia

ABSTRACT

Microstrains and topography of silver coatings made under ground-based conditions and in the outer space are compared. The coatings were made with the use of a manual tool developed at the E.O. Paton Electric Welding Institute, Academy of Sciences of Ukraine. First-kind strains arising in silver coatings 350 – 500 nm thick on the D16 alloy base are –30 – +90 MPa when the coatings are made under ground-based conditions. Similar coatings 600 – 800 nm thick made in the outer space have virtually no first-kind strains. We believe that the silver coatings made in orbiting laboratories will have longer operating time than the coatings made on the Earth.

Key words: *space, material evaporation, electron beam heating, microgravity, surface topography.*

When technological operations are performed in raw space an extensive use of different kinds of coatings is required [1 – 4]. The need to apply the reflective, optical and other coatings in space even recently has led to the emergence of a separate field namely optical technology within the space technology [5, 6].

A whole range of practical tasks related to the position of coatings in space can be successfully solved using an all purpose manual tool (VHT) designed by the employees of the E.O. Paton Electric Welding Institute of the NAS of Ukraine. In 1984 cosmonauts S.E. Savitskaya and V.A. Dzhanibekov tested the tool in raw space [7, 8]. Besides performance of cutting, brazing and welding of materials, samples with silver coatings were also produced. The main goal of the tests was demonstration of broad capabilities of the tool proper, therefore the experiment on production of silver coatings cannot be regarded as quite correct. However, under the conditions of an almost complete absence of the data on the properties of coatings produced in raw space, even the smallest information about it, is of an indubitable interest. It should also be noted that the investigations in question were conducted right after the completion of the experiment. The results however were in classified reports in view of the specifics of those times.

Evaporation of silver of 99.99 purity was carried out from molybdenum crucibles using external electron beam heating of the crucible. In orbit the coating was applied at the pressure of $10^{-4} - 10^{-5}$ Pa and microgravity level $g = 1\times10^{-5}\ g_0$, where g_0 is gravity on the surface of the Earth. On the Earth the coating was produced in the vacuum chamber with the pressure of the residual atmosphere of 5×10^{-2} Pa. Two substrates were produced with a coating from silver as well as their two ground analogs. Sheet rolled stock from D16 alloy was used as 240×180×2 mm substrates. Prior to coating deposition, each substrate had passed such stages of processing as degreasing and etching in an alkaline solution, washing in water, anodizing: H_2SO_4 180 g/l; $T = 20$ °C; $I = 1.0 - 1.5$ A/dm^2; $U = 18 - 20$ V, $t = 40$ min, washing in water, painting to TY 6-14-515–70; final washing in water, drying. As a result of such processing the substrates acquired a black mat colour. The initial direction of the rolled stock texture was quite clearly seen visually.

The present paper contains information on the influence of the conditions of production of silver coatings on value σ of stresses of kind I, lattice parameter a and topography of their surface. Stresses of kind I in silver coatings were determined by the change in the shift of the peak of line (420) silver in the diffractograms taken in cobalt radiation in DRON-3 unit by the a certain procedure [9]. When measurements were taken, a considerable widening of the line was found because of the finely dispersed structure of the coatings, this naturally somewhat lowering the accuracy of the measurements. It can be assumed that it was equal to 20 MPa in determination of stresses of kind I. The error of the lattice parameter measurement was 0.00014 nm.

*Published in *Kosmichna Nauka i Tekhnologia*, 1997, vol. 3, **3/4**, P. 71 – 75.

Values of stresses of kind I and of lattice parameter

Production conditions	$\sigma \pm \Delta\sigma$, *MPa*	*a*, *nm*	$a_{tabl} - a$, *nm*
Space	−16 ± 20	0.40833	0.00027
Space	+25 ± 20	0.40805	0.00055
Earth	+72 ± 20	0.40770	0.00090
Earth	−52 ± 20	0.40800	0.00060

The Table shows values σ (average for 10 samples) and lattice parameter a in silver coatings produced with VHT at different gravity levels.

The given data are indicative of the fact that the coatings produced in space and on the Earth have both compressive and tensile stresses, this most probably resulting from a pronounced relief of the initial substrate.

However, by absolute value, stresses of kind I in the coatings produced on the Earth are equal to -30 – +90 MPa, and in the coatings produced in space they are within the range of measurement error.

From the results given in the Table, it can be seen that the lattice parameter of silver coatings produced in space differs less from the tabulated value than the one for the coatings deposited on the Earth. The table value of the lattice parameter of silver is 0.40860 nm.

Study of surface topography of the silver coatings was conducted in the scanning electron microscope SEM-515. Samples of 10×10 mm size were cut using guillotine type shears. In the photographs given in Figure 1 it can be seen that as a result of the deformation impact in cutting the coatings fail in the locations adjacent to the sample edges. However, the nature of fracture of the coatings deposited in space and on the Earth is different. In the coatings deposited on the Earth (Figure 1, *a*) a dense net of cracks is found and there is much spallation of the coating areas. The silver coatings deposited in space do not have any spallation in cutting up to the very edge of the sample (Figure 1, *b*, *c*), whereas the formed cracks propagate predominantly along parallel lines. The surface of coatings produced in space follows the substrate relief (Figure 2, *b*). The initial texture of the substrate can be seen in the photograph selected from a large number of similar ones. This is not observed in analogous coatings produced on the Earth (Figure 2, *a*). Moreover, reproduction of the substrate

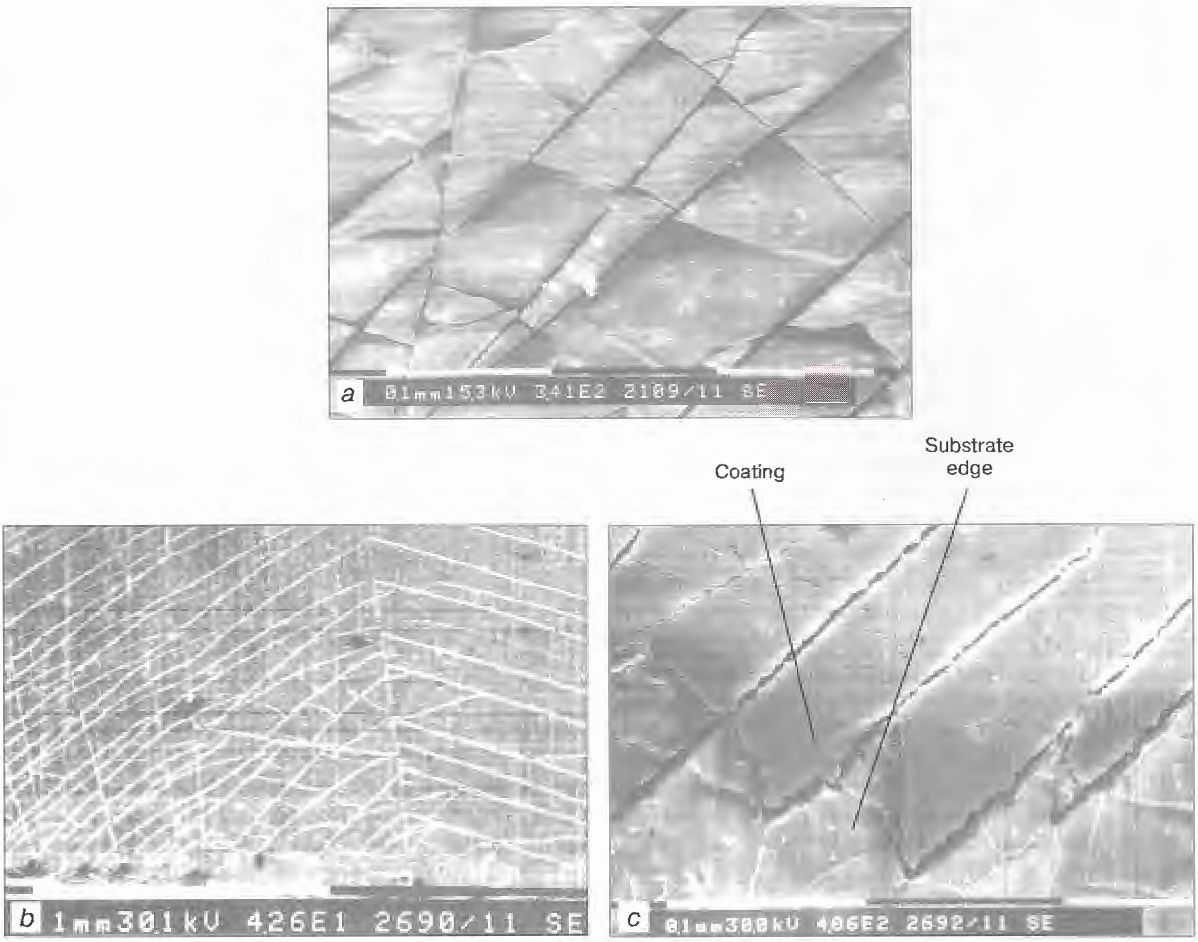

Figure 1. Topography of the surface of silver coatings deposited using the VHT on the Earth (*a*) and in space (*b*, *c*) (edge of samples cut out for investigations).

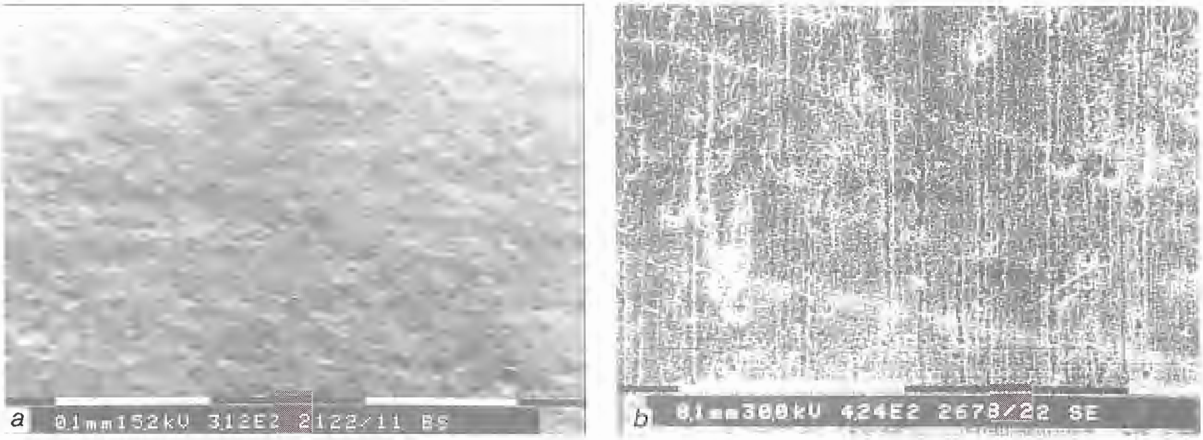

Figure 2. Topography of the surface of silver coatings produced on the Earth (*a*) and in space (*b*).

relief in silver coatings produced in space is found with the thicknesses (600 – 800 nm) greater than that of the corresponding coatings produced under the ground conditions (350 – 500 nm). As was already noted [10], with the same modes of evaporation the coatings deposited in space have a thickness greater than their ground analogs, because of a higher rate of material evaporation at zero gravity. The thickness of the coatings studied in this paper was assessed by transverse macrosections.

Silver coatings produced on the Earth are also characterized by the fact that the cracks appearing in their fracture, have the nature of cleavage (Figure 3, *a*) and those in similar coatings produced under conditions of space have the nature of tough fracture (Figure 3, *b*). Illustration of the nature of fracture of silver coatings produced in space and on the Earth confirms the conclusion that the coatings produced at zero gravity have lower stresses.

It is difficult to give a fully substantiated cause of the found differences in the properties of silver coatings produced at different gravity levels because of the absence of control of many parameters during the experiment performance. It can however be assumed that as the evaporation material during the production of the coating initially stays in the liquid phase for a long time, then goes into the vapour phase and finely condenses on the substrate in the form of a hard film, the environment, as well as deposition rate, coating thickness, substrate temperature, energy of condensing particles [11] and their interaction essentially influence the properties of the produced coatings. It is shown [12] that submicroporosity of silver coatings produced in space is smaller than of their appropriate ground analogs. Distribution of submicropores by dimensions is more uniform in the space samples, than in the ground ones. Since stresses of kind I being macrostresses, are balanced through the entire volume of the studied coatings, the results derived in this paper correlate with the conclusions of [12], as it is known that (up to a certain limit) the more defects in the material, the higher the stresses. Figuratively speaking, the process of production of silver coatings at different gravity levels can be represented as follows: forces of electromagnetic interaction between the silver atoms act in such a way under the influence of different external fac-

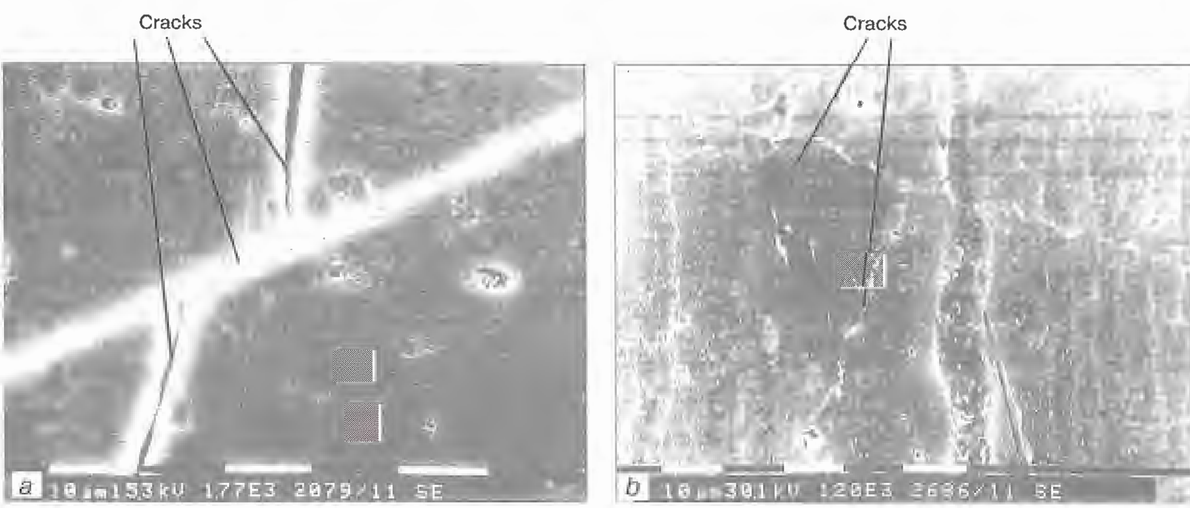

Figure 3. Nature of cracking in fracture of silver coatings deposited on the Earth (*a*) and in space (*b*).

tors, that on the Earth the atoms have to «squeeze» into the space above the substrate, whereas in space they «are freely arranged».

As a result of the conducted research the following conclusions can be made.

1. Stresses of kind I which develop in silver coatings of 350 – 500 nm thickness deposited using VHT on the Earth on D16 alloy substrates are -30 – +90 MPa. In similar coatings of 600 – 800 nm thickness produced in space, stresses of kind I are practically absent.

2. Lattice parameter of silver coatings produced in the space conditions differs less from the lattice parameter of monolithic silver, than in their ground analogs.

3. Unlike their ground analogs, silver coatings produced in raw space reproduce the substrate relief, and at thicknesses greater than in the corresponding ground samples.

4. In fracture of silver coatings deposited on the Earth, the cracks have the nature of cleavage and in those made in raw space the nature of tough fracture.

5. Analysis of the results of measurement of kind I stresses and lattice parameter of silver coatings and study of the topography of the coatings surface, allow the assumption to be made that silver coatings produced under the conditions of raw space will have a greater service life, than similar coatings produced on the Earth and taken to space by a cargo spaceship.

In view of the above-said, there is every ground to believe that the space environment is more favourable for production of coatings than the terrestrial one. The authors support the opinion [5, 13] on the expediency of conducting directly in raw space the process operations related to coating deposition.

REFERENCES

1. Paton, B.E. (1977) Problems of space technology. In: *Space Material Science and Technology*. Moscow: Nauka.
2. Paton, B.E., Dudko, D.A., Lapchinskii, V.F. (1984) Welding processes in space. In: *Welding and Special Electrometallurgy*. Kiev: Naukova Dumka.
3. Nikitskii, V.P., Zhukov, G.V. (1984) Thin films in space systems and technology. In: *Transact. of XVIII Lectures, dedicated to development of scientific inheritance and ides of K.E. Tsiolkovsky*. Moscow: IIET AN USSR.
4. Zagrebelnyi, A.A., Lukash, E.S., Nikitskii, V.P. *et al.* (1988) Development of a procedure of thin-film coatings deposition under real conditions. In: *Transact. of XXII Lectures dedicated to development of scientific inheritance and ideas of K.E. Tsiolkovsky*. Moscow: IIET AN USSR.
5. Petrovskii, G.T., Voronkov, G.L. (1984) *Optics technology in space*. Leningrad: Mashinostroyeniye.
6. (1980) Space optics. In: *Transact. of IX Int. Congr. of Int. Com. on Optics*, Santa-Monica, 1972, Oct. 9 – 13. Moscow: Mashinostroyeniye.
7. Lapchinskii, V.F., Nikitskii, V.P., Zagrebelnyi, A.A. *et al.* (1985) Test of manual electron beam tool in raw space. In: *Problems of Space Technology of Metals*. Kiev: Naukova Dumka.
8. Paton, B.E., Dzhanibekov, V.A., Savitskaya, S.E. *et al.* (1989) The test of the versatile hand electron beam tool in space. In: *Proc. of Int. Conf. under the auspices of the International Institute of Welding on Welding Under Extreme Conditions*. Helsinki: Pergamon Press.
9. Barret, Ch.S., Massalskii, T.B. (1984) *Structure of metals*. Moscow: Metallurgia.
10. Lukash, E.S., Lapchinskii, V.F. *et al.* (1985) Some analysis results of coatings samples produced in space. In: *Problems of Space Technology of Metals*. Kiev: Naukova Dumka.
11. Stetsenko, V.V., Movchan, B.A., Michenko, V.A. (1983) Structure and reflective properties of silver coatings produced by direct electron beam evaporation and ion spraying. *Problemy of Spets. Electrometallurgii*, **19**, 47 – 49.
12. Cheremskoi, P.G., Toptygin, A.L., Neznamova, L.O. (1990) Diagnostics of volume inhomogeneities of coatings being condensed in flight conditions of orbital stations. In: *Abstr. of pap. of V Korolyov Lectures of II Republ. Conf., on Fundamental and Applied Problems of Cosmonautics*. Kiev: PWI.
13. Bruns, A.V., Grechko, G.M., Gubarev, A.A. *et al.* (1977) Orbiting solar telescope on «Saliut-4» station. *Acta Astronautica*, **4**, 1121 – 1125.

APPLICATION OF RESISTANCE MEASUREMENT METHOD FOR DETERMINATION OF THE PARAMETERS OF THERMAL CYCLE OF WELDING

A.E. KOROTYNSKY
The E.O. Paton Electric Welding Institute, NASU, Ukraine

ABSTRACT

The features of application of resistance measurement effect for investigation of the welding thermal cycle are considered. Practical recommendations are given to eliminate the ambiguity of evaluation of the sample reisistance which arises in Curie point transition. The structural-fuctional diagram of the sample temperature measuring device is described which is based on an alternating current double transformer bridge with quasimodulation balancing, capable of providing the measurement rate of ≥ 400 counts per second with ≤ 1.0 % error. This device is the basis for a computerized facility for thermal cycle of welding (TCW) investigation.

Key words: *arc welding, thermal cycle of welding, resistance measurement effect, instrument transducer, sensor.*

Temperature measurement in determination of TCW is, as a rule, performed using thermocouples [1]. Contactless thermometers based on different types of pyrometers are used much more seldom [2].

The disadvantage of the first process consists in the locality of measurement, its low noise immunity, as well as poor dynamic properties of thermocouples at high-rate heating and cooling of the sample being studied. The time constant of the thermocouples can be lowered to 0.2 to 0.3 s, but in the majority of cases this turns out to be insufficient.

The pyroelectric thermometers are characterised by high dynamic characteristics, they, however, requiring a thorough calibration of the metrological parameters. In investigation of TCW specific conditions are found when implementation of the required accuracy of temperature measurement by this method becomes practically impossible.

In this connection, we have made an attempt to develop a temperature measurement unit on the basis of the resistance measurement method [3], which essentially consists in the use of the functional dependence of electric resistance of the sample being tested on temperature $R_x = F(T)$.

References [3, 4] describe several devices applied for resistance measurement studies of metals when the phase transformation points are determined. More promising are the instrument transducers based on bridge circuits using high frequency currents (10 – 50 kHz). In this case the skin-effect is rather strongly manifested, thus allowing the sensitivity of this method of temperature measurement to be increased.

We studied a sample of St.3 steel which is schematically represented in Figure 1, *a* ($d = 4$ mm, $L = 100$ mm). The measurement unit in points *1*, *2* is connected to the signal contacts mounted on the sample. A double transformer bridge is used as the measurement unit [5] balanced by one parameter. Its circuit is given in Figure 1, *b*.

The bridge circuit incorporates a voltage transformer (VT), current comparator (CC) and two matching transformers MT1 and MT2. A four-terminal circuit of connection of the object being measured is used, in order to eliminate the influence of the connecting wires on the result of $R(T)$ measurement [6]. The signals of balancing of the bridge measurement circuit are formed by processing the output current of winding n_3 of CC. Automatic balancing of the bridge is performed by quasimodulation extremum detector (ED) [7], to whose output the automatic balancing circuit is connected (ABC). The latter generates the commands for control of the contactless keys module (CKM), which switch the appropriate sections of the inductive voltage dividers made up by m_2, m_4, m_7 windings.

As CC performs the operation of adding the ampere turns (allowing for their connection phase), the condition of balance of the bridge measurement circuit corresponds to $\Sigma\, n_j I_j = 0$. From this condition the following expression can be derived for determination of the sought $R(T)$ parameter:

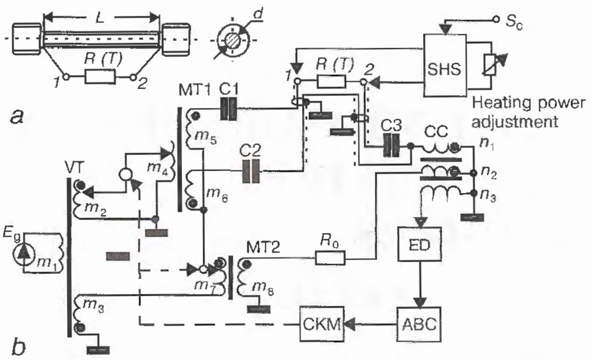

Figure 1. Sample being tested (*a*) and diagram of temperature measuring unit (*b*).

$$R(T) = \frac{n_1\, m_2\, m_4\, m_7}{n_2\, m_3\, m_5\, m_8}\, R_0 \,.$$

Therefore, direct count in the electric resistance units can be achieved with the appropriate switching of turns of n_1, m_2, m_4 and m_7 windings. Switching of CC windings usually involves certain difficulties related to provision of the required level of noise immunity. In this connection it is used in special cases while the turns are mostly switched in the VT circuit. This is exactly why windings of VT, MT1 and MT2 have been selected as the regulated windings (Figure 1, *b*).

The block diagram of the test facility for implementation of the resistance measurement method, is given in Figure 2. It includes a device for mounting the sample being tested, sample heating source with the current transducer (CT) based on Hall generator, technological interface module (TIM), tested object interface MacLab (AD Instruments), and Machintoch PB 180 c personal computer. TIM designed for processing the information signals received from the primary transducers of CT, thermocouple (TC) and $R(T)$ measurement unit, as well as for generation of the command of control S_c of sample heating source (SHS) incorporates CT of heating current I_h, TC temperature monitoring sensor, unit for measurement of sample resistance change with its heating, and matching module (MM) which determines the mode of SHS operation.

The facility is designed to fit into a standard CAMAC rack based on the single-crate system

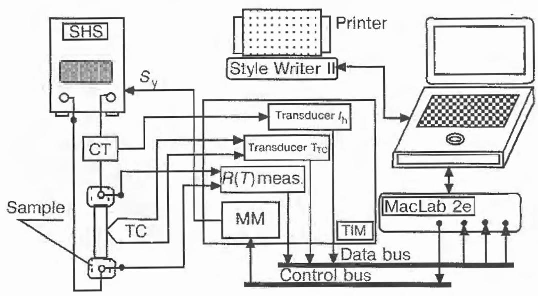

Figure 2. Block-diagram of the testing facility.

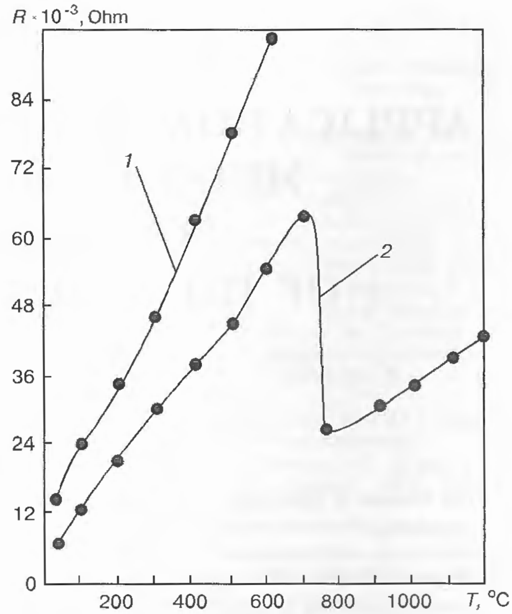

Figure 3. Curves of variation of sample resistance at the frequencies of 15 (*1*) and 8 (*2*) kHz.

which accommodates the sample heating source and the main modules of TIM. The size of SHS is 12 M, of the module of $R(T)$ measurement 2 M, of facility control module 1 M.

The results of experimental testing of $R(T)$ measurement unit designed for resistance measurement studies of standard samples, are given in Figure 3. The curves shown in the graph represent the resistance measurement spectrum (RMS). Its formal description is assigned by $R(T, f)$ expression, where f is the measurement frequency at which evaluation of the sample surface resistance is performed. For a sample of dimensions L = 100 mm and d = 4 mm made of St.3 (Figure 1, *a*), an essential increase in the resistance was recorded with the temperature rise. Here grad $R(T)$ is the higher, the higher the measurement frequency, this being attributable to the surface effect becoming stronger (the depth of the skin-layer is reduced). Therefore, for materials with a small grad $R(T)$, higher measurement frequencies should be recommended, in order to increase the sensitivity of the measurement equipment, although in this case also, the hardware becomes more sophisticated.

Additional difficulties arising in practical implementation of the proposed method of evaluation of the temperature of the studied sample by its RMS, are related to steels and other ferromagnetics having a Curie point. When it has been achieved, the sample abruptly loses its magnetic properties, and, therefore, its surface resistance also abruptly changes, this making the procedure of interpretation of the measurement results somewhat more complicated. However, in combination with the computer methods of processing the experimental data, this shortcoming is easily overcome due to the ability of compiling a data base on RMS for different materials. The more so, since in assessment of TCW parameters the experimenter has a priori information consisting in that in sample heating always grad $R(T) > 0$, and in cooling, on the contrary, grad $R(T) < 0$.

Calculation of metrological parameters of the temperature measurement unit showed that the error of resistance evaluation is at the level of 0.2 to 0.5 %. Therefore, assessment of the sample temperature in TCW can be performed with not more than 0.7 to 1.0 % error. The dynamic properties of such bridge type measuring units depend, primarily on the selected carrier frequency. At $f = 8$ kHz the speed of 400 counts per second and at $f = 15$ kHz that of 720 counts per second can be provided.

REFERENCES

1. Anosov, A.P. (1988) Thermodeformational processes and fracture of welded joints. In: *Proc. of Yakutsk Branch of SO AN USSR*. Yakutsk: Izd. SO AN USSR.
2. Cherepin, V.T. (1968) *Experimental equipment in physical metal science*. Kiev: Tekhnika.
3. Motalo, V.P., Pyzh, A.D., Shmorgun, E.I. *et al.* (1975) *Semi-automatic device for resistance measurement studies of metals at a higher frequency*. Lvov: LPI.
4. Belov, K.P. (1959) *Magnetic transformations*. Moscow: Fizmatgiz.
5. (1970) *Transformer measurement bridges*. Edited by K.B. Karandeev. Moscow: Energia.
6. Grinevich, F.B., Novik, A.I. *Double transformer bridge for measurement of complex impedances connected in a four-terminal circuit*. USSR author's certificate **265272**, Int. Cl. B 23/1. Publ. 05.07.70 .
7. Novik, A.I. (1983) *Systems of automatic balancing of digital extremum alternating-current bridges*. Kiev: Naukova Dumka.

METHODS FOR APPLICATION OF ACTIVATORS IN TIG WELDING OF STEELS

M.M. SAVITSKY, A.F. LUPAN, G.M. MELNICHUK and **O.I. OLEINIK**
The E.O. Paton Electric Welding Institute, NASU, Kyiv, Ukraine

ABSTRACT

Different methods for application of activators in argon-arc welding and their introduction into the welding arc are considered. A new device, fluxograph, has been suggested for introducing activators into the arc zone.

Key words: *argon-arc welding, activator, flux pencil, aerosol canister, fluxograph.*

The problem of raising productivity of TIG welding was resolved at the E.O. Paton Electric Welding Institute as far back as the 1960s. The solution consisted in adding special activators to the arc zone. The effect of these activators is in causing contraction of the welding arc, increase in energy density in the arc, decrease in surface tension of liquid metal and its resistance to immersion of the arc and, finally, substantial increase in metal penetration depth [1, 2]. This solution has sufficient theoretical and experimental grounding. At present, the main consideration is given to the development of formulations and methods for introduction of activators into the welding zone.

Activators for welding steels can be used in the form of mixtures of gases or solid chemicals [2] with the components containing elements characterized by an increased affinity for electron. Solid activating agents (fluxes) are made in the form of powders with an addition of binders, thus producing flux pastes, pencils, fibres and wires. With a properly selected composition and method of application, their consumption in welding is no more than gram per meter of the weld.

One of the most common methods for application of an activator involves deposition of a thin layer of this activator on the surface of metal near the weld edges. In this case the flux in the form of a paste-like suspension is applied to the surface using a paint brush. A drawback of this method is that diluents used to make the suspension, which are relatively volatile, are evaporated from an open vessel, causing a change in viscosity of the paste and inconsistency of thickness of the flux layer deposited on the surface of a workpiece. The use of low-volatility liquids leads to certain improvement in consistency of the deposited flux layer, although this increases the time of drying prior to welding and, if the paste flows into the gap between the weld edges, causes porosity. Another drawback of this method is that it is necessary to store the flux and diluent in different vessels and mix them in small portions just before the use. Besides, this often causes changes in consistency and uniformity of the layer of the flux paste on the workpiece surface.

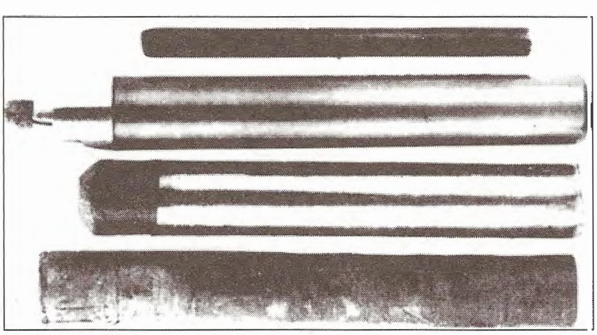

Figure 1. Flux pencils.

The field of application of welding using activators is increasingly widened now. This process is successfully employed for the fabrication of structures of high-, medium- and low-alloy, as well as carbon and slightly deoxidized steels. The wide commercial application of the activators requires improved methods for their introduction into the welding zone.

For instance, for welding titanium, it was suggested that the activators could be added to the cores of flux-cored filler wires [3]. However, in the case of welding steels the use of such wires turned out less effective. This is attributable to the fact that components of the cores of the wires intended for steels are normally more refractory than those intended for titanium. Thus, in their transfer to the weld pool they form non-metallic inclusions in the welds because of incomplete dilution.

The guaranteed stability in addition of the activators into the welding zone was achieved owing to the use of neutral low-melting point binders. The use of the latter enabled fabrication of the flux pencils (Figure 1). Such a pencil allows the activator to be easily applied to the surface of a steel

Figure 2. Aerosol canister.

Figure 3. Fluxograph — a new device for application of the flux paste.

part after sand blasting or preheating. During welding, the binder is as a rule evaporated at a distance of 5 – 10 mm from the leading edge of the weld pool and forced out by the flow of plasma of the arc column from the arc burning zone. Thus, it has no effect on the processes occurring in the arc and the weld pool. However, it is not always possible to preliminarily prepare the surfaces of parts for application of the flux by the above methods. Therefore, the authors in collaboration with associates of the Tsentroenergomontazh Company developed the method and devices for spraying activators onto the surfaces of workpieces using air brushes or aerosol canisters (Figure 2). This method found its application mostly for field operations. In particular, at the beginning of the 1980s this method was employed for position butt welding of pipes in construction of power units for Smolensk and Kursk nuclear power stations [4].

The positive feature of this method was that during operation the consistency of the flux paste did not change, and that it was not necessary to mix components at a work place, as the mixture was prepared under stationary conditions and then fed into the aerosol canister or other hermetically sealed packing to exclude any evaporation of a volatile diluent during storage. This allowed a more uniform layer to be deposited onto the surface of metal near the weld edges and provided a stable burning of the welding arc.

The method described is not versatile. With this method it is almost impossible to avoid overconsumption of the flux and ingress of the liquid fraction into the gap between the weld edges, which is known to cause porosity. In addition, insoluble particles of the flux often settle out on walls of the channel via which the mixture is fed to a sprayer and clog it, which makes the aerosol packing unfit for use. However, the main drawback of this method is in its limited utility in enclosed spaces, because it causes their dusting with harmful matters which could lead to welders' occupational diseases.

To eliminate these drawbacks, the authors offer a new device, i.e. fluxograph, for application of the flux pastes thus avoiding their spraying. The pastes in the form of suspensions or homogeneous solutions are prepared under stationary conditions and stored in hermetically sealed vessels. An attachment to them is a reusable device (Figure 3) which serves as the working tool. This device is periodically filled with the paste in the amount required for work. When not in use, the device is hermetically closed. To make it ready for use, it is enough to remove the protective cap and then, using the working tool, just deposit a thin layer of the flux onto the metal surface.

This method allows consumption of the flux to be precisely measured and safe working conditions for welders to be ensured.

REFERENCES

1. Gurevich, S.M., Zamkov, V.N., Kushnirenko, N.A. (1965) Increasing the efficiency of penetration in argon-arc welding. *Avtomaticheskaya Svarka*, **9**, 1 – 4.
2. Makara, A.M., Kushnirenko, B.N., Savitsky, M.M. *et al. Method for non-consumable electrode welding*. USSR author's certificate **284214**, Int. Cl. B 23 K 35/30. Publ. 03.05.70.
3. Prilutsky, V.P., Zamkov, V.N., Gurevich, S.M. (1975) Argon-arc welding of titanium alloys using flux-cored filler wire. *Avtomaticheskaya Svarka*, **7**, 41 – 44.
4. Stankevich, I.Ya., Dmitriev, V.I., Karida, V.L. *et al.* (1982) The use of the activating flux in automatic welding of nuclear power station piping. *Energeticheskoye Stroitelstvo*, **10**, 19 – 20.

MODE OF FRACTURE OF WELDED JOINTS OF HEAT-RESISTANT STEEL IN GAS MEDIUM OF AMMONIA SYNTHESIS

V.A. BORISENKO[1], Yu.Ya. NIKHAENKO[1], A.N. KUSYUKOV[1], A.V. TUGOLUKOV[2] and S.V. PANCHENKO[2]
[1]NIIKHIMMASH, Severodvinsk, Russia
[2]JSC Concern Stirol, Gorlovka, Ukraine

ABSTRACT

The mode of fracture of welded joints in heat-resistant steel 18Kh3M under conditions of synthesis of ammonia is considered. It has been established that the main cause of fracture is a combined unfavourable effect of postweld heat treatment of welded joints and creep process. The cold cracks are initiated in the higher-hardness quenching structures and contribute to the initiation of creep microfractures. Atomic hydrogen formed under a pressure of 32 MPa and 340 °C temperature causes the accelerated propagation of cracks until they penetrate through a parent metal.

Key words: *electric arc welding, heat-resistant steels, pipelines, site welds, cracks.*

The experience of service of high-pressure pipelines in which the gas, containing ammonia, nitrogen and hydrogen, is transported from a column of the ammonia synthesis showed that at the number of enterprises the welds are subjected to fracture.

Thus, at one of the enterprises after 14-year service the gas was on fire due to complete failure of one of the welded joints of such pipeline. The removable part of the pipeline had seven welds, two of them were site welds, the rest welds were made under the shop conditions.

The site weld adjacent to the column of synthesis failed. The pressure in pipeline was 32 MPa, the gas temperature was 335 – 345 °C. The pipeline was manufactured from steel 17CrMoV10, corresponding to steel 18Kh3M which is heat-and hydrogen-resistant under the given service conditions.

Welded joints were made by an electric arc welding using imported electrodes AUS A/SF A 5.5:E9018-B3a. Welding was performed with preheating at 200 °C and postweld heat-treatment at 680 – 720 °C for 2 h. However, the investigations showed that in case of a site weld with cracks the technology of heat-treatment was not properly followed.

To investigate the causes of failure two site welds were cut out. In metal of weld No.1, after the gas passing, nine longitudinal cracks were revealed, among them seven cracks were through. In metal of weld No.2 several cracks were revealed. By their nature they were like cold welding cracks [1], located inside the weld metal. They had no escape neither to the inner, nor to the external surface of the weld.

Chemical analysis of the parent metal and weld metals of welded joints is given in Table 1. Content of chromium and molybdenum in weld metal was higher than that in the parent metal at a comparatively low content of carbon, that is envisaged for case of welding heat-resistant steels.

Carbide analysis showed that the share of molybdenum in carbides is 32.2 % as compared with initial 10 – 20 %.

Mechanical tests of specimens cut out from welds and parent metal showed that the strength of the weld No.1 1.5 times exceeds that of the

Table 1

Object of analysis	*Elements, mass %*							
	C	*Si*	*Mn*	*Cr*	*Mo*	*V*	*P*	*S*
Parent metal (steel 18Kh3M)	0.19 – 0.20	0.10 – 0.11	0.34 – 0.41	2.60 – 3.00	0.26	0.170	Not determ.	
Weld No. 1	0.10	0.34	0.59	3.17	0.94	0.015		
Weld No. 2	0.10	0.22	0.59	3.11	0.90	0.030		
Parent metal (steel 17CrMoV10)	0.15 – 0.20	0.15 – 0.35	0.30 – 0.50	2.70 – 3.00	0.20 – 0.30	0.10 – 0.20	0.025	0.025

parent metal at reduction of the ductility by 30 – 40 % as compared with the parent metal (Table 2).

Hardness of metal of the weld No.1 reaches *HB* 345 at hardness of the parent metal *HB* 185 – 187 (Table 3).

Macrostructure of welds of the welded joints of the pipes examined is typical of multilayer joints of pipes (dia. 419×42 mm) made from Cr-Mo steels. In weld No.1 the macrostructure of metal is more coarse-grained in sites of clearly expressed dendrites with a smooth transition of HAZ to the farest parent metal from the weld (Figure 1, *a*).

Metallographic examination showed that the metal of welds has a sorbite-troostite and sorbite-bainite structure typical of heat-resistant steels. One of cracks is propagated from the weld metal to HAZ and then to the parent metal. Along the path of avalanche cracks the adjacent zones of metal, consisting of microcracks, are fractured. The avalanche crack, which contacts the inner surface, is filled with products of corrosion, and its edges are contaminated with compounds of nitride types and, possibly, with hydrides. These compounds were revealed in cracks at the depth of 10 – 12 mm (Figure 2) from the inner surface of the pipe. Moreover, a partial decarburization of metal along the crack path was revealed.

The mode of propagation of macrocracks can be evaluated from the fracture examined in two through cracks. The examination of surface of the crack fracture showed that there are 10 – 12 disoriented planes (Figure 1, *b*) of propagation of cracks which are characteristic of a low-cycle fatigue, having a fan-shaped progressing. The presence of radial scars in the form of a chevron is explained by a gradual transition of a plane-deformed state into a complex-deformed state with intensifying the role of tangent stresses.

Investigation of hydrogenation of welded joints using the method of a heat degassing showed that in weld metal section the hydrogen content is not uniform. If from the side of a medium it reaches 36 – 38 $cm^3/100$ g of metal, then at the external surface it is amounted to 3.6 – 3.7 $cm^3/100$ g of metal. The large amount of hydrogen was also revealed in separate regions in height of the weld metal.

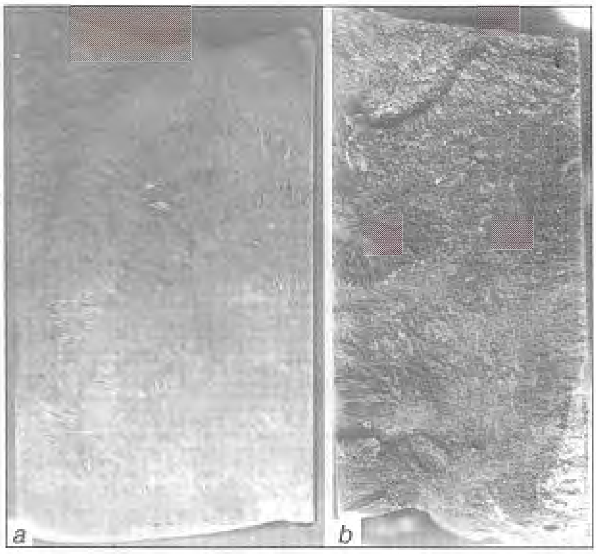

Figure 1. Macrostructure of weld metal (*a*) and appearance of fracture surface of one of cracks (*b*) (×2) (reduced by 0.75).

The investigations can explain the causes of fracture of the welded joint of heat-resistant steels in gas medium of the ammonia synthesis. At unproper selected conditions of heat treatment the weld metal of welded joints has a quenching structure with an increased hardness as compared with that of the parent metal. The higher strength properties of such welds and their lower ductility and also the presence of residual welding stresses lead to the formation of hard microcracks.

In the medium containing hydrogen at high values of pressure and temperature the atomic hydrogen [2] is appeared at steel-medium interface, which penetrates to welded joints and is moved from their inner surface to the external surface. When reaching microcracks the hydrogen is accumulated and forms a molecular hydrogen. The hydrogen pressure is growing, thus intensifying the propagation of welding cracks and creep microfractures.

In case, when the crack reaches the inner surface, its propagation is more accelerated under the action of the gas medium, causing the nitriding, and, possibly, decarburization, because of the hydrogen corrosion. Decarburization is due to the de-

Table 2

Test region	σ_t, *MPa*	σ_y, *MPa*	ψ, *%*	δ, *%*	*KCV*, *J/cm²*
		Test temperature 20 °C			
Weld No. 1	1065 – 1070	928 – 947	20.8 – 51.0	10.0 – 18.7	Not determ.
Weld No. 2	734 – 791	594 – 686	67.7 – 71.1	16.5 – 19.8	140 – 236
Parent metal (steel 17CrMoV10 acc. to standard D1)	650 – 850	450	Not determ.	16	80
		Test temperature 350 °C			
Weld No. 2	597 – 645	499 – 557	66.4 – 69.4	11.0 – 15.0	Not determ.

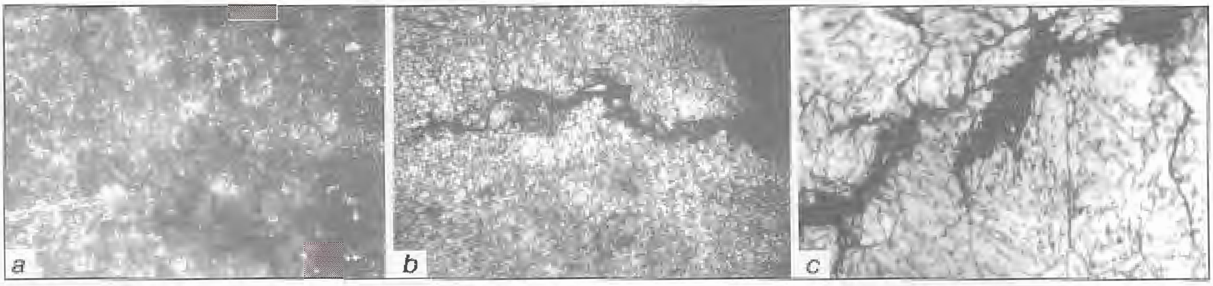

Figure 2. Microcracks along the path of avalanche crack: *a* — weld root, *b*, *c* — weld middle part (×100 and ×1000, respectively) (reduced by 0.75).

Table 3

Object of analysis	*Hardness, HB*	
	Welded joint with weld No.1	*Welded joint with weld No.2*
Weld	308 – 345	217 – 246
HAZ	192 – 229	179 – 229
Parent metal (steel 18Kh3M)	185 – 187	175 – 179

pletion of matrix with chromium and molybdenum which are transferred to the secondary phases.

A high stability to such type of fracture of welded joints made under the shop conditions is explained by a longer incubation period of formation and propagation of welding cold cracks and cracks of the creep process.

The parent metal is more stable to failure under these conditions. However, when metallurgical defects and large amount of non-metallic inclusions caused by the action of the atomic hydrogen, which penetrates to the steel, are present in pipes, the pipes are subjected to lamination that was observed by the authors in other similar cases.

The fractures of site welds were also observed at many other similar enterprises.

To repair the damaged pipeline the recommendations were developed for welding pipelines by the electric arc method using the electrodes of TsL-17 type (GOST 9466–75). The cutting-out of defective welded joints and edge preparation for welding were performed by mechining. Pipes with prepared parallel ends were assembled by using aligning devices with allowance for arrangement of heaters. To remove hydrogen from the pipe metal saturated with it during service the butts were subjected to heating up to 550 °C temperature during 1 h. To remove the residual magnetizing of metal (due to magnetic blow occurred) the wire was coiled to the butts, prepared for welding, through which the electric current was supplied with impulses (power source VD-356, I = 200 A, U = 28 V, impulse duration — 2 – 3 s).

Thus, it was managed to avoid the magnetic blow. Welding was performed with a preheating to 350 – 400 °C and between the separate passes — to 350 °C.

To reduce the probability of fracture of welded joints after welding they were heat treated, thus relieving the welding stresses and providing the structure of tempering. Heat treatment condition included a preheating of butts to 690 °C at a rate of 100 °C/h, soaking at 690 °C for 3.5 h with a next cooling to 200 °C at a rate of 100 °C/h.

Inspection of welded joint did not reveal macrodefects. After repair the pipeline was put into service for a limited period with an obligatory control of welds during regular interruptions of operation.

REFERENCES

1. (1974) *Technology of electric welding of metals and alloys*. Edited by B.E. Paton. Moscow: Mashinostroyeniye.
2. Archakov, Yu.I. (1985) *Hydrogen corrosion of steel*. Moscow: Metallurgia.